Australian Government
Geoscience Australia

Nutrient Cycling In St Georges Basin, South Coast NSW

Report on Field Survey November 2003

Emma J. Murray, Ralf R. Haese, Craig S. Smith And David T. Heggie

Record
2005/22

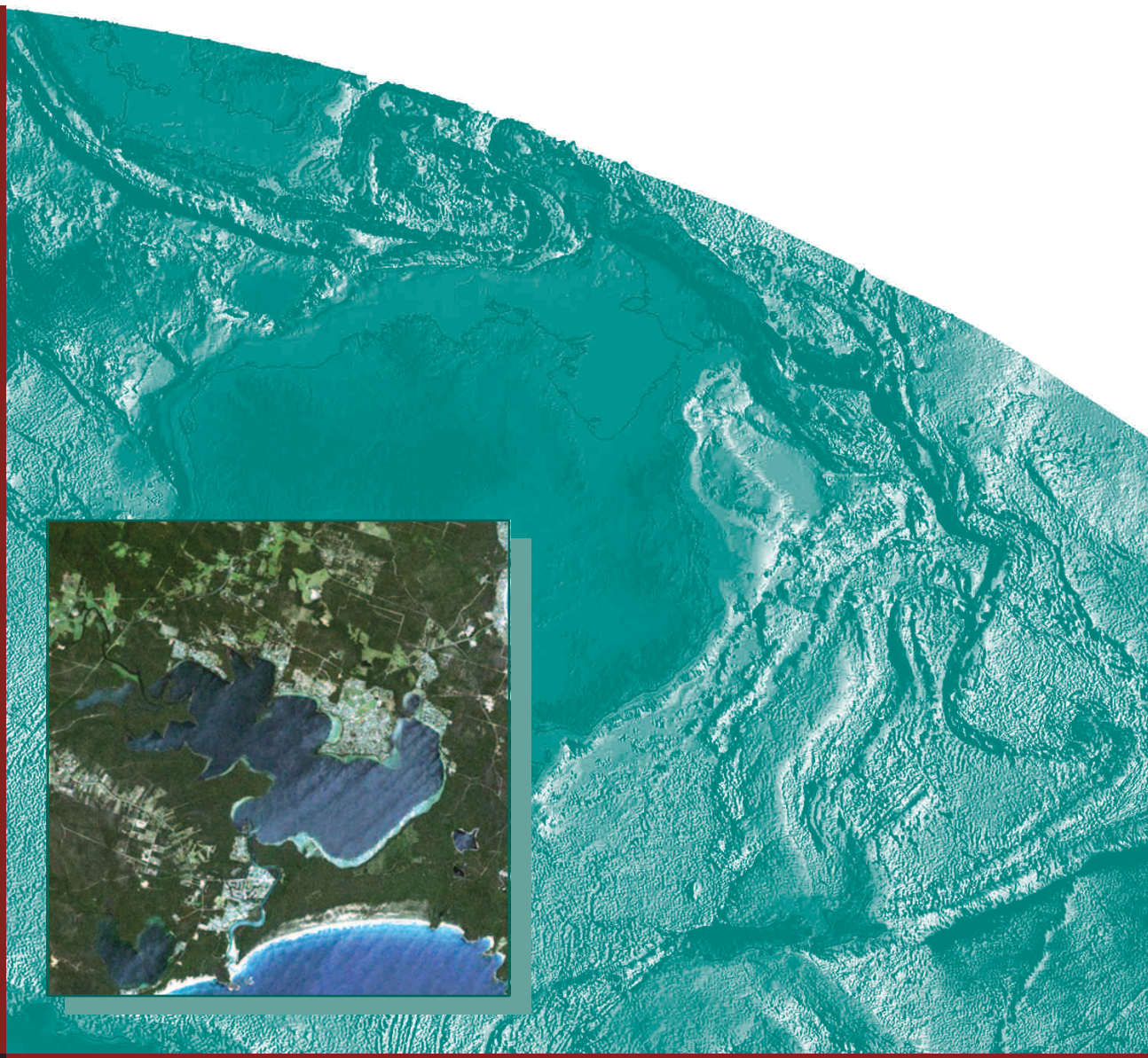

NUTRIENT CYCLING IN ST GEORGES BASIN, SOUTH COAST NSW

Report on Field Survey November 2003

EMMA J. MURRAY, RALF R. HAESE, CRAIG S. SMITH AND DAVID T. HEGGIE

Geoscience for Coastal Waterways Management Project

Australian Government
Geoscience Australia

GEOSCIENCE AUSTRALIA RECORD 2005/22

Department of Industry, Tourism & Resources

Minister for Industry, Tourism & Resources: The Hon Ian Macfarlane, MP
Parliamentary Secretary: The Hon. Bob Baldwin, MP
Secretary: Mark Paterson

Geoscience Australia

Chief Executive Officer: Dr Neil Williams

ISSN: 1448-2177
ISBN: 1 920871 63 2 (Hardcopy)
ISBN: 1 920871 64 0 (Web)

GeoCat No. 61611

Bibliographic Reference: Murray, E. J., Haese, R. R., Smith, C. S. and Heggie, D. T. 2005. *Nutrient Cycling in St Georges Basin, South Coast NSW: Report on Field Survey November 2003*. Geoscience Australia, Record 2005/22.

EXECUTIVE SUMMARY

Objectives

Geoscience Australia conducted a survey of lakebed (benthic) nutrient fluxes in St Georges Basin, November 2003. The objectives were to (1) determine the nature of nutrient cycling between the sediment and overlying water, and (2) determine the implications of benthic nutrient fluxes for water quality in the estuary. The relevance to management of this work is that it gives an indication of the susceptibility of the estuary to eutrophication from increased nutrient loads from the catchment.

Activities

In November 2003, we sampled five sites in St Georges Basin (the Central Basin, Erowal Bay, the entrance to Wandandian Creek, One Tree Bay, and Pats Bay). Site selection aimed to capture the variability of nutrient loads from different sub-catchments. We measured the rate of O_2 uptake and release of TCO_2, NH_4^+, N_2, and SiO_4^{4-} to the water column using benthic chambers. Denitrification efficiencies (DE) were calculated, representing the percentage of nitrogen released as N_2 gas compared to total dissolved inorganic nitrogen remineralised from degrading organic material. A caesium tracer was injected into the chambers to determine the extent of bioirrigation in the sediments.

In addition to benthic chambers, we performed core incubations and collected sediment cores. The down core profiles of pore water (TCO_2, NH_4^+, NO_x, PO_4^{3-}, SiO_4^{4-}) and solid phase (TOC, Chl-a, δ^{13}C-TOC, porosity) constituents gave information on organic matter source and diffusive fluxes. Comparing benthic fluxes derived from core incubations and benthic chambers with diffusive fluxes derived from down core profiles revealed aspects of spatial heterogeneity.

Background

Organic matter breakdown in the sediments and exchange (flux) of solutes between the sediment and overlying water are key processes influencing water quality in estuaries. The release of nutrients to the overlying water from organic matter breakdown is often a major source of nutrients for plant growth. Also, the process has a significant influence on dissolved oxygen levels because during respiration, bacteria use oxygen, when available, to oxidize the dead organic matter. In general, nutrients in runoff from the catchment can enter an estuary and stimulate plant growth, especially phytoplankton, and macroalgae. When these plants fall to the lakebed and die, they are broken down by bacteria, which results in the release of nutrients back into the water column. Therefore, through these linkages, we consider the magnitude of benthic fluxes (this study specifically measured TCO_2, NH_4^+, N_2, SiO_4^{4-} and O_2) to be proportional to the amount of organic matter degrading in the sediments, which in turn is a measure of the levels of nutrient supplied from the catchment and available in the water column.

Excessive plant growth (eutrophication), which is often associated with undesirable consequences such as nuisance algal blooms, seagrass decline, and low dissolved oxygen levels, can occur when there is an oversupply of nutrients. In addition to nutrients arriving from the catchment, the nutrient nitrogen (N) can be released from organic matter breakdown in the sediment as ammonium (NH_4^+), a form which is readily available for plant growth. The process of denitrification is an important control on eutrophication, as it can result in the loss of N to the atmosphere as N_2 gas. N can also be lost through water exchange with the ocean and burial. However, sedimentation rates are likely not rapid enough to bury significant amounts of organic material and nutrients before they are remineralised and the restricted entrance to St Georges Basin limits exchange with the ocean. It takes approximately 80 days to exchange a volume equal to that of the Basin with the ocean.

Key Findings

- St Georges Basin was mesotrophic to eutrophic at the time of the survey (spring) based on relatively high respiration rates and O_2 demand in the sediments measured by in situ benthic chambers. Especially the shallower sites in the embayments around the edge of the basin showed high benthic nutrient, oxygen and inorganic carbon fluxes.

- Respiration rates were linked to phytoplankton biomass (mainly diatoms) where local fluvial discharge of dissolved nutrients created enhanced primary productivity in the water column, which in turn enhanced mineralisation rates.

- St Georges Basin had comparatively low denitrification efficiencies (less than 60%). This was especially so for the shallower areas around the edge of the basin, where over 50% of N was returned to the water column as NH_4^+.

Management Implications

Wave-dominated estuaries such as St Georges Basin have restricted entrances and little capacity to 'flush' N to the sea. In order to maintain water quality and prevent eutrophication, these estuaries depend on high denitrification efficiencies to maintain low levels of bioavailable N in the water column. At the time of sampling, St Georges Basin had relatively high respiration rates and low denitrification efficiencies. Therefore, the basin is likely prone to eutrophication and may have little tolerance for increases in nutrients and organic matter from the catchment.

ACKNOWLEDGMENTS

We would like to thank Colin Tindall, Ian Atkinson and Alex McLachlan for sample processing and analysis in the field and field survey logistics. Craig Wintell for additional benthic chamber construction and maintenance. We also thank the NSW EPA, Wollongong University, and Shoalhaven City Council for use of their boats, and Martin Bergs from Shoalhaven City Council for general assistance and advice.

ABBREVIATIONS AND UNITS

Chl-a	Chlorophyll a
C	Carbon
Cl^-	Chloride
Cs	Caesium
CsCl	Caesium Chloride
DO	Dissolved Oxygen
Fe^{2+}	Ferrous Iron
GA	Geoscience Australia
H_2S	Hydrogen Sulfide
ICOLL	Intermittently Closed and Open Lake/Lagoon
mAHD	metres above Australian Height Datum
mL	milliliter
ML	Mega Litres
mM	millimoles per litre
mmol/kg	millimoles per kilogram
mmol m^{-2} day^{-1}	millimoles per metre squared per day
N	Nitrogen
N_2	Dinitrogen Gas
NH_4^+	Ammonium
NLWRA	National Land and Water Resources Audit
NO_2^-	Nitrite
NO_3^-	Nitrate
NO_x	Nitrate + Nitrite
O_2	Oxygen
P	Phosphorus
Si	Silica
SiO_4^{4-}	Silicate
TOC	Total Organic Carbon
wt%	Weight Percent
TCO_2	Total Carbon Dioxide
TN	Total Nitrogen
TP	Total Phosphorus
µg	microgram
µL	microlitre
µM	micromolar

CONTENTS

LIST OF FIGURES

LIST OF TABLES

1. INTRODUCTION

Declining water quality is a growing problem in Australian estuaries. This is especially the case along the south-east and south-west coasts where estuaries are predominantly: (1) 'modified' (NLWRA 2002, p133) and thus subject to increasing nutrient loads from agricultural, urban, and industrial expansion; and (2) 'wave-dominated', with restricted entrances, and a limited capacity to flush nutrients to the ocean (Harris and Heap 2003).

This report outlines the results and findings of a recent survey to St Georges Basin. The study aimed to build upon our present understanding of nutrient cycling in Australian estuaries, which in turn, informs the sustainable management of these ecosystems. This knowledge is of particular importance to management because it gives an indication of the susceptibility of different types of Australian estuaries to a decline in ecosystem health from increased nutrient loads from the catchment. The present study in St Georges Basin allowed us to ascertain the susceptibility of a relatively large coastal lake to water quality decline. The lake foreshores and catchment are relatively undeveloped with over 80% covered in forest. Urban areas are largely restricted to the northern shoreline and the eastern side of Sussex Inlet, which links the basin to the ocean (Shoalhaven City Council 1998, p 2.6). Residential development is set to expand in the future, along with the potential for increased nutrient and sediment loads to the estuary.

Organic matter breakdown in sediments, and the resulting exchange (flux) of oxygen, carbon dioxide, and nutrients between the sediments and overlying water, is a key influence on water quality in estuaries. Geoscience Australia has conducted research into estuarine-sediment (benthic) nutrient fluxes in Australian coastal waterways for over 10 years, mainly focusing on estuaries along the south-eastern and south-western Australian coasts. Studies have been conducted in Port Phillip Bay (Heggie *et al*. 1999a; Heggie *et al*. 1999b; Berelson *et al*. 1998), Moreton Bay (AGSO 1998), Wallis Lake (Smith *et al*. 2000; Smith and Heggie 2003b), Myall Lake (Palmer *et al*. 2000a), Smiths Lake (Smith and Heggie 2003a), Durras Lake (Palmer *et al*. 2000b) and Lake Wollumboola (Murray *et al*. 2003) in south-eastern Australia, and Swan-Canning River (Fredericks *et al*. 2002), and Wilson Inlet (Fredericks and Heggie 2000) in south-western Western Australia. These studies, and others measuring benthic nutrient fluxes (for example Ullmann and Sandstrom 1987; Hansen *et al*. 1987; Alongi 1989a; Alongi 1989b; Alongi 1990; Douglas *et al*. 1996; Eyre and Ferguson 2002), have improved our understanding of nutrient cycling in Australian coastal waterways, especially in respect of nitrogen cycling and the importance of denitrification as a major process controlling eutrophication in wave-dominated estuaries (Heggie *et al*. 1999a; Webster and Harris 2004).

Figure 1-1 is a simplified illustration of organic matter breakdown and nutrient cycling in wave-dominated type estuaries, mainly focusing on the nutrient nitrogen (N). Nutrients in runoff from the catchment can enter an estuary and stimulate plant growth, especially that of phytoplankton and macroalgae. Bacteria subsequently break down these plants when they fall to the lakebed and die. The resulting flux of nutrients to the overlying water from organic matter breakdown is often a major source of nutrients for further plant growth. Also, the process has a significant influence on dissolved oxygen levels, where bacteria will use oxygen during respiration, when available, to oxidise the dead organic material. Therefore, through these linkages, we consider the magnitude of benthic fluxes (this study specifically measured TCO_2, NH_4^+, N_2, SiO_4^{4-} and O_2) to be proportional to the amount of organic matter degrading in the sediments, which in turn is a measure of the levels of nutrient supplied from the catchment and available in the water column.

Excessive plant growth (eutrophication), which is often associated with undesirable consequences such as nuisance algal blooms, seagrass decline, and low dissolved oxygen levels, can occur when there is an oversupply of nutrients. In addition to nutrients arriving from the catchment, the nutrient nitrogen (N) can be released during organic matter breakdown in the sediment as ammonium (NH_4^+), which is readily transferred into nitrate via nitrification and subsequently available for plant growth. Denitrification is an important control on eutrophication because this process of organic matter breakdown releases N as N_2 gas, which can be lost from the system into the atmosphere (Figure 1-1). N can also be lost through water exchange with the ocean and burial. However, sedimentation rates are usually not rapid enough to bury organic material and nutrients before they are remineralised and the restricted entrances of many wave-dominated estuaries along the south-east and south west coasts of Australia limit water exchange with the ocean.

Researchers generally accept that plant growth (primary productivity) in marine ecosystems is N limited (Redfield 1958). Studies have shown denitrification is critical in controlling the amount of N available for plant growth in Australian estuaries, for example, in Port Phillip Bay (Berelson *et al*. 1998; Murray and Parslow 1999). The degree to which denitrification is occurring in the sediments can indicate the susceptibility of an estuary to eutrophication and associated problems such as water quality decline, low dissolved oxygen levels, and nuisance algal blooms.

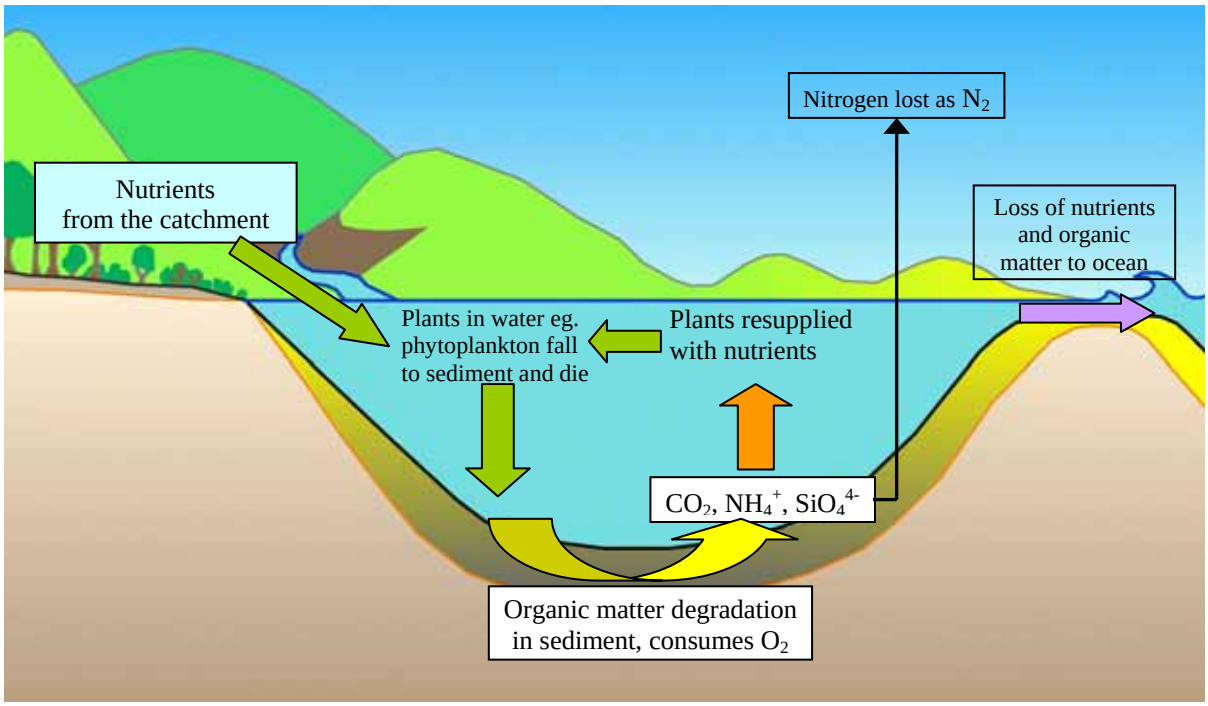

Figure 1-1. Schematic diagram of nutrient cycling in wave-dominated type estuaries. Green arrows show organic matter supply to the sediment, the yellow arrow shows organic matter breakdown (benthic nutrient fluxes), which consumes O_2, and releases TCO_2, SiO_4^{4-}, N_2 and NH_4^+ to the water column, the orange arrow shows re-supply of nutrients to plants, the black arrow shows loss of N through denitrification, and the purple arrow shows loss of nutrients and organic matter to the ocean (this is often limited in wave-dominated estuaries).

Benthic chambers have played an important role in studies of sediment-water interactions in Australia (Heggie *et al.* 1999) and they are the main means by which Geoscience Australia measures benthic nutrient fluxes. Each chamber isolates a volume of water above the sediment. This allows us to measure the rate of exchange (flux) of oxygen, carbon dioxide, nutrients, and any other solutes of interest between the sediment and overlying water by monitoring changes in solute concentrations inside the chamber over time (Berelson *et al.* 1998). The main advantage of benthic chambers over other methods of measuring benthic fluxes, such as core incubations, is that measurements are made under in-situ temperature, pressure, and light conditions, with a minimum of disturbance to the sediment and the organisms living within the sediment. This study used benthic chambers to determine the magnitude of metabolite fluxes across the sediment-water interface at five different sites in St Georges Basin. In addition, we performed core incubations and collected sediment cores to examine aspects of spatial heterogeneity and organic matter source respectively.

During the survey, we also investigated the influence of bioirrigation on measured fluxes. Bioirrigation is the enhanced exchange of solutes resulting from the action of macrofauna, which regularly exchange their burrow water with the overlying water (Aller and Aller 1992). In the absence of bioirrigation, solutes are transported mainly by molecular diffusion, which is driven by the difference in solute concentration between the porewaters and overlying water.

1A. OBJECTIVES

The overarching objectives of this study were to (1) contribute to our growing understanding of nutrient cycling in temperate Australian estuaries and how we can use this knowledge to assist managers achieve better environmental outcomes, and (2) contribute information for underpinning environmentally sustainable management of St Georges Basin.

More specifically, the study aimed to:

1. characterise and compare the sediment-water interactions at a selection of sites across St Georges Basin, regarding the:
    - magnitude of total carbon dioxide (TCO_2), oxygen (O_2), ammonium (NH_4^+), silicate (SiO_4^{4-}), and nitrogen gas (N_2) fluxes;
    - denitrification efficiencies;
    - dominant organic matter source to the sediments;
    - ratio of aerobic to anaerobic respiration; and
    - influence of bioirrigation on the magnitude of benthic nutrient fluxes.
2. assess the susceptibility of St Georges Basin to increased nutrient loads from the catchment based on the magnitude of fluxes, degree of anaerobic respiration, and denitrification efficiencies, and compare these to other wave-dominated, temperate Australian estuaries.

In order to achieve these objectives, we measured the consumption of dissolved oxygen (DO), and the flux of carbon dioxide (TCO_2), ammonium (NH_4^+), nitrogen gas (N_2), and silicate (SiO_4^{4-}) from the sediments into the water column. We also calculated the relative proportion of N released as plant-available NH_4^+ to non-plant available N_2 (denitrification efficiency), which is an indicator of the potential for eutrophication. We investigated the source of organic matter through comparing the stoiciometries of TCO_2, total N, and SiO_4^{4-} fluxes, and determining the Chl-a and carbon isotopic composition (δ^{13}C-TOC) of organic matter in the sediment. Measuring sediment total organic carbon, (TOC) indicated the amount of organic matter supply to the sediment.

1B. THE STUDY AREA

St Georges Basin is about 150 km south of Sydney, situated immediately southwest of Jervis Bay (Figure 1-2). The basin covers an area of approximately 42 km^2 and has a catchment area of 348 km^2. Wandandian Creek and Tomorong Creek are the main tributaries, draining 46% and 13% of the total catchment respectively. Most land clearing has occurred along Wandandian and Tomorong Creeks for grazing purposes and along the northern shores of the basin and the eastern side of Sussex Inlet for residential uses. The western, southern and eastern foreshores are largely unmodified, and the fringing native vegetation contributes significantly to the high visual amenity of the basin. Small towns located along the northern shore include Basin View, St Georges Basin, Pelican Point, Sanctuary Point, and Erowal Bay. The town of Sussex Inlet is built on the western shore of the narrow channel linking the basin to the ocean. The township incorporates a large canal development, the initial stages of which were constructed in the 1950s.

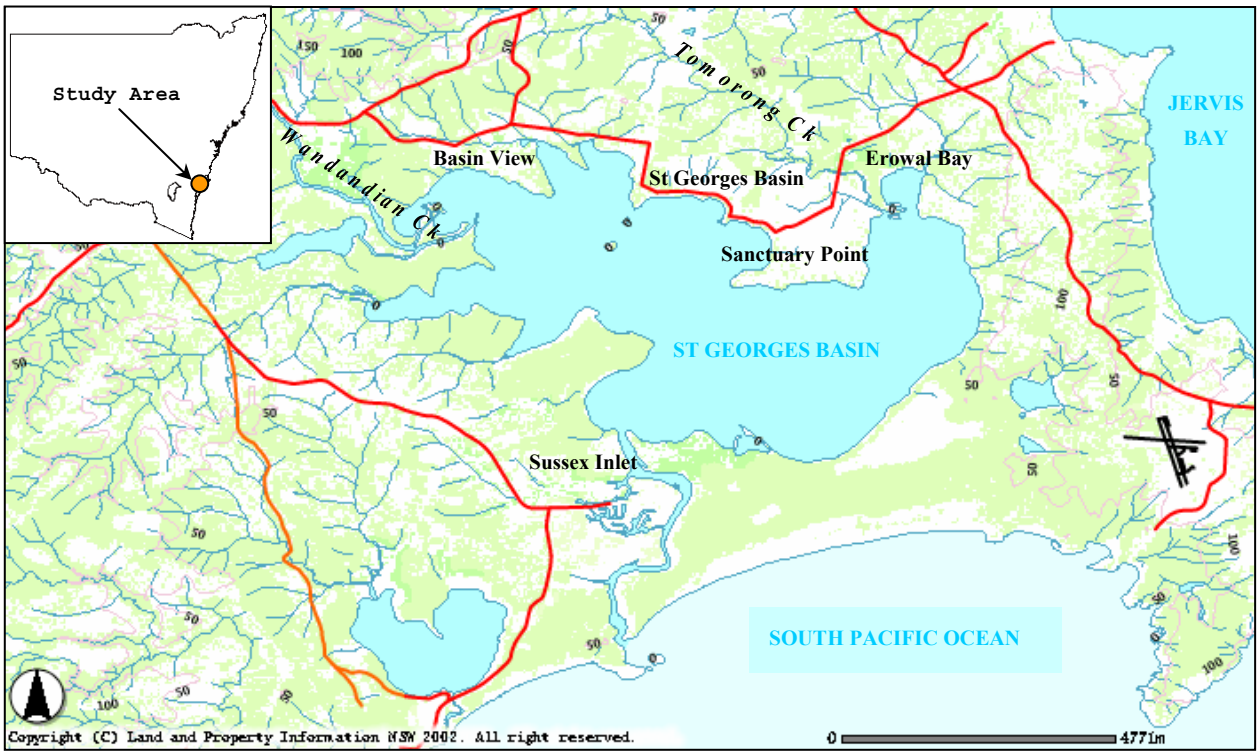

Figure 1-2. Map of St Georges Basin showing surrounding towns and waterways, and the location of St Georges Basin on the New South Wales south coast (inset map). Vegetated areas are green, and cleared and urban areas white. Base map source: NSW Land and Property Information.

The residential population around the shores of St Georges Basin is estimated at 15 000. However, this is set to increase along with expanding urban development. The area is also a popular holiday destination and the focus for recreational activities such as fishing, sailing, water skiing, bushwalking and sightseeing.

The basin incorporates a wide variety of sedimentary habitats (Figure 1-3). These are typical of wave-dominated type estuaries (See OzEstuaries Website www.ozestuaries.org "Query Database" section for sizes of each habitat type, and see "Conceptual Models" section for more information on wave-dominated estuaries and other estuary types) and comprise a relatively small flood and ebb-tide delta, small areas of mangrove, saltmarsh, and intertidal flats and a relatively large fluvial delta, central basin, and sandy barrier separating the estuary from the ocean. Freshwater wetlands also exist around the western and northern fringes of the basin.

The basin is permanently open to the ocean; however, the entrance (Sussex Inlet) is long and narrow, restricting water exchange. It takes approximately 80 days to exchange a volume equal to that of the Basin (235 000 ML) with the ocean (Shoalhaven City Council 1998, p 3.2.7). The central basin is relatively large and deep (up to 10 m; Figure 1-4) compared to most other lakes and lagoons on the NSW south coast. The basin margins and embayments are shallow (3m – 7m).

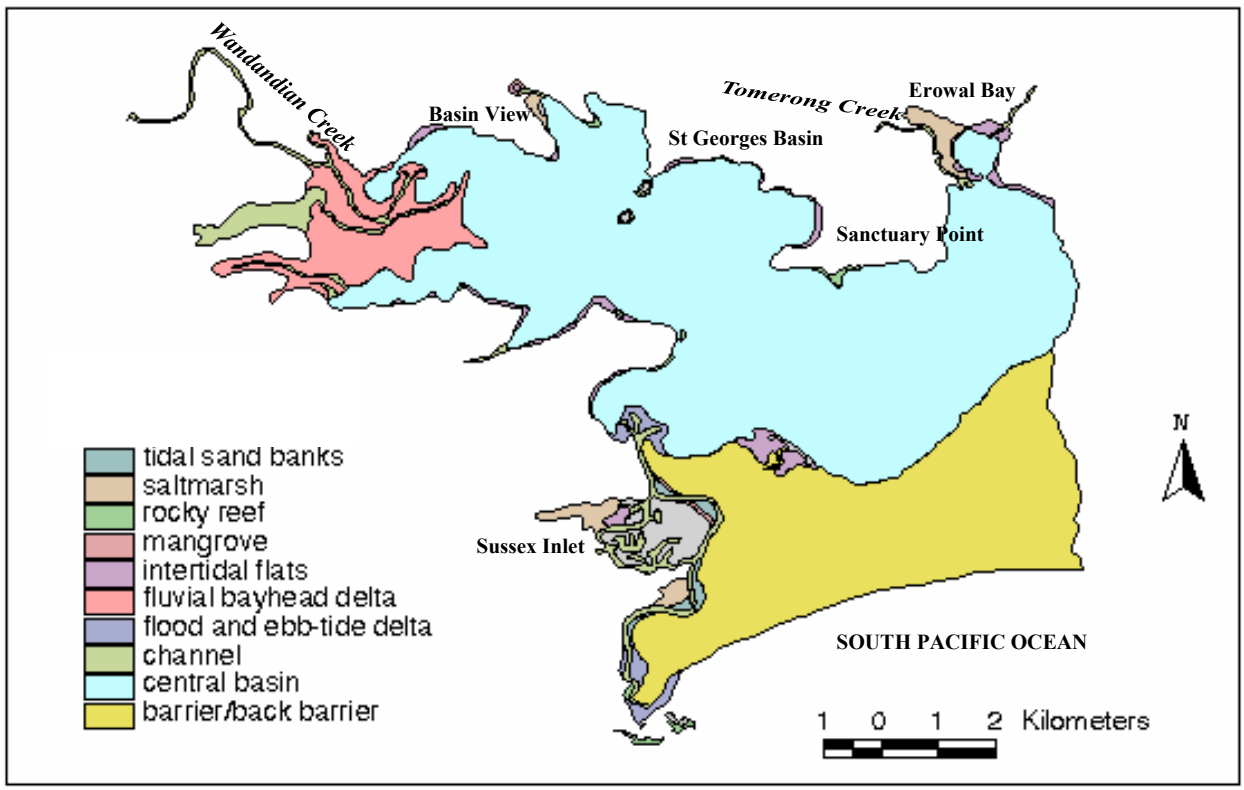

Figure 1-3. Sedimentary habitats of St Georges Basin mapped during the National Land and Water Resources Audit (NLWRA 2001).

Seagrass communities made up of *Posidonia australis*, *Zostera* spp., *Ruppia* spp., and *Halophila* spp occupy shallow areas around the margins of the basin and are valuable habitat for fish and other animals. Current seagrass cover is approximately 292 ha (Figure 1-4). Meehan (2001), using historic aerial photographs, showed that seagrass area in the basin has decreased by 23% since 1961. Seagrass communities growing along the northern shore experienced the largest declines, with complete loss of seagrass from shallow water shoals in the bay west of Sanctuary Point. A change in species composition was also evident, where *Posidonia australis* had the largest declines, and *Zostera* spp., *Halophila* spp., and *Ruppia* spp. actually increased in some areas. *Ruppia* spp. increased sevenfold in Erowal Bay. Higher nutrient levels and freshwater runoff are possible causes for these changes, as a number of studies (Lukatelich *et al.* 1987; Geddes 1987) have correlated *Ruppia* spp. increases and *P. australis* decreases with increasing nutrient and freshwater input (Meehan 2001).

To date, the basin has had no serious water quality problems. However, there have been cases of localised water quality deterioration in the lake and high faecal coliform and low dissolved oxygen levels in tributaries (Shoalhaven City Council 1998, p3.2.3). A CSIRO study conducted between 1974 and 1978, and reported in the St Georges Basin Estuary Management Plan (Shoalhaven City Council 1998, p3.2.4), measured elevated levels of total phosphorus (TP) and total nitrogen (TN) in the sediments. A more recent study by the Shoalhaven City Council in 1998 measured lower TP and TN concentrations at comparable sites to the CSIRO study. The reason for this drop in levels is likely the progressive elimination of septic sewerage systems from around the basin since construction of a sewerage reticulation system (Shoalhaven City Council 1998, p3.2.4).

Infestations of the invasive seaweed *Caulerpa taxifolia* were recently (April 2004) discovered in the basin (Martin Bergs, Shoalhaven City Council, Pers Comm, June 2004). At present, outbreaks are mainly restricted to the Basin View area. *Caulerpa taxifolia* spreads easily and can overrun seagrasses and alter marine habitats. The NSW government lists it as *noxious marine vegetation*. The weed has established and spread throughout several coastal waterways in NSW, including the nearby Burrill Lake and Lake Conjola. NSW Fisheries is currently attempting to eradicate it from St Georges Basin.

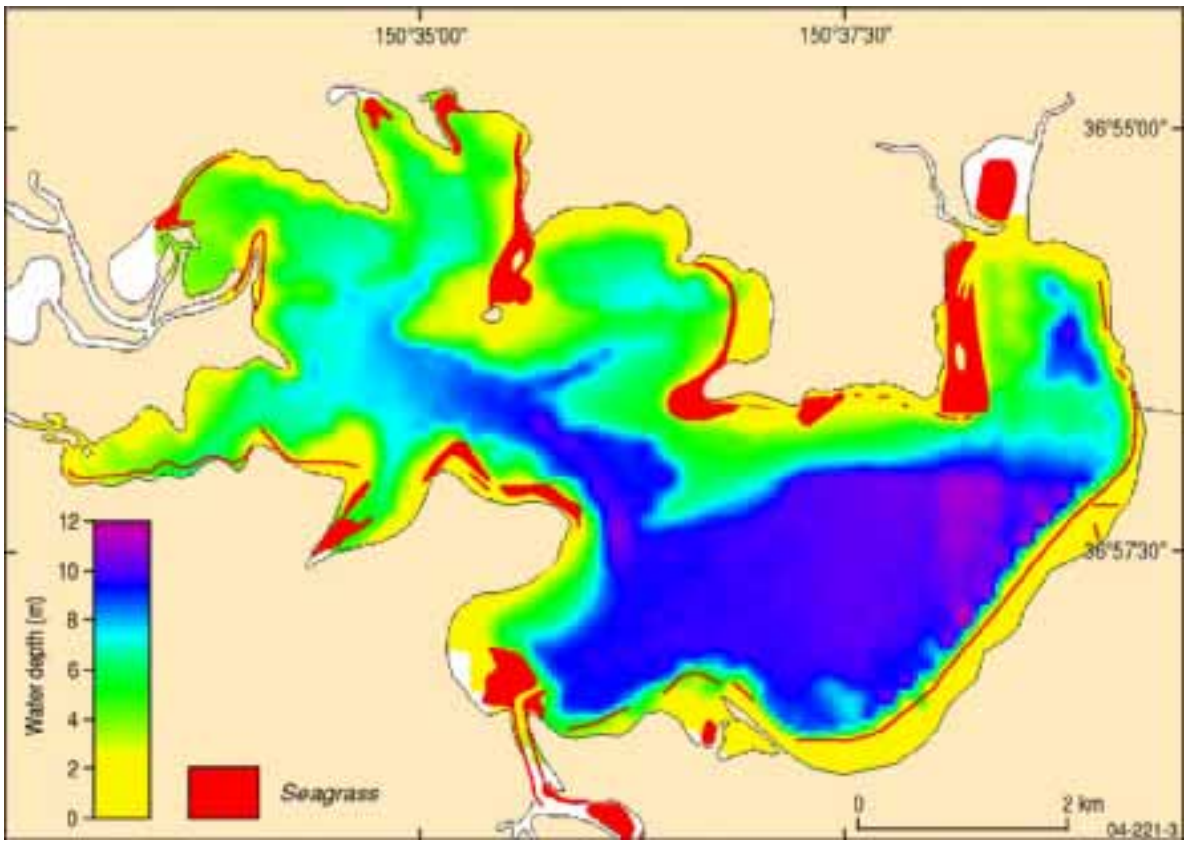

Figure 1-4. Bathymetry (from DLWC 2000) and current seagrass distribution (from Meehan 2001) for St Georges Basin.

2. METHODS

2A. SAMPLING STRATEGY

We sampled five sites within St Georges Basin (Figure 2-1). Site selection aimed to capture the variability of nutrient loads from different sub-catchments surrounding the basin (Table 2-1). For example, Erowal Bay (Site 2) is a semi-enclosed bay with limited water exchange with the rest of the basin, and potentially high nutrient loads from urban runoff; whereas Site 4 (One Tree Bay) has a relatively well-vegetated and undeveloped catchment and probably less nutrient input than Erowal Bay. Sites 2, 3, 4, and 5 were around the edge of the basin in shallow water (less than 3 m deep), and Site 1 was in the deep central basin (10 m deep; Figure 2-1 and Figure 1-4).

Figure 2-1. False colour Landsat image showing the five sample sites in St Georges Basin. Site 1 – Central Basin, Site 2 – Erowal Bay, Site 3 – Wandandian Creek, Site 4 – One Tree Bay, and Site 5 – Pat's Bay. Densely vegetated areas are green. The urban areas on the northern side of the basin and around Sussex Inlet are indicated by white to pink, and cleared and naturally occurring less densely-vegetated areas are pink.

Site 1 was chosen to represent conditions in the deep central basin (Figure 2-1; Figure 1-3). This sedimentary environment encompasses most of the estuary and is characterised by relatively deep water (5-10 m; Figure 1-4) and muddy sediments. We expect the central basin site receives inputs from all surrounding catchments, whereas the other sites receive more localised inputs from their respective catchments. Site 2 was in Erowal Bay, a shallow (1-2 m deep) bay with a narrow entrance linking it to the rest of the basin (Figure 2-1). Sediment at this site was fine, black, organic-rich muds. Site 3 was at the entrance to Wandandian Creek, which is the major tributary entering the basin. This site had sticky, clayey sediments characteristic of a fluvial bayhead delta (Figure 1-3). Site 4 was in One Tree Bay, a small bay on the relatively undeveloped and well-vegetated southern side of the basin (Figure 2-1). Sediments here were organic-rich muds. Site 5 was in Pat's Bay, which is relatively open to the rest of the basin and subject to some urban runoff from the township of St Georges Basin.

Table 2-1. Sample site location and character.

Site	Latitude	Longitude	Depth	Comments
Site 1 Central Basin	35°07.620'S	150°38.477'E	9.8 m	Deep central basin, muddy, black, organic-rich sediments
Site 2 Erowal Bay	35°06.006'S	150°38.739'E	1.6 m	Limited water exchange with rest of basin, subject to (relatively nutrient rich?) urban runoff, muddy, black, organic-rich sediments
Site 3 Wandandian Ck	35°06.017'S	150°33.419'E	1.6 m	Entrance to main watercourse entering basin, relatively well vegetated catchment, clayey, brown-black, organic-rich sediments
Site 4 One Tree Bay	35°07.659'S	150°34.399'E	2.0 m	Relatively undeveloped/well vegetated catchment, apparently less nutrient loading than all other sites, muddy, black, organic-rich sediments
Site 5 Pat's Bay	35°05.445'S	150°34.756'E	2.2 m	Subject to urban (relatively nutrient rich?) runoff, good water exchange with rest of the basin, muddy, black, organic-rich sediments

2B. SAMPLE COLLECTION

2B1. Benthic Chambers

We determined metabolite fluxes at the sediment-water interface by measuring the change (either positive or negative) in metabolite concentrations over time inside each benthic chamber according to the methods of Berelson *et al*. (1998). Five *manually* sampled chambers (Figure 2-2) were deployed at each of the four shallow water sites (Sites 2, 3, 4, and 5), and two *automatically* sampled chambers (Figure 2-3) at the deep central basin site (Site 1; Table 2-2). Four chambers at each of the shallow water sites, and one at the deep-water site, were blacked out to stop sunlight entering (dark chambers), and one chamber at each site was transparent to sunlight (light chamber; Table 2-2). Dark chambers recorded oxygen consumption and nutrient release from respiration processes, whereas light chambers recorded *net* oxygen flux (production minus consumption) and nutrient release from both respiration and photosynthesis.

Timing of sample draws from each chamber involved: an initial water sample representing ambient conditions (bottom water) taken immediately before lid closure; a sample draw taken 30 min after lid closure; then, a sample drawn every 1.5 to 2 hours, with the last sample taken 6 to 7 hours after lid closure. Sample draws from each chamber were analysed for carbon dioxide (TCO_2), ammonium (NH_4^+), nitrogen gas (N_2), pH, alkalinity, caesium chloride (CsCl), and silicate (SiO_4^{4-}). TCO_2 concentrations were calculated using the alkalinity and pH measurements. YSI data loggers recorded dissolved oxygen (DO) concentrations, salinity, and temperature both inside and outside each chamber. Appendix 1 details chamber specifications, as well as sample draw, CsCl spike, sample handling, and sub-sampling procedures. Appendix 4 outlines the analytical methods used to measure each parameter and Appendix 5 explains how benthic fluxes and denitrification efficiencies were calculated from the raw benthic chamber data. Appendix 5 also outlines the diffusion and irrigation models used to determine irrigation rates in the sediment.

Table 2-2. Number and type of chambers deployed, and metabolites measured at each site.

Site	Chamber Type	No. of Chambers	Parameters Measured
Site 1 Central Basin	Automatic	1 Light 1 Dark	O_2, TCO_2, NH_4^+, N_2, SiO_4^{4-}, Alkalinity, pH, Cs
Site 2 Erowal Bay	Manual	1 Light 4 Dark	O_2, TCO_2, NH_4^+, N_2, SiO_4^{4-}, Alkalinity, pH, Cs
Site 3 Wandandian Ck	Manual	1 Light 4 Dark	O_2, TCO_2, NH_4^+, N_2, SiO_4^{4-}, Alkalinity, pH, Cs
Site 4 One Tree Bay	Manual	1 Light 4 Dark	O_2, TCO_2, NH_4^+, N_2, SiO_4^{4-}, Alkalinity, pH, Cs
Site 5 Pat's Bay	Manual	1 Light 4 Dark	O_2, TCO_2, NH_4^+, N_2, SiO_4^{4-}, Alkalinity, pH, Cs

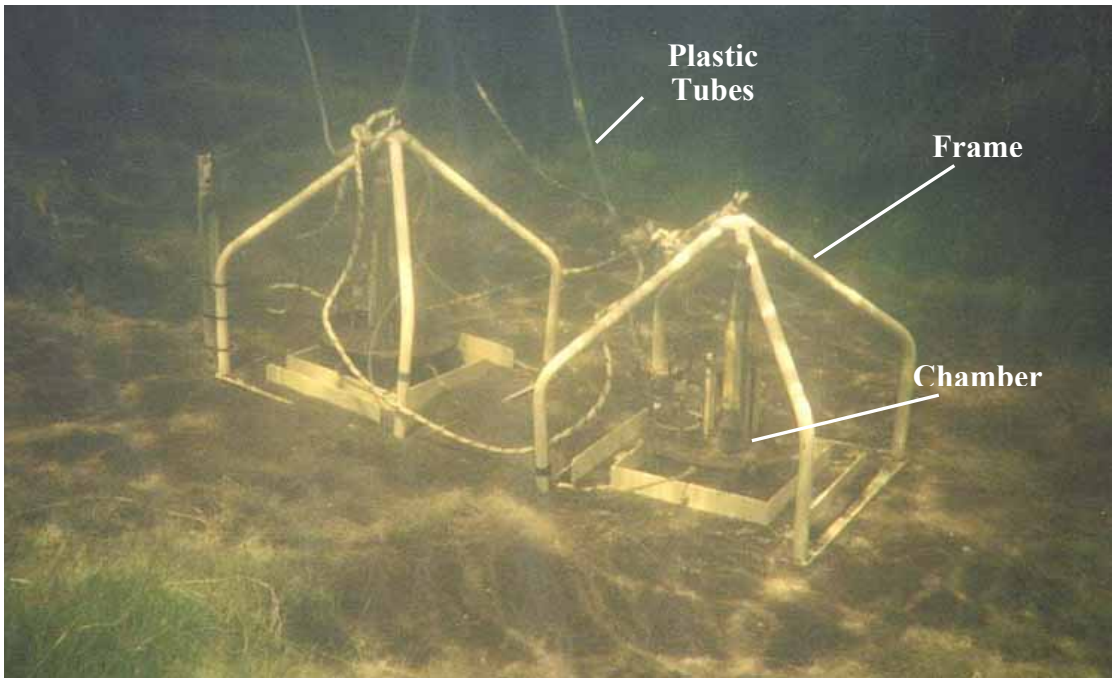

Figure 2-2. Manually sampled benthic chambers deployed on the bottom of an estuary. We drew water samples from within each chamber through the plastic tubes.

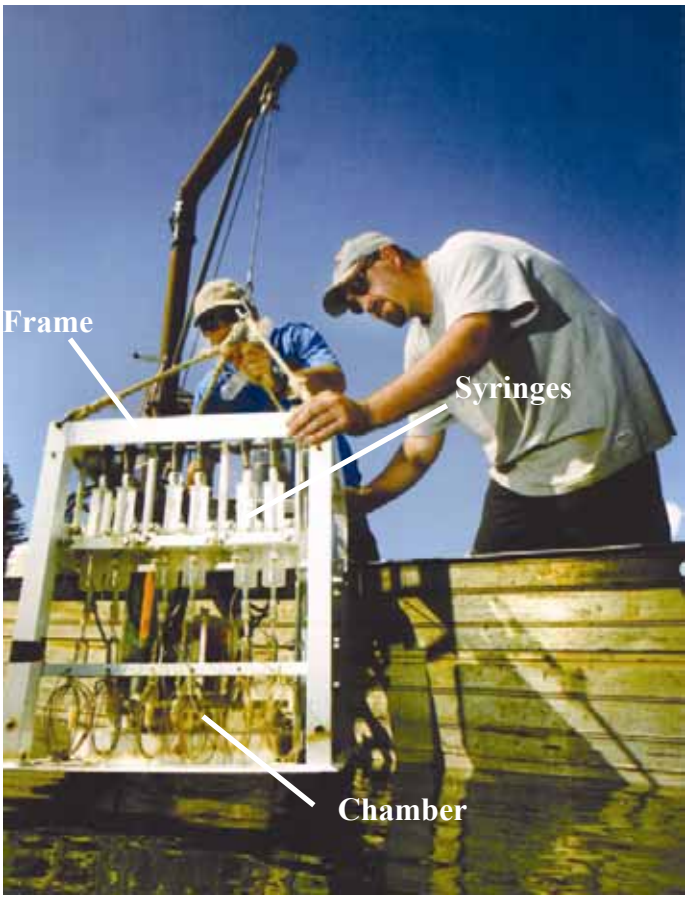

Figure 2-3. Deploying an automatically sampled chamber. Spring-loaded syringes are arranged around the chamber and supported by the frame. (Photo: Newcastle Herald).

2B2. Water Column Conditions

Water column temperature, salinity and DO were measured at the top, middle and bottom of the water column using a YSI probe. We did this at around midday on the same day benthic chamber experiments were undertaken at each site.

2B3. Sediment Cores

Two closely spaced sediment cores were collected at each site for porewater and sediment analysis. We collected these cores using a manually operated corer, which we pushed into the soft sediment using a long pole (pole corer; Figure 2-4). Cores were sliced into depth intervals and centrifuged to separate porewaters from the solid phase. Porewaters were analysed for PO_4^{3-}, NO_3^-, NO_2^-, NH_4^+, SiO_4^{4-}, TCO_2, and Chlorophyll a (Chl-a). TCO_2 was measured by means of conductivity as outlined in Appendix 4.

The solid phase was analysed for total organic carbon (TOC), major oxides, and nitrogen and carbon stable isotopes. We also measured the sediment porosity of each depth interval.

Appendix 3 gives more detail on core collection and sample handling, and Appendix 4 outlines the analytical methods used to measure each metabolite. details how diffusive fluxes were calculated from the raw down core metabolite data

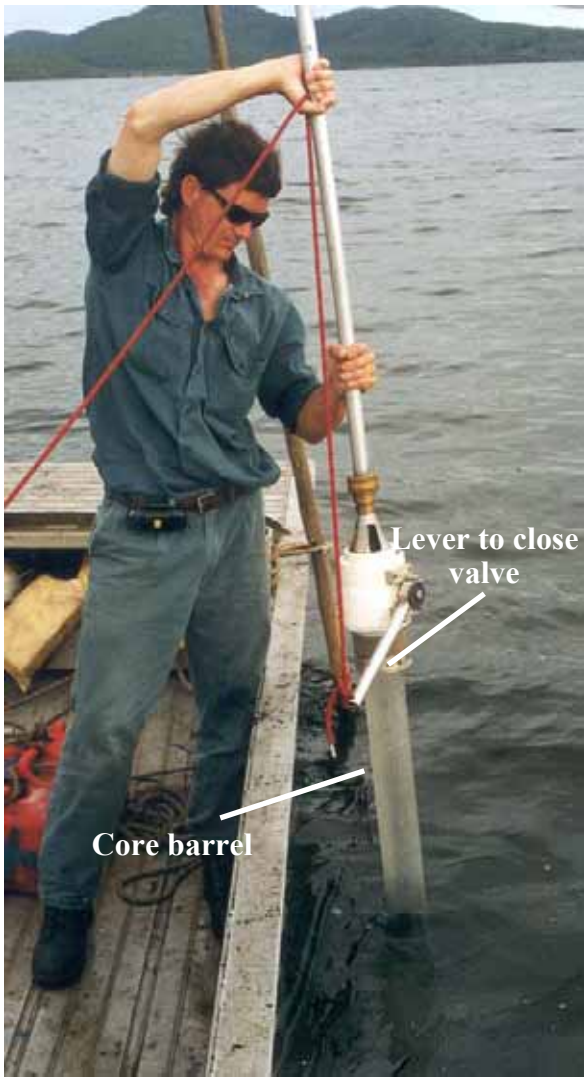

Figure 2-4. An operator about to collect a sediment core using a pole corer.

2B4. Core Incubations

For core incubation experiments, we collected three closely spaced sediment cores of about 200 mm depth from each site. These were obtained using the same pole-coring system referred to in Section 2B3. Core incubations proceeded in darkness and at in-situ temperature (20 ± 1 °C) for approximately 24 hours using the set up in Figure 2-5. Bottom water

samples for nutrients (SiO_4^{4-}, NO_2^-, NO_3^-, NH_4^+, PO_4^{3-}), alkalinity, pH, and TCO_2 were collected at the beginning (t_0) and end (12 - 24 h = t_1) of each incubation. YSI probes measured DO in the bottom water at t_0 and t_1.

We incubated three replicate cores from each site to determine the reproducibility of each flux estimate.

Appendix 3 gives more detail on the core incubation procedure and sample handling, and Appendix 4 outlines the analytical methods used to determine each metabolite. Appendix 5 explains how benthic fluxes were calculated from the raw core incubation results.

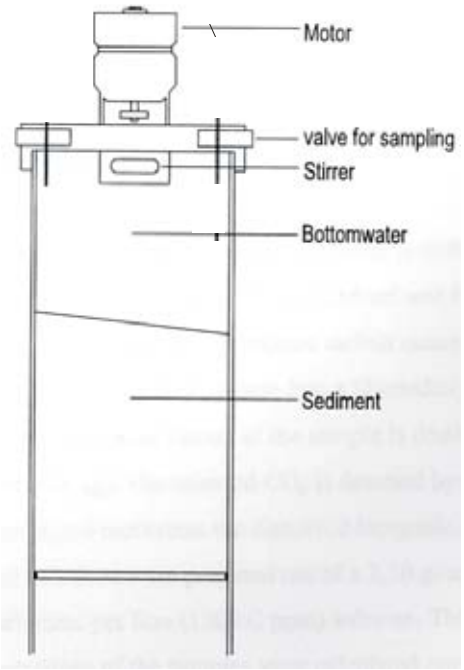

Figure 2-5. Core incubation experimental set up for the determination of total fluxes across the sediment-water interface.

.

3. RESULTS

3A. WATER COLUMN CONDITIONS

Table 3-1 lists the temperature, salinity and dissolved oxygen (DO) measured at the top, middle, and bottom of the water column at each of the five sites.

Temperature

The profiles show the water column was well mixed in regard to temperature for all sites, except the central basin site (Site 1), which was more than 1°C lower in bottom waters compared to surface waters. The higher temperatures recorded at Erowal Bay compared to all other sites may result from the shallow, enclosed nature of the bay and its limited exchange with the rest of the basin.

Salinity

The profiles show the water column was well mixed in regard to salinity for all sites. Erowal Bay (Site 2) had the highest salinity. This was probably a consequence of evaporation and limited exchange of water between Erowal Bay and the main basin. Wandandian Ck (Site 3) had the lowest salinity. This is likely a result of fresh water runoff from a heavy rain event that occurred before and during sampling of this site. We had completed sampling of all other sites prior to this rain event.

Dissolved Oxygen

All sites showed lower DO concentrations in bottom waters compared to surface waters except at Pats Bay (Site 5). DO was significantly lower (~10%) in bottom waters relative to surface waters for the Central Basin, Wandandian Creek, and One Tree Bay sites; indicating the water column was poorly mixed and O_2 consumption at the sediment-water interface was greater than could be replenished from the atmosphere or photosynthesis. In addition, surface waters were depleted in oxygen compared to atmospheric equilibrium (100%) at all sites except One Tree Bay (Site 4). Erowal Bay was the most depleted, followed by Wandandian Creek.

Table 3-1. Depth profiles of temperature, salinity, and dissolved oxygen (DO % saturation) measured at each site.

Site	Date	Depth (m)	Temp (°C)	Salinity	DO (%sat)
Site 1	19/11/03	0.5	21.7	31.7	91.8
Central Basin		3.0	20.9	31.7	89.3
		6.3	20.7	31.6	89.5
		9.8	20.4	31.7	80.0
Site 2	21/11/03	0.3	23.6	32.1	83.1
Erowal Bay		1.0	23.5	32.7	81.3
		1.6	23.6	32.8	80.0
Site 3	23/11/03	0.5	20.9	30.2	89.6
Wandandian Ck		1.0	21.1	29.5	82.2
		1.6	21.1	30.8	80.7
Site 4	16/11/03	0.6	21.3	31.1	110.6
One Tree Bay		1.6	21.3	31.1	105.2
		2.0	21.1	31.1	101.3
Site 5	14/11/03	0.4	22.0	31.9	92.1
Pat's Bay		1.3	22.8	31.6	93.8
		2.2	22.4	31.5	92.2

3B. SEDIMENT BIOGEOCHEMISTRY

3B1. Benthic Chambers

All 22 chamber deployments (5 chambers at four sites and 2 chambers at the central basin site) were successful, and we obtained fluxes for all solutes except in three chambers where a YSI probe failed and O_2 was not measured (Table 3-2). The Cs spike failed in two chambers at Site 5. Cs tracer results are described below in *Section 3B4 Tracer Experiments*. Appendix 6 shows plots of TCO_2, O_2, NH_4^+, N_2; alkalinity, and SiO_4^{4-} against time, for all chambers, at all sites. In these plots, linear regression lines incorporate only those points used in flux calculations, that is, those measured during the period of linear O_2 uptake (See Appendix 5: A5a).

Table 3-2 shows solute fluxes measured across the sediment-water interface, calculated from the plots shown in Appendix 6. We calculated the median, mean and coefficient of variance using the dark chamber replicates at each site. We excluded light chamber results from these calculations because additional processes (e.g. photosynthesis) were occurring in these chambers. We treated the Site 1 "light" chamber results the same as for dark chamber results because water depths at Site 1 were 9.8 m and sunlight would not have reached the chambers.

The coefficient of variance gives a measure of the degree of variance as a percentage of the mean. One Tree Bay (Site 4) had the most variable TCO_2, NH_4^+, SiO_4^{4-}, and alkalinity fluxes (not including Site 1, which had high coefficient of variance values because of the low number of replicates). Pat's Bay (Site 5) had the most variable O_2 fluxes and Wandandian Creek (Site 3) had the most variable denitrification efficiencies. Coefficient of variance typically ranged between 15 and 40% for all metabolites at all sites.

O_2 fluxes were negative, in both light and dark chambers at all sites. Light chamber O_2 fluxes were appreciably lower than dark chamber O_2 fluxes at Sites 4 and 5. In contrast, light chamber O_2 fluxes did not differ significantly from dark chamber fluxes at Sites 2 and 3.

To aid site comparisons, the fluxes for dark chambers were plotted as box and whisker diagrams (Figure 3-1). TCO_2, and NH_4^+ fluxes at Sites 2, 5 and 4 were noticeably higher than at Sites 1 and 3 (Figure 3-1 a and c). O_2 consumption was higher at Sites 2, 3, 4, and 5, than at Site 1, in the central basin (Figure 3-1 b). It was difficult to differentiate between sites regarding SiO_4^{4-} fluxes (Figure 3-1 d). However, similarly to TCO_2 and NH_4^+ fluxes, Sites 2, 5, and 4 had higher median SiO_4^{4-} fluxes than Sites 1 and 3.

Denitrification efficiencies (DEs) calculated using equation (1) in Appendix 5: A5b were significantly lower than those calculated using equation (2), for all but two chambers. It appeared that direct N_2 measurements failed to detect a component of the N_2 flux (perhaps due to N_2 fixation). Therefore, we made site comparisons based on DEs calculated using equation (2) (Table 3-2 and Figure 3-1 e). DEs for Site 1 were significantly higher (50-68%) than at Sites 2, 3, 4, and 5, where all DEs were below 53% (Figure 3-1 e).

Comparing SiO_4^{4-} and NH_4^+ fluxes also indicated denitrification. SiO_4^{4-} and NH_4^+ fluxes should be similar if organic matter was degrading at the same rate as silica was released from the dissolution of silicate frustules, and no secondary reaction, such as denitrification was occurring. However, SiO_4^{4-} benthic fluxes always exceeded NH_4^+ benthic fluxes suggesting that some N was released as N_2 instead of NH_4^+.

Table 3-2. Benthic fluxes for all chambers, at all sites, in mmol m^{-2} day^{-1}. Light chamber results were excluded from median and coefficient of variance calculations. Denitrification Efficiency (DE %) is the percentage of total inorganic nitrogen recycled as N_2, calculated using equation (2) in Appendix 5: A5b. Negative fluxes (e.g. for O_2) indicate consumption, whereas positive fluxes indicate production. Cells marked with (-) indicate where O_2 was not measured due to YSI probe failure. Error = Standard Error.

Site	Chamber Type	Chamber ID	TCO_2	Error	O_2	Error	NH_4^+	Error	SiO_4^{4-}	Error	Alk	Error	N_2	Error	DE %
Site 1 Central Basin	Dark	1	30.7	3.0	-33.7	0.3	2.3	3.0	4.9	3.0	6.7	2.3	-0.3	5.0	49.5
	Light	2	77.3	9.2	-	0.3	3.7	0.4	10.7	0.2	34.9	5.0	2.6	3.1	68.3
Median			**54.0**		**-33.7**		**3.0**		**7.8**		**20.8**		**1.2**		**58.9**
Mean			**54.0**		**-33.7**		**3.0**		**7.8**		**20.8**		**1.1**		**58.9**
Coefficient of Variance			**61.1**		**-**		**31.9**		**52.5**		**96.0**		**184.9**		**22.6**
Site 2 Erowal Bay	Dark	3	94.3	7.6	-	-	7.3	0.2	13.1	0.4	45.5	4.2	-1.1	0.4	48.8
	Dark	4	95.6	17.3	-71.4	0.6	8.3	0.4	11.2	0.6	36.0	17.0	0.2	0.5	42.2
	Dark	7	89.5	11.3	-57.2	0.1	6.3	0.2	6.7	0.1	35.6	11.5	1.2	0.2	53.1
	Dark	8	63.3	6.4	-60.3	0.6	6.7	0.3	12.1	0.6	17.3	6.1	1.0	0.3	30.3
	Light	9	140.9	4.6	-69.9	0.5	10.0	0.7	16.1	0.4	76.2	7.4	0.2	0.1	53.0
Median			**91.9**		**-60.3**		**7.0**		**11.7**		**35.8**		**0.6**		**45.5**
Mean			**85.7**		**-63.4**		**7.2**		**10.8**		**33.6**		**0.3**		**43.6**
Coefficient of Variance			**17.7**		**11.8**		**12.4**		**26.4**		**35.1**		**324.4**		**22.8**
Site 3 Wandandian Ck	Dark	3	72.2	1.5	-70.8	0.5	5.2	0.8	11.4	0.0	24.4	1.0	0.8	0.2	52.5
	Dark	4	61.4	2.6	-54.5	0.3	5.0	0.1	9.1	0.1	22.6	2.0	0.0	0.0	45.6
	Dark	7	39.3	2.6	-49.0	0.5	4.1	0.3	7.3	0.2	2.3	4.1	1.2	0.3	30.1
	Dark	8	57.0	2.6	-	-	6.6	0.1	10.6	0.2	17.0	1.6	1.7	0.4	23.3
	Light	9	70.9	6.4	-68.6	0.4	7.6	1.0	11.7	0.5	17.7	7.4	0.4	0.9	29.3
Median			**59.2**		**-54.5**		**5.1**		**9.9**		**19.8**		**1.0**		**37.9**
Mean			**57.5**		**-58.5**		**5.2**		**9.6**		**16.6**		**0.9**		**37.9**
Coefficient of Variance			**23.8**		**19.4**		**19.4**		**18.7**		**60.4**		**77.5**		**35.7**
Site 4 One Tree Bay	Dark	3	53.7	4.3	-57.1	0.5	4.6	0.1	7.3	0.3	1.6	2.4	2.2	0.3	42.7
	Dark	4	108.0	2.6	-79.3	0.4	10.8	0.3	16.9	0.7	41.6	4.6	0.7	0.2	33.8
	Dark	7	58.6	1.2	-73.3	0.6	6.9	0.1	13.9	1.2	20.2	4.2	2.0	0.2	22.5
	Dark	8	116.8	2.7	-63.1	0.5	11.1	0.5	18.1	1.2	60.4	2.9	0.5	0.1	37.1
	Light	9	73.2	6.5	-45.6	0.2	5.3	0.2	5.9	0.2	29.9	2.7	3.6	0.4	52.5
Median			**83.3**		**-68.2**		**8.9**		**15.4**		**30.9**		**1.4**		**35.5**
Mean			**84.3**		**-68.2**		**8.3**		**14.1**		**31.0**		**1.3**		**34.0**
Coefficient of Variance			**38.9**		**14.4**		**37.5**		**34.4**		**82.5**		**64.6**		**25.1**
Site 5 Pat's Bay	Dark	3	93.2	0.2	-76.0	0.8	7.8	0.3	12.1	0.3	19.1	4.2	2.7	1.2	44.7
	Dark	4	81.5	2.5	-58.9	0.3	8.3	0.1	13.5	0.3	39.0	4.2	0.6	0.0	32.4
	Dark	7	74.1	3.8	-49.5	0.5	7.2	0.2	11.0	0.2	21.4	4.3	1.4	0.3	35.7
	Dark	8	61.3	6.2	-40.3	0.2	5.6	0.2	11.7	0.2	24.2	5.5	0.2	0.0	39.6
	Light	9	33.5	25.0	-25.9	0.3	3.1	0.4	12.8	0.4	11.3	0.9	1.7	1.2	38.6
Median			**77.8**		**-54.2**		**7.5**		**11.9**		**22.8**		**1.0**		**37.7**
Mean			**77.5**		**-56.2**		**7.2**		**12.1**		**25.9**		**1.2**		**38.1**
Coefficient of Variance			**17.3**		**27.2**		**16.4**		**8.6**		**34.5**		**89.6**		**13.9**

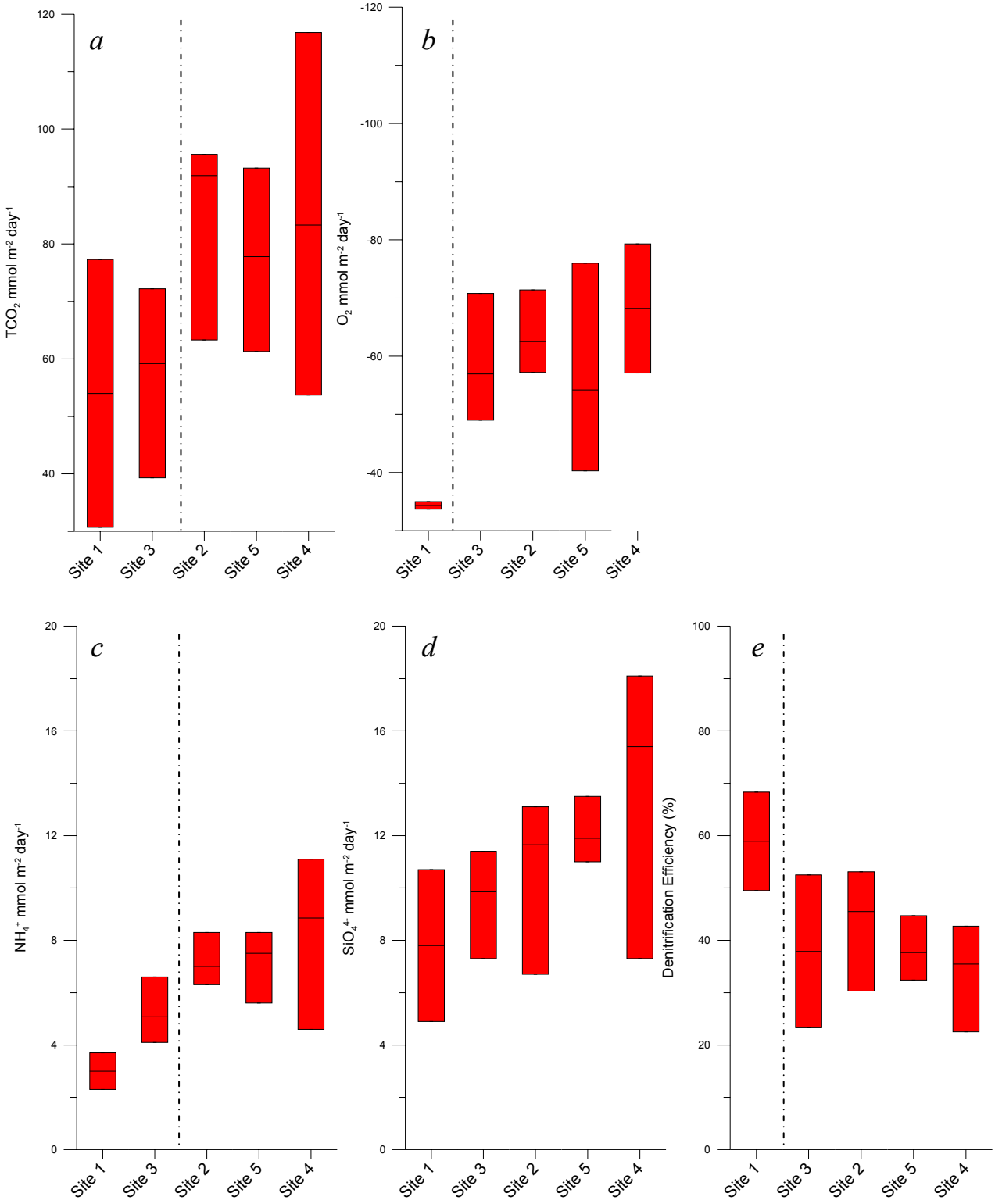

Figure 3-1. Box and whisker diagrams showing the range of (a) TCO_2, (b) O_2, (c) NH_4^+, and (d) SiO_4^{4-} fluxes, and (e) denitrification efficiencies measured using dark benthic chambers and shown in Table 3-2. The median is the horizontal line within the boxes, the bottom end of each box is the 25th percentile, and the top end is the 75th percentile. The dashed lines in (a), (b), (c), and (e) separate distinct groupings of sites. Denitrification efficiency, the percentage of total inorganic nitrogen recycled as N_2, was calculated using equation (2) in Appendix 5: A5b.

3B2. Core Incubations

Figure 3-2 shows the benthic fluxes derived from core incubations. Note that TCO_2 and O_2 fluxes were plotted using the left-hand y-axis, and NH_4^+ and SiO_4^{4-} fluxes were plotted using the right-hand y-axis. The left and right y-axes are scaled according to Redfield ratio (7C : 1N : 1Si), so that bars for TCO_2, O_2, NH_4^+, and SiO_4^{4-} will be at the same height, if diatoms degraded as a whole, that is, silicate frustules and biomass decomposed at the same rate, and if there were no secondary reactions, for example, denitrification.

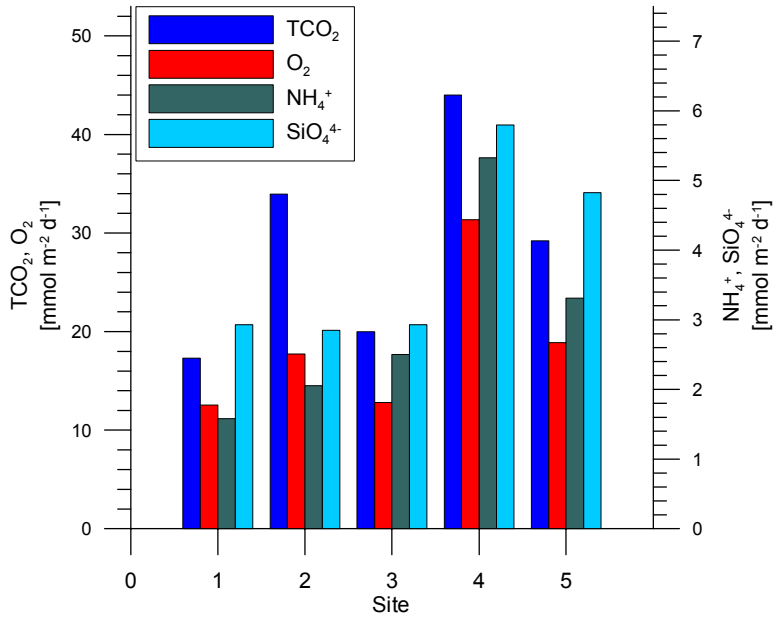

Figure 3-2. Comparison of average (n=3) benthic nutrient and gas fluxes for TCO_2, O_2, NH_4^+, and SiO_4^{4-} for each site. Note that NH_4^+, SiO_4^{4-}, and TCO_2 were fluxing out of the sediment, whereas O_2 was fluxing into the sediment. TCO_2 was determined by alkalinity titrations for Sites 1, 2, and 3, and by means of conductivity for Sites 4 and 5.

Sites 1 and 3 had the lowest TCO_2, O_2, NH_4^+, and SiO_4^{4-} fluxes and also similar bar heights, suggesting near-congruent decomposition of diatoms. However, for these and all other sites, SiO_4^{4-} and TCO_2 fluxes exceeded the NH_4^+ flux; indicating that other reactions were imposed, for example, denitrification, carbonate dissolution or decoupled decomposition of organic matter and frustules. A flux ratio of $1TCO_2 : -1.3O_2$ is expected for aerobic respiration in coastal and estuarine sediments. However, TCO_2 fluxes significantly exceeded this ratio; indicating that anaerobic degradation pathways were playing a major role.

3B3. Sediment Cores: Solid Phase and Pore Waters

Appendix 7 shows down core solid phase and pore water data. All sediments were muddy with porosities of about 90%, except Site 3, which had porosities closer to 80%. Average total organic carbon concentrations (TOC) varied between 5.0 wt% (Site 3) and 9.8 wt% (Site 4). Surface sediment TOC concentrations from lowest to highest were: Site 3 (5.5 wt%) > Site 1 (7.4 wt%) > Site 5 (7.8 wt%) > Site 2 (8.1 wt%) > Site 4 (10.5 wt%).

Distinct differences in the carbon isotopic composition of the TOC, δ^{13}C-TOC, were observed. Site 3 had the lowest value of -21‰, wherea sites 4, 5, and 2 had values close to -18‰. Site 1 had an intermediate δ^{13}C-TOC of -19‰ (Appendix 7).

Sedimentary chlorophyll-a (Chl-a) represents a highly reactive fraction of TOC that decomposes rapidly, ($t_{1/2} \approx 10$ d, Sun *et al.*1994) and is readily mixed downward into the sediments by bioturbation (Boon and Duineveld 1998). Therefore, elevated concentrations of Chl-a relative to background values, at several centimetres depth, indicates the presence of bioturbation. All sites had elevated Chl-a concentrations relative to background values down to at least 10 cm. Site 4 had the highest Chl-a concentrations at 10 cm depth (Appendix 7).

It has been suggested that the Chl-a inventory, that is, the total mass of excess Chl-a in surface sediments, can quantify the flux of organic matter to the sediment (Boon *et al*. 1998). In St. Georges Basin, Chl-a inventories were highly variable, with Site 4 (38.1µg cm^{-2}) > Site 5 (22.3µg cm^{-2}) > Site 2 (17.6µg cm^{-2}) > Site 3 (16.0µg cm^{-2}) > Site 1 (6.8µg cm^{-2}) (Appendix 7).

Table 3-3. Surface sediment properties: porosity, TOC concentration, and carbon isotopic composition in the top 0.5 cm of sediment, and chlorophyll-a content per volume of 1 cm^2 x 12 cm.

	Site 1	Site 2	Site 3	Site 4	Site 5
Porosity (%)	91	92	86	93	93
TOC (wt. %)	7.37	8.08	5.5	10.56	7.82
δ^{13}C-TOC (‰ PDB)	-19.15	-18.3	-21.35	-17.78	-17.91
Chl-a [µg/12cm^3]	6.8	17.6	16.0	38.1	22.3

Appendix 7 shows porewater concentration profiles for all sites. The concentration gradient between the bottom water and surface sediment porewaters gave an estimate of molecular diffusion at the sediment-water interface (See Appendix 5: A5c). Table 4-1 in the Discussion lists the diffusive fluxes for all sites.

Replicate pore water concentration profiles were typically very similar, except for Site 4, where replicates of TCO_2 and NH_4^+ profiles significantly deviated from each other for depths below about 3 cm. The steepest concentration gradients for pore water TCO_2 and all nutrients except for NO_3^- were typically at the sediment-water interface. These increasingly flattened with depth (Appendix 7).

NO_3^- was only present in (sub)micromolar concentrations and depth profiles revealed significant scatter. In some cases, however, a subsurface maximum was identified, for example, core 1 of Site 2 and core 2 of Site 4 (Appendix 7).

SiO_4^{4-} concentration gradients always exceeded NH_4^+ gradients (Appendix 7) indicating some N was released as N_2 (through denitrification) instead of NH_4^+. SiO_4^{4-} and NH_4^+ fluxes should be identical if organic matter was degrading at the same rate as silica was released from the dissolution of silicate frustules, and no secondary reaction, such as denitrification was occurring.

3B4. Tracer Experiments

Figure 3-3 illustrates the rate of tracer loss and the loss predicted from diffusion at each of the 5 sites in St Georges Basin. All tracer concentrations are expressed as fractions (C/C_0) of the initial concentration at time t_0. The initial concentration of Cs in the chamber (C_0) was determined by extrapolating the Cs concentration in the chamber back to time (t_0). It is clear from Figure 3-3 that at all sites the rate of Cs loss was greater than predicted from diffusion. We therefore concluded that bioirrigation was active at all sites.

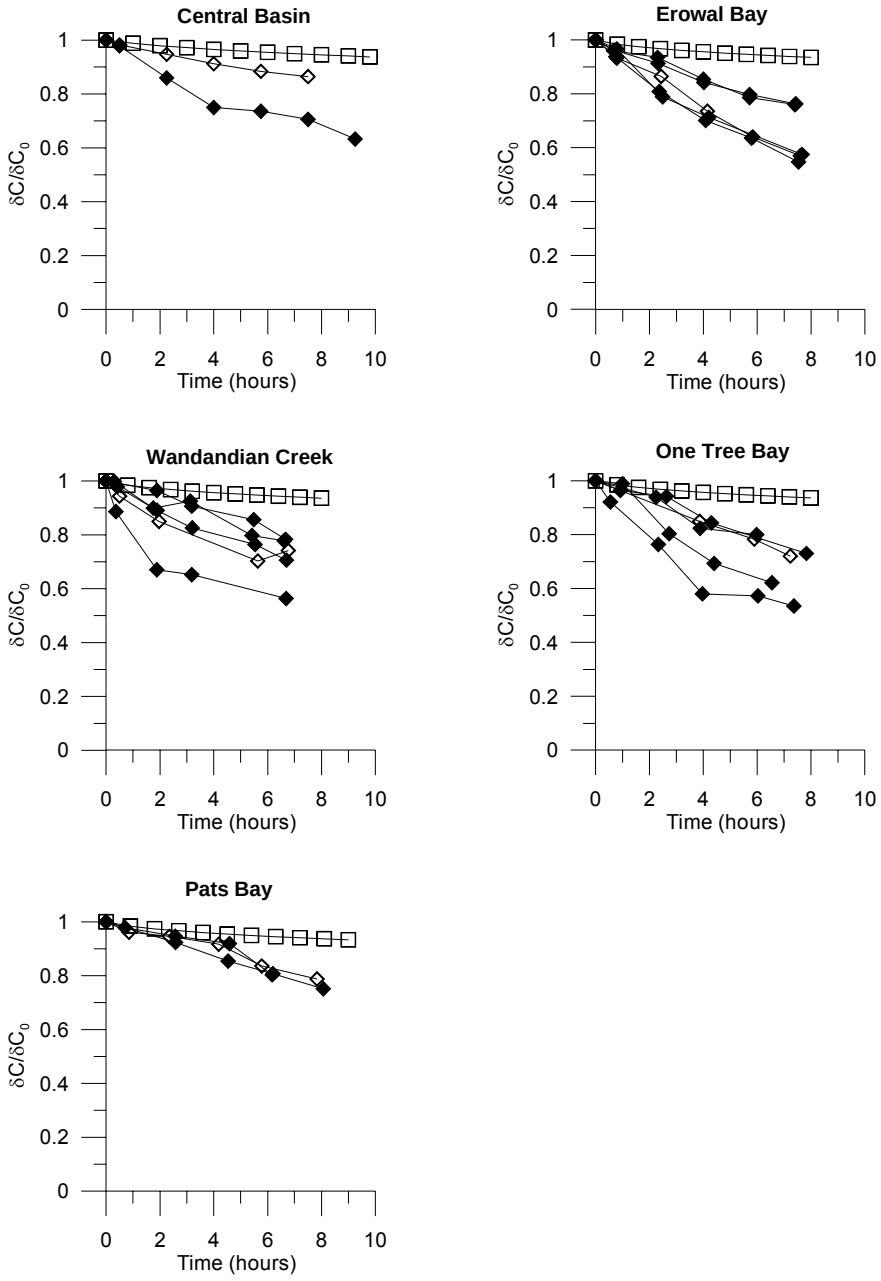

Figure 3-3. Comparison of measured tracer loss with modelled diffusive loss at each of the 5 sites in St Georges Basin. Open diamonds (◊) represent light chamber incubations, while closed diamonds (♦) represent dark chamber incubations. The open squares (□) represent the rate of tracer loss predicted from the diffusion model.

Figure 3-4 is an example of how the bioirrigation model (dashed lines) was fitted to the measured data. A bioirrigation rate that describes the velocity, beyond diffusion, at which the biota are transporting the tracer between the water column and underlying sediments was then derived from the model. Table 3-4 shows the bioirrigation rates from each chamber deployed in St Georges Basin.

Bioirrigation rates measured in different chambers at the same site were extremely variable, with most sites recording both high and low irrigation rates. For example, irrigation rates at Site 3, Wandandian Creek ranged between 110 m/yr and 1671 m/yr, where 110 m/yr was one of the lowest rates, and 1671 m/yr was the highest rate measured for all sites.

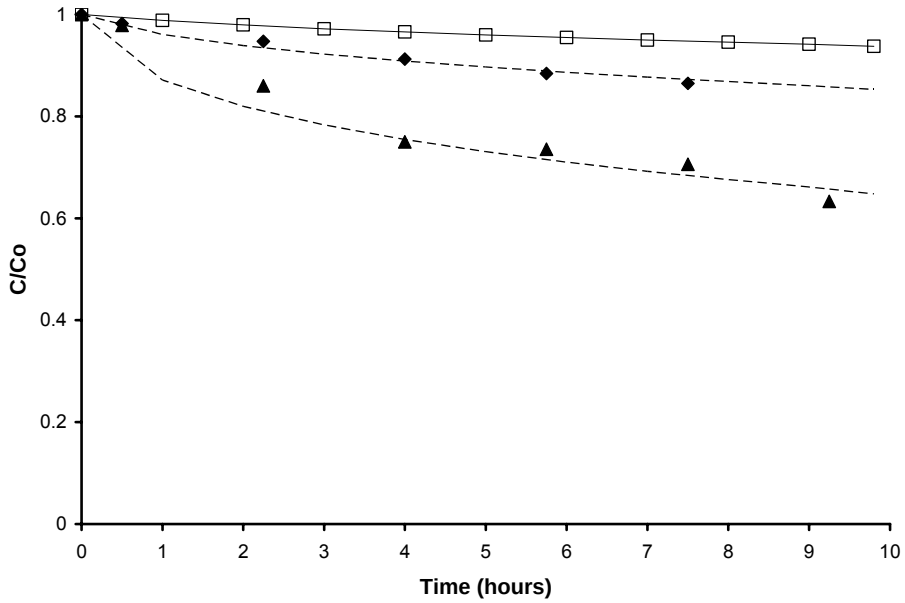

Figure 3-4. Tracer loss from two chambers (♦ and ▲) deployed at Site 1, modelled diffusive loss (□) and modelled bioirrigation (dashed lines).

Table 3-4. Irrigation rates (m/yr) for each benthic chamber deployed in St Georges Basin.

Site	Chamber	Irrigation Rate (m/yr)
Central Basin	1A_1	66
	1A_2	473
Erowal Bay	2A_3	1072
	2A_4	788
	2A_7	189
	2A_8	189
	2A_9	1104
Wandandian Creek	3A_3	306
	3A_4	1671
	3A_7	136
	3A_8	110
	3A_9	410
One Tree Bay	4A_3	136
	4A_4	107
	4A_7	1041
	4A_8	631
	4A_9	246
Pats Bay	5A_4	50
	5A_8	148
	5`A_9	101

4. DISCUSSION

Benthic nutrient fluxes and denitrification efficiency are major influences controlling eutrophication in wave-dominated estuaries such as St Georges Basin (Webster and Harris 2004; Murray and Parslow 1999). The results of this study reveal some important aspects of benthic nutrient cycling influencing water quality in St Georges Basin.

4A. SITE COMPARISONS

4A1. Organic Matter Loads

The magnitude of benthic fluxes measured using dark benthic chambers (Table 3-2 and Figure 3-1) and core incubations (Figure 3-2) are proportional to the rate of organic matter break down in the sediment (See *Introduction* Figure 1-1). In general, high rates of TCO_2, NH_4^+, and SiO_4^{4-} production, and O_2 consumption, indicate high benthic respiration rates, sustained by high organic matter loads to the sediment. This in turn, through organic matter degradation and nutrient release to the water column, influences the level of nutrients available for plant growth.

In both benthic chamber (Figure 3-1 a, b, c, and d) and core incubation (Figure 3-2) experiments, One Tree Bay (Site 4), Erowal Bay (Site 2), and Pats Bay (Site 5) had higher benthic respiration rates than the central basin (Site 1), and Wandandian Creek (Site 3) sites. This indicated Sites 4, 2, and 5, located in bays around the basin margin, were receiving higher inputs of organic matter than Site 1 in the central basin and Site 3 at the entrance to Wandandian Creek. The sediment at Sites 4, 2, and 5 also had higher TOC concentrations and Chl-a inventories, compared to Sites 1 and 3, and almost identical carbon isotopic compositions of -18‰ (Appendix 2).

4A2. Oxygen Status of the Sediments

All sites had negative O_2 fluxes in light chambers (Table 3-2), indicating they were net respiratory and more oxygen was consumed by respiration than was produced by photosynthesis during the time of sampling. This was despite four of the sites having shallow water depths (<3 m). Sites 4 and 5 had significantly lower O_2 uptake rates in light chambers compared to dark chambers (Table 3-2), whereas O_2 uptake rates were comparable between dark and light chambers at Sites 2 and 3. This suggests photosynthesis at the lakebed was possibly more significant at Sites 4 and 5 than at Sites 2 and 3.

All chamber results from Sites 5 and 2 plotted to the right of the 1:1 line, indicating anaerobic pathways (e.g. sulfate reduction) of organic matter degradation were important at these sites. All chamber results for Site 3 plotted within or just outside the envelope, indicating aerobic respiration was the major pathway for organic matter degradation at this site. Sites 1 and 4 were highly variable, with some chamber data plotting within the envelope and some plotting outside the envelope.

For core incubation results, consistently higher TCO_2 fluxes as compared to O_2 fluxes (Figure 3-2) suggested that anaerobic pathways of organic matter degradation were occurring at all sites. Therefore, it appears that anaerobic respiration was present at all sites but was highly variable, ranging from not important at Site 3 to moderately important at Sites 1 and 4, to a significant organic matter pathway at Sites 2 and 5.

Figure 4-1 shows O_2 versus TCO_2 fluxes for all dark benthic chamber experiments. The *1:1* line represents the conversion of O_2 to TCO_2, and the *1:1.3* line represents the oxidation of NH_4^+ to nitrate during nitrification. Data that plot within the envelope bound by these two lines arose from aerobic respiration, whereas data plotting to the right of the envelope had a component of TCO_2 flux attributable to anaerobic respiration; assuming carbonate dissolution was not contributing to TCO_2 fluxes.

All chamber results from Sites 5 and 2 plotted to the right of the 1:1 line, indicating anaerobic pathways (e.g. sulfate reduction) of organic matter degradation were important at these sites. All chamber results for Site 3 plotted within or just outside the envelope, indicating aerobic respiration was the major pathway for organic matter degradation at this site. Sites 1 and 4 were highly variable, with some chamber data plotting within the envelope and some plotting outside the envelope.

For core incubation results, consistently higher TCO_2 fluxes as compared to O_2 fluxes (Figure 3-2) suggested that anaerobic pathways of organic matter degradation were occurring at all sites. Therefore, it appears that anaerobic respiration was present at all sites but was highly variable, ranging from not important at Site 3 to moderately important at Sites 1 and 4, to a significant organic matter pathway at Sites 2 and 5.

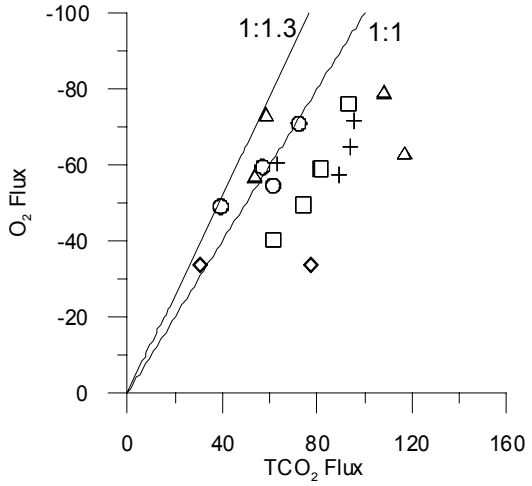

Figure 4-1. O_2 versus TCO_2 fluxes for all dark benthic chambers at all sites in mmol m2 day-1. The 1:1and 1:1.3 lines represent the scenarios of O_2 being used to: convert organic carbon to TCO_2, and; oxidize NH_4^+ to nitrate respectively. Diamonds represent Site 1 (◊), crosses Site 2 (+), circles Site 3 (o), triangles Site 4 (Δ), and squares Site 5 (□).

4A3. Organic Matter Source

Diatoms are microscopic algae that have thick outer cell walls made of silicate (SiO_4). They are very common in estuaries and can live in the water column, on plants such as seagrass or macroalgae, or at the sediment surface. The plot of TCO_2 against SiO_4^{4-} flux can indicate if diatoms are the major source of organic matter undergoing degradation in the sediments.

SiO_4^{4-} versus TCO_2 fluxes for most (dark) benthic chamber and core incubation experiments, plotted close to the 106 C : 17 Si ratio for diatoms (Brezezinski 1985) (Figure 4-2). Therefore, it appears the fluxes were closely related, and the two distinct processes, namely chemical dissolution of opal and microbial decomposition of organic matter, were coupled. Secondly, this observation suggested that carbonate dissolution was a negligible component of TCO_2 fluxes, and that diatoms were the major organic matter source; otherwise TCO_2 fluxes would lie above the C:Si ratio for diatoms (Figure 4-2).

It is interesting to note, when looking at the plots of NH_4^+ and SiO_4^{4-} versus TCO_2 (Figure 4-2 and Figure 4-4), that fluxes measured using core incubation measurements were consistently lower than fluxes measured using benthic chambers. We discuss this observation below in *Section 4B1 Spatial Heterogeneity of Fluxes*.

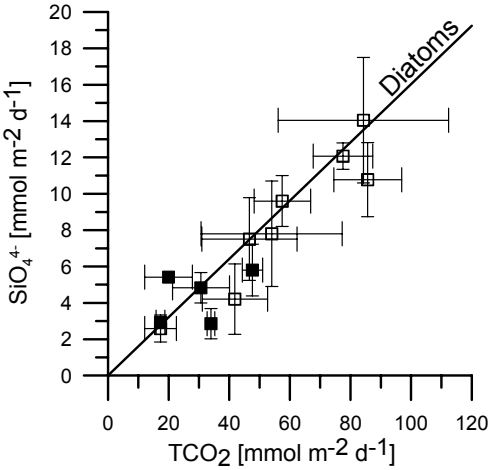

Figure 4-2. Plot of TCO_2 fluxes versus SiO_4^{4-} fluxes in mmol m^{-2} day^{-1} for all dark benthic chambers (□), and core incubations (■) for all sites. The error bars represent the coefficient of variation per site. The "Diatoms" line represents the ratio of 17 Si:106 C for diatomaceous material (Brezezinski 1985).

Researchers have used differences in the carbon isotopic composition of organic matter, δ^{13}C-TOC, between sites to reconstruct differences in the composition and origin of the organic matter (Rullkötter 2000). However, temporal

variation in the composition of terrestrial input and seasonal variations in the δ^{13}C-TOC of marine organic matter may complicate the interpretation of individual values of the δ^{13}C-TOC in terms of terrestrial versus marine organic matter (Cloern *et al*. 2002). Despite this, it is interesting to note that the sites with the lowest δ^{13}C-TOC (Table 3-3, Sites 4, 5, 2) also reveal highest Chl-a inventories and highest benthic nutrient fluxes. We speculate that these sites receive the highest proportion of terrestrial organic matter and that the proximity to stream discharge, with its associated particulate and dissolved organic matter load, appeared to drive benthic remineralisation.

Comparing the Chl-a inventory to benthic nutrient fluxes (Figure 4-3) can indicate whether high benthic nutrient fluxes resulted from the load of terrestrial organic matter deposited in certain areas of the estuary or the dissolved fraction of nutrients entering the estuary led to locally enhanced primary productivity. Terrestrial organic matter, being derived from soils and transported over distance, is not expected to be rich in Chl-a, whereas in-situ formed phytoplankton rapidly settles and predominantly contributes to the sedimentary Chl-a inventory. A good correlation was observed between both NH_4^+ and Chl-a (Figure 4-3 a), and SiO_4^{4-} and Chl-a (Figure 4-3 b). This suggested that local fluvial discharge of dissolved nutrients created enhanced primary productivity, which in turn enhanced mineralisation rates.

Not only does Figure 4-3 provide evidence for the above interpretation, but more generally the relationship between NH_4^+ and SiO_4^{4-} benthic fluxes and Chl-a inventories indicates Chl-a inventories could potentially provide a proxy for estimating NH_4^+ and SiO_4^{4-} benthic fluxes. This is a useful proposal since Chl-a is easier to measure than benthic fluxes.

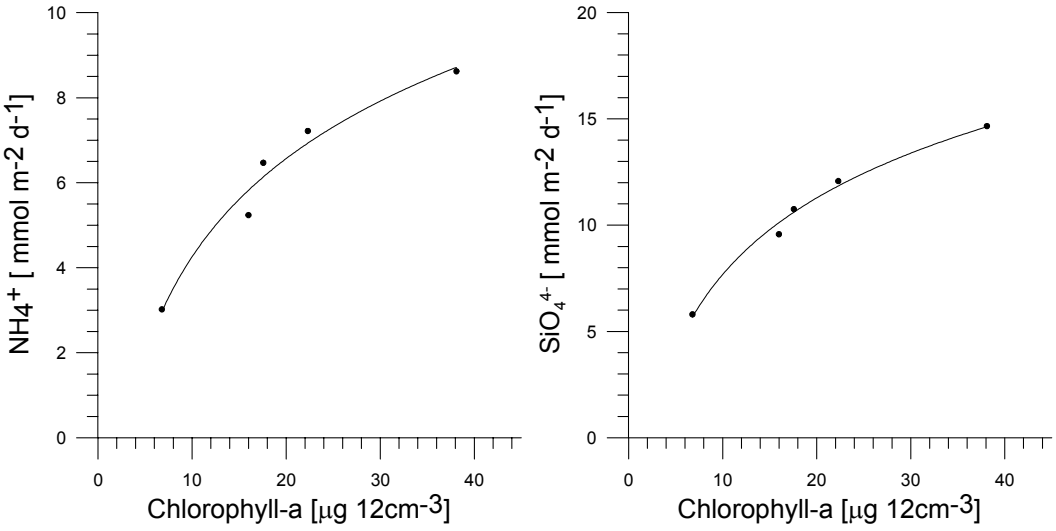

Figure 4-3. Plots of NH_4^+ (a) and SiO_4^{4-} (b) versus Chl-a. Average NH_4^+ and SiO_4^{4-} fluxes were derived from dark benthic chamber experiments and Chl-a concentrations were measured to a depth of 12 cm in surface sediments.

4A4. Denitrification Efficiency

Denitrification is a bacterial process of organic matter breakdown that results in the production of N_2 gas. The N_2 gas is subsequently lost to the atmosphere, reducing the pool of nitrogen available for plant growth. Therefore, denitrification is a process by which an estuary can rid itself of some nitrogen and thereby reduce the likelihood of the accumulation of nutrients within the system and eutrophication (Figure 1-1).

Denitrification efficiencies, calculated using equation (2) in *Appendix A5b,* were all less than 53% for all sites, except the central basin site (Table 3-2). This means that less than 53% of nitrogen was released in the form of N_2 gas; the remainder recycled in forms available for plant growth (mainly NH_4^+). Plots of NH_4^+ versus TCO_2 fluxes for dark benthic chambers and core incubations, also revealed to what degree denitrification was present (*Figure 4-4*). In the case of 100% denitrification efficiency, NH_4^+ fluxes would be zero, and all N recycled as N_2. However, NH_4^+ fluxes plotted slightly below the Redfield-ratio (106 TCO_2 : 16 NH_4^+) for most chambers and core incubations at all sites, indicating that most N was returned to the water column as NH_4^+, and denitrification efficiencies were low (*Figure 4-4*).

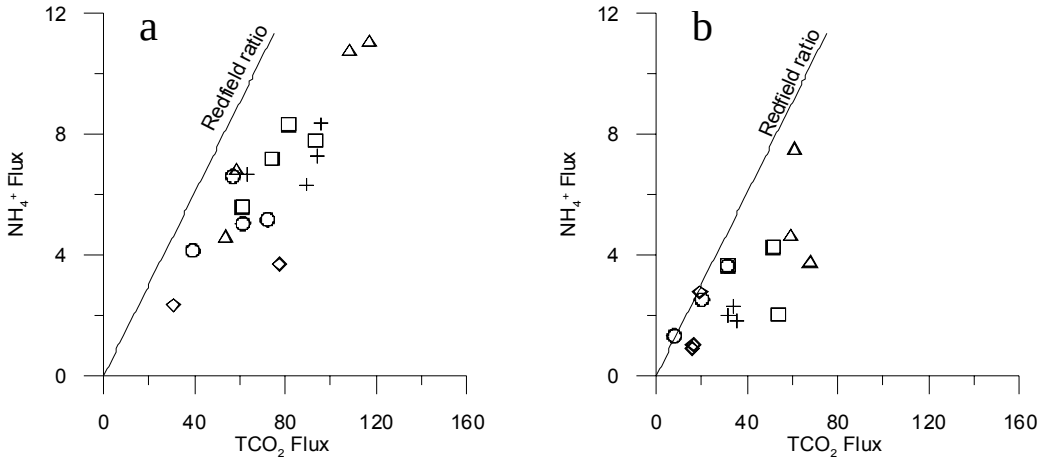

Figure 4-4. Plot of NH_4^+ fluxes versus TCO_2 fluxes in mmol m^{-2} day^{-1} for all dark benthic chambers (a) and core incubations (b) for all sites. The "Redfield ratio" line represents the ratio of 106 C : 16 NH_4^+ for the break down of Redfield composition organic matter. Diamonds represent Site 1 (◊), crosses Site 2 (+), circles Site 3 (o), triangles Site 4 (Δ), and squares Site 5 (□).

4B. SOLUTE TRANSPORT ACROSS THE SEDIMENT-WATER INTERFACE

4B1. Spatial Heterogeneity of Fluxes

Solute fluxes across the sediment-water interface have been calculated based on pore water concentrations, core incubations, and benthic chamber experiments (Table 4-1). Vertical porewater concentration gradients were steepest between bottom water and surface sediment porewaters (Appendix 2), indicating respiration rates were highest at the sediment-water interface. Note, however, that calculations based on vertical pore water concentration gradients only gave molecular diffusive fluxes, whereas bottom water concentration changes in core incubations and dark benthic chambers represented total solute fluxes, i.e. they comprised diffusive fluxes and bioirrigation induced fluxes. Consequently, studies have found diffusive fluxes to be systematically lower than total fluxes (Forster *et al*. 1999).

Table 4-1 gives a comparison of TCO_2, NH_4^+, and SiO_4^{4-} fluxes. As expected, diffusive fluxes were systematically the lowest for all solutes. However, significantly lower fluxes derived from core incubations as compared to fluxes derived from in-situ dark benthic chamber deployments were unexpected for such shallow sites. Similar differences have been observed when comparing in-situ and ex-situ fluxes in continental shelf and slope environments and were attributed to artifacts related to decompression during core recovery (Hammond *et al*. 2004). Given the shallow water depths of St. Georges Basin (<10 m), this argument may not hold in this situation. Possibly, this observation was related to the area covered by the incubation. Three cores cover a total of 150 cm^2, while four (dark) chambers cover 2500 cm^2. We suggest that 'hot' spots with highly enriched organic matter were randomly distributed in surface sediments and that their spacing was large enough, so that hot spots were not sampled when taking three cores. Various species of benthic macrofauna, e.g. shrimp, are known to accumulate organic debris at discrete sites serving as future feeding reservoirs. This would also explain, why in a recent study using benthic chambers with a surface area of 3850 cm^2 they found 'higher than most fluxes reported previously in other coastal systems' (Forja *et al*. 2004).

Macrofauna, and their tendency to create heterogeneity in the sediment, may also explain the high variability of benthic nutrient fluxes within sites, where coefficients of variance typically ranged between 15 and 40% (Table 3-2).

Table 4-1. Comparison of the diffusive flux (diff.), the average total fluxes derived from core incubations (CI), and the average total flux derived from dark benthic chamber incubations (BC).

	TCO_2 (mmol m^{-2} d^{-1})			NH_4^+ (mmol m^{-2} d^{-1})			SiO_4^{4-} (mmol m^{-2} d^{-1})		
Site	**diff.**	**CI**	**BC**	**diff.**	**CI**	**BC**	**diff.**	**CI**	**BC**
1	9.65	17.30	54.01	2.70	1.58	3.02	3.86	2.93	5.80
2	3.89	33.97	85.66	0.40	2.05	6.47	0.58	2.85	10.75
3	4.39	19.96	57.47	1.51	2.50	5.24	2.52	5.41	9.57
4	21.90	43.99	68.99	2.77	5.33	8.62	4.73	5.80	14.66
5	17.09	29.21	72.58	3.30	3.31	7.22	4.43	4.83	12.07

4B2. Bioirrigation

There was high variability in bioirrigation rates both between and within sites (Table 3-4). This was most likely a result of different amounts (and possibly types) of bioirrigating macrofauna captured within each benthic chamber.

We tested the relationship between bioirrigation rates and benthic fluxes to determine if increased macrofaunal activity (bioirrigation) led to larger benthic flux rates. We would assume the larger benthic fluxes would correspond to the largest bioirrigation rates. However, this was not the case. We found there was no significant relationship between benthic fluxes and irrigation rates. Therefore, it appeared the increased exchange of water between the sediments and overlying water caused by macrofauna was not directly influencing solute flux rates.

4C. COMPARISONS WITH OTHER AUSTRALIAN ESTUARIES

The rates of organic matter degradation in St Georges Basin were relatively high when compared to other temperate Australian estuaries (Figure 4-5). The fluxes shown for other estuaries in Figure 4-5 were measured with dark benthic chambers using similar methods to those used in St Georges Basin and were measured at varying times of the year.

St Georges Basin had the highest median TCO_2, NH_4^+ and SiO_4^{4-} fluxes (Figure 4-5 a, c, and d), and the second highest O_2 consumption rate (Figure 4-5 b). We measured these in late spring, a time of year when we would expect relatively high plant productivity. Benthic fluxes may be even higher in late autumn when plant biomass is decreasing and more dead organic material is falling to the sediments.

N_2 fluxes and denitrification efficiencies averaged for all sites in St Georges Basin were lower than most other estuaries (Figure 4-6). This indicated a greater proportion of nitrogen was recycled as bioavailable NH_4^+ in St Georges Basin than most other estuaries. Myall Lake was the only estuary with lower denitrification efficiencies, and these were measured shortly before an algal bloom.

The high respiration rates measured in St Georges Basin indicate the estuary was mesotrophic to eutrophic, according to the trophic classification of Nixon (1995), where oligotrophic estuaries have low primary productivity, eutrophic estuaries have high primary productivity, and mesotrophic estuaries are in between. Mesotrophic estuaries have TCO_2 fluxes between 23 and 69 mmol m^{-2} day^{-1}, whereas eutrophic estuaries exhibit TCO_2 fluxes above 69 mmol m^{-2} day^{-1}. High respiration rates, coupled with low denitrification efficiencies compared to other temperate Australian estuaries, indicated St Georges Basin is relatively susceptible to eutrophication.

The calculated bioirrigation rates can be used to estimate the time taken to pump the overlying water column through the sediments (turn-over time). For St Georges Basin, this time was estimated between 1 and 36 days (Table 4-2). This time is similar to Wilson Inlet in Western Australia, however, Wilson Inlet has a smaller water volume (average depth of 1.7m compared to 5m in St Georges Basin). San Francisco Bay, USA, has a similar average depth to St Georges Basin (6m), but has a turn-over time of between 170 and 1150 days. St Georges Basin, therefore, appeared to have a comparatively high level of biological activity.

Table 4-2. Turn-over time in selected Australian and US estuaries and coastal waterways.

Location	Average Depth (m)	Turn-over Time (days)	Reference
San Francisco Bay, USA	6	170-1150	Hammond *et al*. (1985)
Los Angeles Harbour, USA	15	85-1730	Townsend (1998)
Washington Shelf, USA	100	11500-116000	Christensen *et al*. (1987)
Port Phillip Bay, VIC	14	50-270	Berelson *et al*. (1996)
Wilson Inlet, WA	1.7	0.5-39	Fredericks & Heggie (2000)
St Georges Basin, NSW	5	1-36	This study

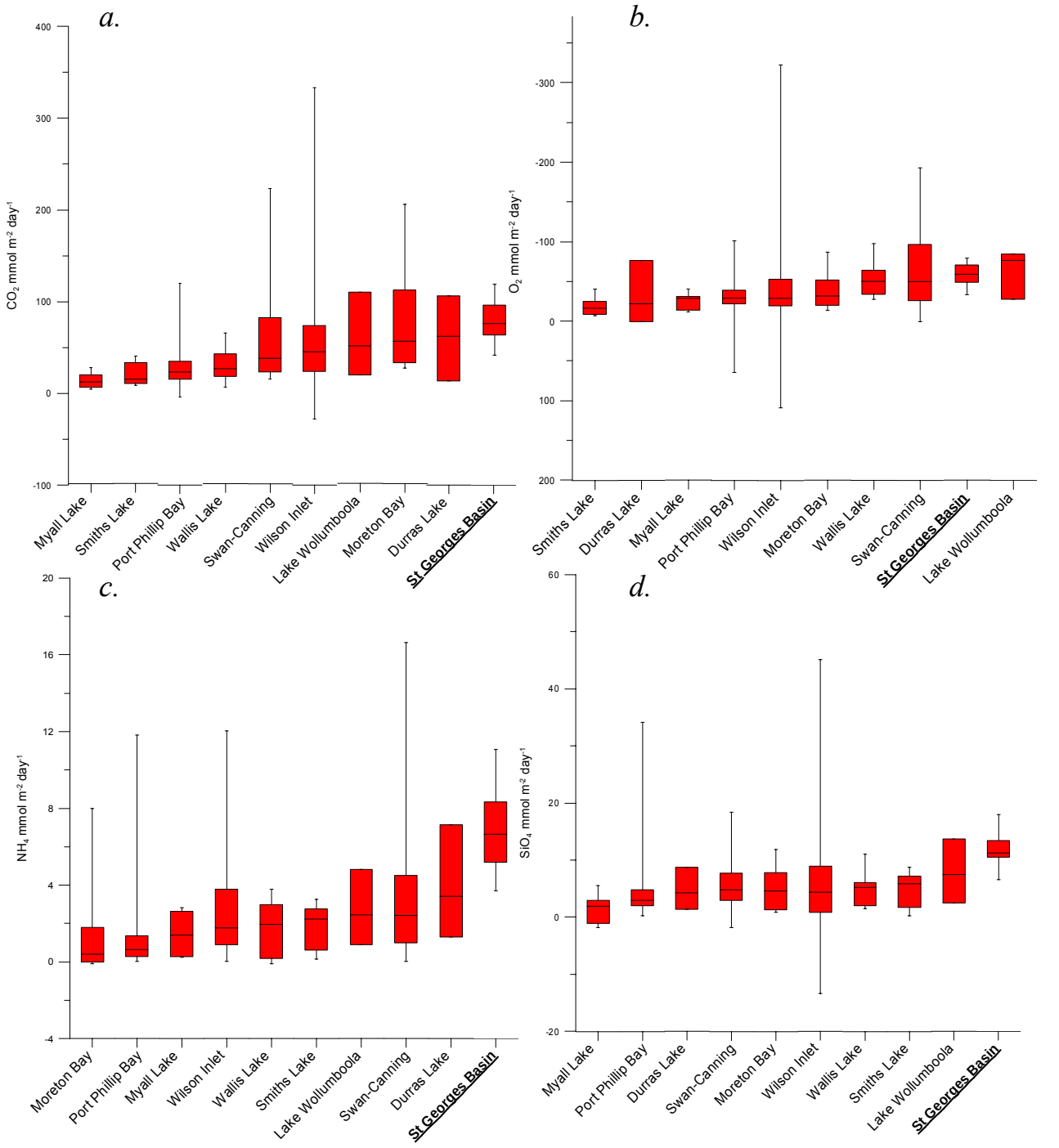

Figure 4-5. Box and whisker diagrams showing the range of (a) TCO_2, (b) O_2, (c) NH_4^+, and (d) SiO_4^{4-} fluxes measured using dark benthic chambers in St Georges Basin (for all 5 sites combined) compared to other temperate Australian estuaries. The median is the horizontal line within the boxes, the bottom end of each box is the 25th percentile and the top end is the 75th percentile, and the vertical lines show the range of the outliers. Myall Lake, Smiths Lake, Wallis Lake, Lake Wollumboola and Durras Lake are in NSW; Port Phillip Bay is in Victoria; Moreton Bay is in south-east Queensland; and the Swan-Canning River system and Wilson Inlet are in south-west Western Australia. Data sourced from previous Geoscience Australia studies 1997-2003 and measured using similar methods as for this study.

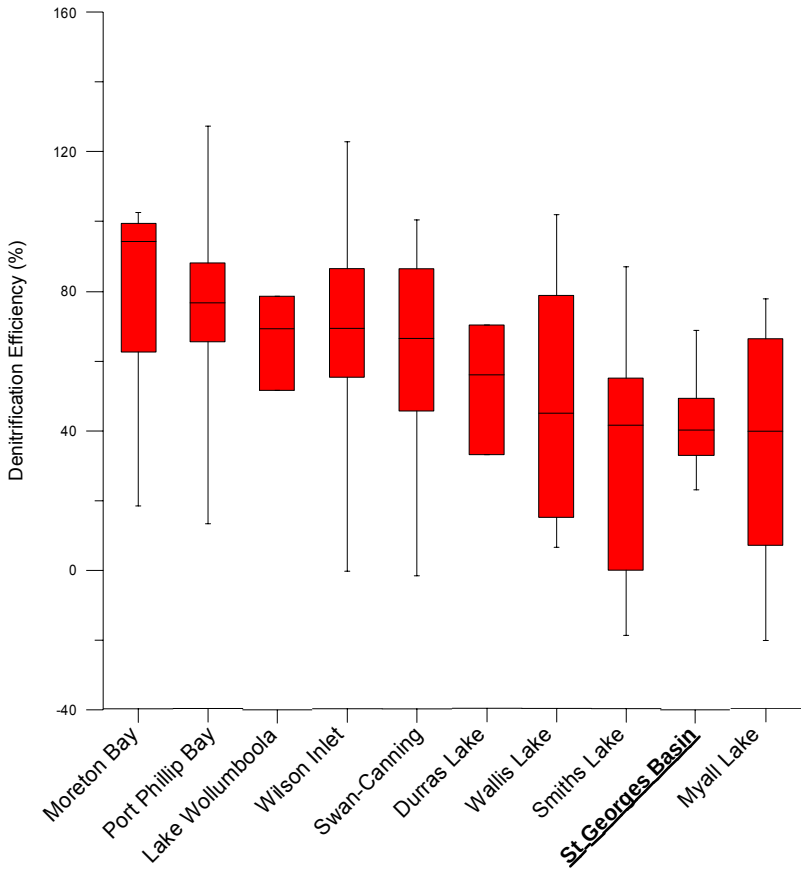

Figure 4-6. Box and whisker diagram showing the range of denitrification efficiencies (%) measured in St Georges Basin using dark benthic chambers and calculated using equation (2) in Section A5b (for all 5 sites combined) compared to other temperate Australian estuaries.

5. CONCLUSIONS

5A. KEY FINDINGS

This study focused on the exchange of dissolved nutrients and gases at the sediment-water interface. Processes occurring at this critical interface can give useful information on estuarine health and susceptibility to human impacts. Key findings of this study were:

(1) Respiration rates and O_2 demand in the sediments of St Georges Basin were relatively high at the time of the survey, especially the shallower sites in the embayments around the edge of the basin.

- St Georges Basin was mesotrophic to eutrophic according to the classification of Nixon (1995) and had the highest median TCO_2, NH_4^+ and SiO_4^{4-} fluxes, and second highest median O_2 consumption rate compared to other temperate Australian estuaries (those with benthic flux data).

- The shallower sites in embayments around the edge of the basin (Sites 2, 4, and 5) had higher median TCO_2, O_2, NH_4^+, and SiO_4^{4-} fluxes then the Wandandian Creek site (Site 3) and the deep central basin site (Site 1).

- All sites in the basin recorded negative O_2 fluxes in light chambers, indicating they were net heterotrophic, where more oxygen was consumed by respiration than was produced by photosynthesis. This was despite four sites having shallow water depths (<3 m).

- Water column profiles revealed that O_2 consumption at the sediment-water interface was greater than could be replenished from the atmosphere or by deep photosynthesis. We found bottom water O_2 concentrations were depleted compared to surface water and atmospheric O_2 concentrations.

- All sites displayed evidence for anaerobic degradation pathways (e.g. sulfate reduction) to varying degrees. This was indicated by the complete exhaustion of O_2 in the sediments.

(2) Respiration rates were linked to phytoplankton biomass, where local fluvial discharge of dissolved nutrients, created enhanced primary productivity in the water column, which in turn enhanced mineralisation rates.

- The ratio between NH_4^+, and SiO_4^{4-} fluxes indicated diatoms (phytoplankton with a Si-frustule) were the major source of organic matter at all sites.

- There was a good correlation between NH_4^+ and SiO_4^{4-} fluxes, and Chl-a, where the sedimentary Chl-a inventory predominantly results from in-situ formed phytoplankton that rapidly settles to the sediment.

- Sites 2, 4, and 5 had higher TCO_2, O_2, NH_4^+, and SiO_4^{4-} fluxes, Chl-a inventories, and TOC concentrations, compared to Sites 1 and 3. Sites 2, 4, and 5 also had the lowest δ^{13}C-TOC compositions (of around -18‰). We speculate these sites received the highest proportion of terrestrial organic matter and that the proximity to stream discharge, with its associated particulate and dissolved organic matter load, appeared to drive benthic remineralisation.

- The relationship between NH_4^+ and SiO_4^{4-} benthic fluxes, and Chl-a inventories indicated Chl-a inventories could potentially provide a proxy for estimating NH_4^+ and SiO_4^{4-} benthic fluxes throughout St Georges Basin.

(3) St Georges Basin had comparatively low denitrification efficiencies. This was especially so for the shallower areas around the edge of the basin.

- Median denitrification efficiencies in St Georges Basin sediments were low compared to most other temperate Australian estuaries (those with benthic flux data).

- Sites 2, 3, 4, and 5, located around the basin margins, all had denitrification efficiencies less than 53%, indicating that at least half of all N in organic matter degrading in the sediment, was returned to the water column as NH_4^+, and hence available for primary productivity (plant growth).

- The central basin site (Site 1) had higher denitrification efficiencies (of around 60%) compared to the shallower sites, around the basin margin.

(4) Benthic fluxes in St Georges Basin sediments were heterogeneous within sampling areas (~100 m^2) and systematic flux differences were found when benthic chambers are compared to core incubations.

- The variability of benthic nutrient fluxes within sites was very high and the coefficient of variance typically ranged between 15 and 40%. Within-site variability was possibly a result of the activity of macrofauna causing heterogeneity in the sediment.

- Core incubations systematically derived lower fluxes than in-situ dark benthic chamber deployments. This was possibly related to the area covered by the respective incubations, where benthic chambers potentially captured randomly distributed surface sediment patches with highly enriched organic matter and cores did not. Various species of benthic macrofauna, e.g. shrimp, are known to accumulate organic debris at discrete sites serving as future feeding reservoirs.

5B. MANAGEMENT IMPLICATIONS

Wave-dominated estuaries such as St Georges Basin have restricted entrances and little capacity to 'flush' N to the sea (the residence time in St Georges Basin is around 80 days). These estuaries depend upon efficient denitrification to maintain low bioavailable N concentrations in the water column. At the time of sampling, St Georges Basin had relatively high respiration rates and low denitrification efficiencies. Therefore, the basin is probably prone to eutrophication and may have little tolerance for any human-induced increase in nutrients and organic matter from the catchment.

We cannot accurately predict the ecological response of eutrophication in St Georges Basin, but it could involve nuisance algal blooms, seagrass decline resulting from an increase in phytoplankton biomass shading seagrass meadows (Butler and Jernakoff 1999), or anoxia and fish kills. Shallow embayments around the basin margin would probably contribute overproportionally to eutrophication compared to the deeper central basin, as these sites recorded higher respiration rates and lower denitrification efficiencies than the central basin. In addition, it appears that dissolved nutrients from stream inflow and benthic respiration are tightly coupled, where nutrients in runoff from the catchment drive localised primary productivity in the water column, which subsequently enhances the supply of organic material to the sediment and increases respiration rates at the sediment-water interface.

The variability of benthic fluxes within-sites, and the bioirrigation rates measured, indicated the activity of benthic macrofauna. Benthic macrofauna can influence the distribution of organic matter, microbial activities and growth rates, and the transport of water and solutes in and out of the sediment. Most notably, for this study, the activities of macrofauna may increase coupled nitrification-denitrification in the sediment by creating microenvironments such as faecal pellets and ventilated burrows that increase the volume of sediment where these processes can occur (Kristensen 1988). For example, the pumping of water through the burrows of macroinvertibrates, increases the surface area of sediment exposed to oxic bottom water, which is needed for coupled nitrification-denitrification. However, increased nutrient inputs may overwhelm the capacity of these benthic communities, reducing denitrification efficiencies and increasing the possibility of eutrophication.

Future management would benefit greatly from a better spatial and temporal understanding of benthic nutrient fluxes in St Georges Basin. This could involve another survey, similar to this one, using the same sites but at a different time of year, such as late autumn when primary productivity is lower than in late spring (when this study was conducted). In addition, a better temporal and spatial understanding may be gained by interpreting remotely sensed images of Chl-a distributions at different times of the year. Measuring Chl-a in the surface sediments at many sites across the basin could also improve spatial resolution of nutrient fluxes because this study showed that Chl-a could provide an easily and rapidly measured proxy for benthic fluxes.

6. REFERENCES

Aller, R.C. (1994). The sedimentary Mn cycle in Long Island Sound: Its role as intermediate oxidant and the influence of bioturbation, O_2, and Corg flux on diagenetic reaction balances. *Journal of Marine Research* **52,** 259-293.

Aller, R.C., and Aller J.Y. (1992). Meiofauna and solute transport in marine muds. *Limnology and Oceanography* **37**, 1018-1033.

Alongi, D. M. (1989a). The role of soft-bottom benthic communities in tropical mangrove and coral reef ecosystems. *Reviews in Aquatic Sciences* **1(2)**, 243-80.

Alongi, D. M. (1989b). Benthic processes across mixed terrigenous-carbonate sediment facies on the central Great Barrier Reef continental shelf. *Continental Shelf Research* **9**, 629-63.

Alongi, D. M. (1990). Effects of mangrove detrital outwelling on nutrient regeneration and oxygen fluxes in coastal sediments of the central Great Barrier Reef lagoon. *Estuarine, Coastal and Shelf Science* **31**, 581-98.

Australian Geological Survey Organisation (1998), *Benthic Fluxes and Seafloor Biogeochemistry of Moreton Bay and Brisbane River*. Australian Geological Survey Organisation, Canberra.

Berelson, W. M., and Hammond, D. E. (1986). The calibration of a new free vehicle benthic flux chamber for use in the deep sea. *Deep Sea Research* **33**, 1439-54.

Berelson, W., Kilmore, T., Heggie, D., Skyring, G. and Ford, P. (1996). *Benthic chambers, nutrient fluxes and the biogeochemistry of Port Phillip Bay, 1995 and 1996.* Australian Geological Survey Organisation, Canberra.

Berelson, W., Heggie, D., Longmore, A., Kilgore, T., Nicholson, G., and Skyring, G. (1998). Benthic nutrient cycling in Port Phillip Bay, Australia. *Estuarine, Coastal and Shelf Science* **46**, 917-34.

Berelson, W.M., Townsend, T., Heggie, D., Ford, P., Longmore, A., Skyring, G., Kilmore, T. and Nicholson, G. (1999). Modelling bio-irrigation rates in the sediments of Port Phillip Bay. *Marine and Freshwater Research* **50**, 573-579.

Boon, A. R., and Duineveld, G. C. A. (1998). Chlorophyll a as a marker for bioturbation and carbon flux in southern and central North Sea sediments. *Marine Ecological Progress Series* **162**, 33-43.

Boon A.R., Duineveld, G. C. A., Berghuis, E. M., and Van der Weele, J. A. (1998). Relationships between benthic activity and the annual phytopigment cycle in near-bottom water and sediments in the southern North Sea. *Estuarine, Coastal and Shelf Science* **4**, 1-13.

Butler, A.J., and Jernakoff, P. (1999). *Seagrass in Australia: Strategic Review and Development of an R&D Plan.* FRDC Project 98/223

Brzezinski, M. A. (1985). The Si:C:N ratio of marine diatoms: Interspecific variability and the effect of some environmental variables. *Journal of Phycology* **21(3)**, 347-57.

Caffrey, J. M. (1995). Spatial and seasonal patterns in nitrogen remineralisation and ammonium in San Francisco Bay, California. *Estuaries* **18**, 219-33.

Canfield, D. E. (1993). Organic matter oxidation in marine sediments. In *Interactions of C,N,P and S Biogeochemical Cycles and Global Changes* (Eds Wollast, R., Mackenzie, F. T., Chou, L.). pp 333-63, Springer-Verlag: Berlin.

Christensen, J.P., Smethie, W.M.Jr. and Devol, A.H. (1987). Benthic nutrient regeneration and denitrification on the Washington continental shelf. *Deep-Sea Research* **34**, 1027-1047.

Cloern J. E., Canuel, E.A., Harris, D. (2002). Stable carbon and nitrogen isotope composition of aquatic and terrestrial plants of the San Francisco Bay estuary system. *Limnology and Oceanography* **47**, 713-729.

Douglas, G., Hamilton, D., Gerritse, R., Adeney, J., and Coad, D. (1996). Sediment geochemistry, nutrient fluxes and water quality in the Swan River Estuary, Western Australia. In *Managing algal blooms: Outcomes from CSIRO's multidivisional blue-green algal program*. (Ed J. K. Davis.), CSIRO Land and Water, Canberra.

Eyre, B. D., and Ferguson, A. J. P. (2002). Comparison of carbon production and decomposition, benthic nutrient fluxes and denitrification in seagrass, phytoplankton, benthic microalgae- and macroalgae-dominated warm-temperate Australian lagoons. *Marine Ecology Progress Series* **229**, 43-59.

Eyre, B. D., Rysgaard, S., Dalsgaard, T., and Christensen, P. B. (2002). Comparison of Isotope Pairing and N_2:Ar Methods for Measuring Sediment Denitrification-Assumptions, Modifications, and Implications. *Estuaries* **25**, 6, 1077-1087.

Forja, J. M., Angel DelValls, T. O. T., Gomez-Parra, A. (2004). Benthic fluxes of inorganic carbon in shallow coastal ecosystems of the Iberian Peninsula. *Marine Chemistry* **85**, 141-156.

Forster, S., Glud, R. N., Gundersen, J. K., and Huettel, M., (1999). In situ study of bromide tracer and oxygen flux in coastal sediments. *Estuarine, Coastal and Shelf Science* **49**, 813-827.

Fredericks, D. J., and Heggie, D. T. (2000). *Are Sediments a Significant Source of Nutrients in Wilson Inlet?* Australian Geological Survey Organisation, Professional Opinion, 2000/04, Canberra.

Fredericks, D. J., Palmer, D. W., Smith, C. S., and Heggie, D. T. (2002). *Benthic Fluxes and Nutrient Recycling in the Swan Estuary*. Australian Geological Survey Organisation, Professional Opinion, 2002/03, Canberra.

Froelich, P. N., Klinkhammer, G. P., Bender, M. L., Luedtki, N. A., Heath, G. R., Cullen, D., Dauphin, P., Hammond, D., and Hartman, B. (1979). Early oxidation of organic matter in pelagic sediments of the eastern equatorial Atlantic: suboxic diagenesis. *Geochima et Cosmochimica Acta* **43**, 127-68.

Grasshoff, K., Ehrhardt, M., and Kremling, K. (1983). *Methods of seawater analysis*. Verlag Chemie: Weinheim.

Hall, P. O. J., and Aller, R. (1992). Rapid, small-volume, flow injection analysis for ΣCO_2 and NH_4^+ in marine and freshwaters. *Limnology and Oceanography* **37**, 1113-1119.

Hammond, D. E., Fuller, C., Harmon, D., Hartman, B., Korosec, M., Miller, L.G., Rea, R., Warren, S., Berelson, W., and Hager, S.W. (1987). Benthic fluxes in San Francisco Bay. *Hydrobiologia* **129**, 69-90.

Hammond, D. E., Cummins, K. M., McManus, J., Berelson, W. M., Smith, G., and Spagnoli, F. (2004), Methods for measuring benthic nutrient flux on the California Margin: Comparing shipboard core incubations to in situ lander results. *Limnology and Oceanography Methods* **2**, 146-159.

Hansen, J. A., Alongi, D. M., Moriarty, D. J. W., and Pollard, P. C. (1987). The dynamics of benthic microbial communities at Davies Reef, central GBR. *Coral Reefs* **6**, 63-70.

Harris, P. T. and Heap, A. D. (2003). Environmental management of clastic coastal depositional environments: inferences from an Australian geomorphic database. *Ocean and Coastal Management* **46**, 457-478.

Hecky, R. E., and Kilham, P. (1988). Nutrient limitation of phytoplankton in freshwater and marine environments: a review of recent evidence on the effects of enrichment. *Limnology and Oceanography* **33**, 796-822.

Heggie, D. T., Skyring, G. W., Berelson, W. M., Longmore, A. R., and Nicholson, G. J. (1999a). Sediment-water interaction in Australian coastal environments: implications for water and sediment quality. *AGSO Journal of Australian Geology and Geophysics* **17(5/6)**, 159-73.

Heggie, D. T., Skyring, G. W., Orchardo, J., Longmore, A. R., Nicholson, G. J., and Berelson, W. M. (1999b). Denitrification and denitrifying efficiencies in sediments of Port Phillip Bay: direct determinations of biogenic N_2 and N-metabolite fluxes with implications for water quality. *Marine and Freshwater Research* **50**, 589-96.

Kana, T. M., Darkangelo, C., Hunt, M. D., Oldam, J. B., Bennett, G. E., and Cornwell, J. C. (1994). Membrane inlet mass spectrometer for rapid high-precision determination of N_2, O_2 and Ar in environmental samples. *Analytical Chemistry* **66**, 4166-70.

Kristensen, E. (1988). Benthic Fauna and Biogeochemical Processes in Marine Sediments: Microbial Activities and Fluxes. In 'Nutrient Cycling in Coastal Marine Environments'. (Eds T. H. Blackburn and J. Sorensen), John Wiley and Sons Ltd.

Lukatelelich, R. J., Schofield, N. J., and McComb, A. J. (1987). Nutrient loading and macrophyte growth in Wilson Inlet, a bar-built southwestern Australian estuary. *Estuarine, Coastal and Shelf Science* **24**, 141-165.

Meehan, A. (2001). *Conservation status of the seagrass Posidonia australis in south east Australia*. PhD thesis, Environmental Science, University of Wollongong. 230 pp.

Millero, J. (1996). *Chemical Oceanography*. CRC Pr Llc.

Mehrbach, C., Culberson, C. H., Hawley, J. E., and Pytkowitcz, R. M. (1973). Measurement of the apparent dissociation constants of carbonic acid in seawater at atmospheric pressure. *Limnology and Oceanography* **18(6)**, 897-907.

Murray, A. G., and Parslow, J. S. (1999). Modelling of nutrient impacts in Port Phillip Bay – a semi-enclosed marine Australian ecosystem. *Marine and Freshwater Research* **50**, 597-611.

Murray, E. M., Heggie, D. T., and Skyring, G. (2003). Denitrification in the sediments of Lake Wollumboola, a hydrogen sulphide-rich, saline coastal lagoon, southeast Australia, Conference Paper, Australian Marine Sciences Association Conference, Brisbane, July 2003.

Nixon, S. W. (1995). Coastal marine eutrophication: a definition, social causes and future concerns. *Ophellia* **41**, 199-219.

National Land and Water Resources Audit (2002). *Australian Catchment, River and Estuary Assessment 2002*. Commonwealth Government, Canberra. www.audit.ea.gov.au/ANRA/atlas_home.cfm

Palmer, D., Fredericks, D. J., Smith, C., Logan, G., and Heggie, D. T. (2000a). *Benthic Nutrient Fluxes in Bombah Broadwater, Myall Lakes*. Australian Geological Survey Organisation, Professional Opinion, 2000/33, Canberra.

Palmer, D., Fredericks, D. J., Smith, C., Tindall, C., and Heggie, D. T. (2000b). *A Reconnaissance Study of Benthic Fluxes in Durras Lake* Australian Geological Survey Organisation, Professional Opinion, 2000/14, Canberra.

Redfield, A. C., Ketchum, B. H., and Richards, F. A. (1963). The influence of organisms on the composition of sea water. In 'The Sea'. Vol. 2, (Ed. M. N. Hill.) pp. 26-79. Wiley Interscience: New York.

Rullkötter J. (2000). Organic matter: The driving force for early diagenesis, In *Marine Geochemistry*, (eds.: H.D. Schulz and M. Zabel), 129-172. Springer, Heidelberg.

Ryther, J. H., and Dunstan, W. M. (1971). Nitrogen, phosphorus and eutrophocation in the coastal marine environment. *Science* **171**, 1008-13.

Schulz, H. D. (2000). Quantification of early diagenesis: Dissolved constituents in marine pore water, In *Marine Geochemistry*, (eds.: H.D. Schulz and M. Zabel), 85-128, Springer, Heidelberg.

Seitzinger, S. P. (1987). Nitrogen biogeochemistry in an unpolluted estuary: the importance of benthic denitrification. *Marine Ecology Progress Series* **41**, 177-86.

Seitzinger, S. P. (1988). Denitrification in freshwater and coastal marine ecosystems: ecological and geochemical significance. *Limnology and Oceanography* **33**, 702-24.

Seitzinger, S. P., and Nixon, S. W. (1985). Eutrophication and the rate of denitrification and N_2O production in coastal marine sediments. *Limnology and Oceanography* **30**, 1332-9.

Seitzinger, S. P., Nixon, S. W., Pilson, M. E. Q., and Burke, S. (1980). Denitrification and N_2O production in near-shore marine sediments. *Geochmica et Cosmochimica Acta* **44**, 1853-60.

Skyring, G. W. (1987). Sulfate Reduction in Coastal Ecosystems. *Geomicrobiology Journal* **5(3/4)**, 295-374

Shoalhaven City Council (1998). *St Georges Basin Estuary Management Plan.* Shoalhaven City Council, Nowra.

Smith, C. S., Heggie, D. T., Fredericks, D. J., Palmer, D. W., and Logan, G. A. (2000). *Benthic Nutrient Fluxes in Wallis Lake.* Australian Geological Survey Organisation, Professional Opinion, 2000/35, Canberra.

Smith, C. S., and Heggie, D. T. (2003a). *Benthic Nutrient Fluxes in Smiths Lake, NSW.* Geoscience Australia, Record 2003/16, Canberra.

Smith, C. S., and Heggie, D. T. (2003b). *Benthic Nutrient Fluxes in Wallis Lake, NSW – Feb 2003.* Geoscience Australia, Record 2003/22, Canberra.

Smith, S. V. (1984). Phosphorus versus nitrogen limitation in the marine environment. *Limnology and Oceanography* **29**, 1149-60.

Sun, M. Y., Aller, R.C., and Lee, C. (1994). Spatial and temporal distribution of sedimentary chloropigments as indicators of benthic processes in Long Island Sound. *Journal of Marine Research* **52**, 149-176.

Townsend, T.H. (1998). *Numerical simulation of tracer loss from benthic chambers: An investigation of bio-irrigation rates and patterns in marine sediments*. PhD Thesis, University of Southern California, USA.

Tsunogai, S., Nishimura, M., and Nakaya, S. (1968). Complexometric titration of calcium in the presence of larger amounts of magnesium. *Talanta* **15**, 385-390.

Ullman, W. J., and Sandstrom, M. W. (1987). Dissolved nutrient fluxes from the nearshore sediments of Bowling Green Bay, Central GBR Lagoon (Australia). *Estuarine, Coastal and Shelf Science* **24**, 289-303.

Webster, I. T., and Harris, G. P. (2004). Anthropogenic impacts on the ecosystems of coastal lagoons: modelling fundamental biogeochemical processes and management implications. *Marine and Freshwater Research* **55**, 67-78.

Weis, R. F. (1970). The solubility of nitrogen, oxygen and argon in water and seawater. *Deep Sea Research* **17**, 721-35.

West, R. J., Thorogood, C. A., Watford, T. R., and Williams, R. J. (1985). An Estuarine Inventory of NSW, Australia, *Fisheries Bulletin* **No 2**, NSW Department of Agriculture**.**

APPENDIX 1 – BENTHIC CHAMBER OPERATIONS

Both the manual and automatic chambers comprised a plexiglass cylinder, which isolated a volume of water (8.4 L) in contact with 0.066 m^2 of bottom sediment. Divers drew samples from manual chambers using 110 mL syringes attached to the end of tubes connected to the inside of each chamber (Figure 2-2). Spring-loaded syringes sampled the automatic chambers (Figure 2-3), controlled by an electronics module that applied a current across burn wires to release each spring-loaded device. Ambient water from immediately outside each chamber replaced water taken for sample draws. This entered each chamber via a narrow 20 cm tube that permitted water entry only during sample draws. Flux calculations involved a correction for the addition of ambient water.

Divers injected a caesium chloride (CsCl) spike into each manual chamber shortly after lid-closure. In automatic chambers, the electronics module controlled the release of the spring-loaded lid and spike injection. The observed decrease in Cs was used to model transport across the sediment-water interface and determine the rate of bioirrigation.

Water inside each chamber must equilibrate with ambient water before lid closure. We were uncertain of the time needed to achieve this, or whether after a length of time, the presence of the chambers would affect metabolite concentrations. To test this some chambers were left to equilibrate for 12 hours prior to lid closure and others were left for 1 hour before lid-closure. The length of time for equilibration did not appear to affect flux determinations. DO inside the chambers was the same as ambient water prior to all incubations regardless of equilibration time, and the initial metabolite concentrations and DO were also not significantly different.

Sub-samples for:

- NH_4^+ and SiO_4^{4-} were filtered immediately after collection through 0.45 μM filters and then taken to a nearby field laboratory for analysis.
- pH were left unfiltered and analysed immediately at the nearby field laboratory.
- alkalinity were filtered immediately after collection through 0.45 μM filters and analysed by Gran titration within 24 hours of collection at the nearby field laboratory.
- N_2 gas analysis were left unfiltered and carefully transferred (avoiding the introduction of bubbles) into 10 ml gas tight Quickfit glass vials containing 50 μL of concentrated $HgCl_2$ solution to preserve the sample. The glass vials were stored in a water bath at in-situ temperature (~20 °C) until analysed 3 weeks later at the Southern Cross University laboratories in Lismore. .
- Cs determinations were collected and analysed upon return from the survey in the Geoscience Australia laboratories.

APPENDIX 2 – CORE SAMPLE PROCEDURES

Using a pole corer (Figure 2-4), we collected cores using core barrels comprising a PVC tube, 73 mm in diameter. Once in the sediment, the core barrel was sealed by closing a ball valve at the top. This prevented disturbance of the sediment inside the core barrels during retrieval. In each core barrel, we obtained a sediment depth of around 400 mm and left a 100 mm cap of water to prevent exposure of the sediment to air.

Cores were processed at a nearby field laboratory immediately after collection. We extruded and sliced each core into sub-samples according to the following: 0.5cm intervals for the top 3 cm, 1 cm intervals between 3 and 6 cm, and 2 cm intervals between 6 and 12 cm depth. This was done in a nitrogen gas filled glove bag to prevent exposure of the sediment and porewaters to oxygen. Sediment slices were loaded into nitrogen gas filled centrifuge tubes, which were centrifuged at 11 000 rpm for 5 min to separate the solid phase from the porewaters. The porewaters were removed using a syringe and filtered through 0.45 μm filters. Porewaters were immediately analysed for NH_4^+, SiO_4^{4-}, and Chlorophyll a (Chl-a). TCO_2 was analysed by means of conductivity, which Geoscience Australia was trialing for the first time during this survey. The remaining sample was frozen and analysed for PO_4^{3-}, NO_3^- and NO_2^-, upon return to Geoscience Australia.

The solid phase from each core slice was also frozen and returned to the Geoscience Australia laboratories. Here, they were freeze-dried and analysed for total organic carbon (TOC), major elements using XRF, and nitrogen and carbon stable isotopes. We also measured the sediment porosity of each depth interval.

APPENDIX 3 – CORE INCUBATION PROCEDURES

After collection using the pole corer described in Appendix 2, the three cores collected from each site were immediately transported to a field laboratory for incubation. We kept about 200 mm of overlying water (bottom water) above the sediment in each core barrel and sealed the base of each core with an o-ring-fitted plastic plug (Figure 2-5). A gas-tight lid, fitted on the underside with a magnetic stirrer, sealed the top of each core, and constantly mixed the bottom water to avoid stratification. The stirrer was spun by means of a second magnet, situated on top of the lid, driven by a small motor (Figure 2-5).

Sub-samples for SiO_4^{4-}, NH_4^+, alkalinity and TCO_2 were filtered using 0.45 µM disposable filters. SiO_4^{4-}, NH_4^+, alkalinity, pH, and TCO_2 were analysed in the field. TCO_2 was calculated from the alkalinity and pH measurements, and also analysed directly by means of conductivity. The results from these two different methods were subsequently compared.

APPENDIX 4 – CHEMICAL ANALYSIS

A4a. Alkalinity and Carbon Dioxide

The alkalinity was determined by Gran titration, whilst the carbonate alkalinity (CA) was estimated by subtracting the alkalinity contribution of $B(OH)_4^-$. Carbon dioxide (TCO_2) was estimated from pH and carbonate alkalinity according to Mehrbach *et al*. (1973) using:

$$TCO_2 = CA\frac{1+K_2/a_H+a_H/K_1}{1+2K_2/a_H}$$

Where:
a_h is the activity of the hydrogen ion
K_1 and K_2 are the first and second ionisation constants of carbonic acid (H_2CO_3).

A4b. Carbon Dioxide by Means of Conductivity

We also determined TCO_2 by means of conductivity according to the method described by Hall and Aller (1992). The continuous flow system comprised a peristaltic pump supporting three flow channels (sample, acid, and base), a cell mixing the sample and acid channels, a gas permeable membrane separating TCO_2 from the acidified sample flow, and a conductivity cell analysing TCO_2 in the receiving base flow by means of a change of conductivity. The conductivity cell was kept in a water bath with a constant temperature of 30°C. The pump speed was set to '5', and we chose Skalar silicon tubing colours as follows:

Sample: yellow-white; acid (HCl): orange –white; and base (NaOH): blue-white. A conductivity cell with k=0.117 was used, but the instrument was set to k=0.351. Standard solutions (1, 2, 5 mM) were prepared from a 100 mM stock solution, of Na_2CO_3 and purged demineralized water. They were kept gas-tight in small bottles with septa. We used a 30 mM HCl acid solution and 5-10 mM NaOH base solution. The conductivity meter was linked to a computer for continuous recording.

The conductivity of the carbonate-free base flow gave a signal of ~ 1000 mV and standard sea water (2.1 mM TCO_2) mixed with the acid resulted in a drop of ~200 mV. The signal was stable with ± 2 mV resulting in an analytical precision of ±20 µM. Calibration was highly reproducible over several days (Figure 4A).

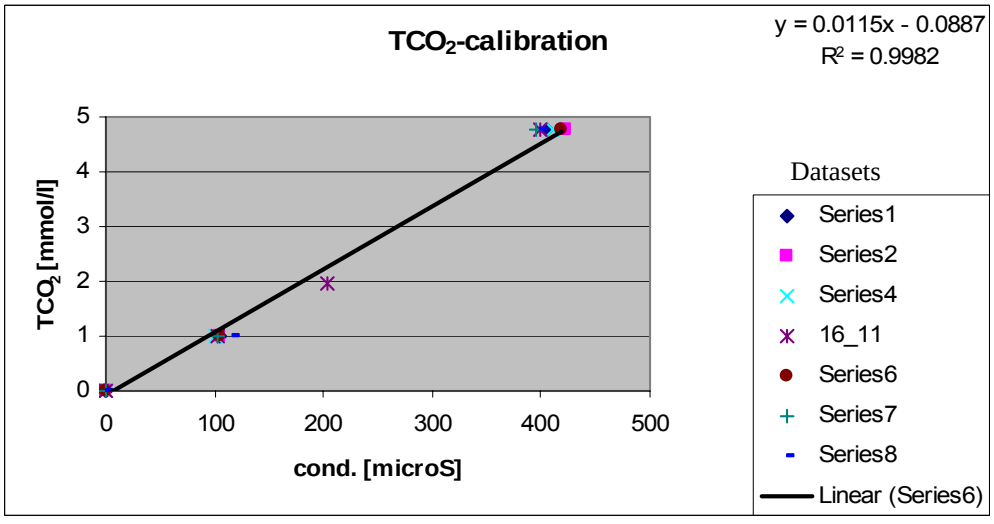

Figure 4A. Calibration results of the direct TCO_2 method over several days.

A4c. Dissolved Inorganic Nutrients

Ammonia (NH_4^+) and silicate (SiO_4^{4-}) were determined immediately after sample collection at our nearby field laboratory. They were analysed using a Bran+Luebbe (B+L) Auto Analyser 3, segmented flow instrument system based on the standard colourimetric methods of Grasshoff (1983).

The colourimetric method used for NH_4^+ was the Berthelot reaction, with phenol, citrate, EDTA and sodium nitroprusside, and for SiO_4^{4-} we used the molybdenum blue method, with ascorbic acid and oxalic acid.

Hydrogen sulfide (H_2S) was removed from the porewaters to prevent its interference in the analysis of nutrients. It was removed at the time of sampling, by sparging high purity nitrogen gas (N_2) through the samples in positive pressured sample vessels until the H_2S odour ceased.

A4d. Nitrogen

Southern Cross University Environmental Analysis Laboratory analysed the benthic chamber samples for N_2. The laboratory used the method and instrumentation of Kana *et al*. (1994) with the following modifications. Gases were detected with a Balzers QMS422 quadrupole mass spectrometer and a water bath (± 0.01°C) was used to stabilize sample temperature in the water line upstream of the membrane. The effect of O_2 in the sample on the N_2 signal measured by the membrane inlet mass spectrometer was corrected by making a standard curve of O_2 concentration against N_2 : Ar ratios using water standards made from the incubation water equilibrated with the atmosphere at constant temperature (Eyre *et al*. 2002).

A4e. Chlorophyll-a

For each chlorophyll-a (Chl-a) analysis, we weighed 3 – 5 g of wet sediment into a 15 ml PE vial (must resist acetone), and added 10 mL of acetone (90 %, saturated with $MgCO_3$). The vial was then closed and placed on a Vertex mixer for vigorous mixing of the sediment and the acetone. Chl-a rich sediments were immediately recognized by the green coloration. The vial was then placed into an ultrasonic bath for ~ 30 min, centrifuged, and the supernatant extraction solution poured into a second vial. From this vial, we transferred 1 mL of solution into a photometric glass cell and placed it in a photospectrometer for the photospectrometric analysis of Chl-a (and pheophytin, a degradation product). The sample was analysed at wavelengths of 664 nm and 750 nm and the result recorded. We then added 100 µl of 0.1 N HCl to the solution in the glass cell and again analysed at wavelengths of 664 and 750 nm. The concentration of Chl-a and pheophytin was given as µg / g dry sediment and calculated according to the following US-EPA equations:

$$Chl-a[\mu g/g] = \frac{26.7((664-750)-(664a-750a))extr-vol}{sed-massL}$$

$$Pheophytin[\mu g/g] = \frac{26.7(1.7(664a-750a)-(664-750))extr-vol}{sed-massL}$$

Where:
664 / 750 is the optical density of original extraction solution,
664a / 750a is the optical density after acidification,
extr-vol is the volume of the extraction solution, e.g. 10 mL,
sed-mass is the weight of dry sediment, e.g. 2 g.,
L is the pathlength of the photospectrometric cell, e.g. 1 cm.

A4f. Caesium

Samples for Caesium (Cs) analysis were diluted 200 fold with polished (milliQ) water and acidified with 10 mL HNO_3. Concentrations were measured using a Perkin-Elmer ELAN 6000 ICP-MS. An internal standard was added and Cs concentration was determined using a standard calibration curve.

A4g. Stable Isotopes

Sediments were analysed for $\delta^{15}N$, $\delta^{13}C$, and total nitrogen (TN) using a Thermo Finnigan Flash EA series 1112 interfaced to a Thermo Finnigan Conflo III. A Finnigan Mat 252 using ISODAT NT software carried out the isotopic measurements and EAGER software operated the Flash EA. The oxidation furnace of the Flash EA was packed with copper oxide and silvered cobaltous oxide and operated at 900°C. The reduction furnace was packed with pure copper and operated at 600°C. Combustion products were separated on a packed GC column run isothermally at 40°C. We conducted carbon and nitrogen analysis separately to improve reproducibility and accuracy.

For nitrogen analysis, ground dry sediment samples were loaded into tin foil cups. These were placed in the auto-sampler along with a series of blanks and standards used for isotope correction and TN calculation. International standards IAEA N1 and IAEA N2 were used along with caffeine, which was used as a secondary standard and has been previously calibrated against international standards. CO_2 was removed in all nitrogen analysis by passing the gas stream from the GC through a trap of Carbosorb As Self-indicating granules (BDH Prod # 331634T). Water was removed from the gas stream using a 6 to 18 mesh Magnesium Perchlorate water trap. All analyses were carried out in duplicate.

For carbon analysis, 0.5 to 1.0 mg ground dry sediment samples were loaded into tin foil cups. Sulfurous acid was added drop wise to the sediment and allowed to react for at least 15 minutes. Samples were then dried for an hour in an oven at 100°C to drive off sulfurous acid and water. Acid addition was repeated and the drying process carried out if no further effervescence was observed. Each acidified sediment sample, still in its tin capsule,was then placed inside a second tin capsule before being placed in the auto-sampler along with a series of blanks and standards used for isotope correction. Standards ANU Sucrose, TO2 and caffeine were used for isotopic calibration. Water was removed from the gas stream using a 6 to 18 mesh Magnesium Perchlorate water trap. All analyses were carried out in duplicate.

APPENDIX 5 - DATA ANALYSIS

A5a. Benthic Fluxes across the Sediment-Water Interface

Fluxes were calculated by linear regression of the benthic chamber solute (nutrient and gas) concentrations, corrected for the addition of replaced water when samples drawn. Figure 5A shows, as an example, a linear regression through O_2 and TCO_2 concentrations measured in a dark chamber at Site 4. For all solutes measured, only data points within the period of linear decrease in O_2 were included, as a linear decrease in O_2 over time indicated that conditions in the chamber were unperturbed, or not effected by the presence of the chamber itself.

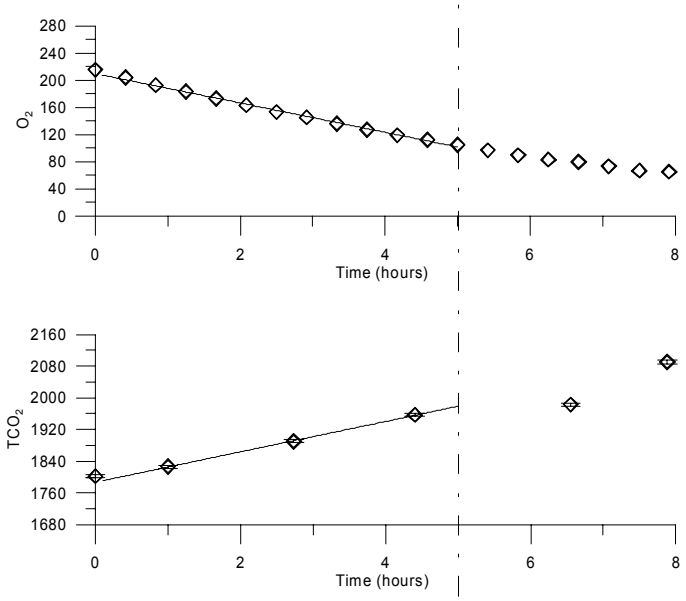

Figure 5A. O_2 and TCO_2 in μM for Chamber 4 at Site 4 (μM). Fluxes were determined only from data points that fell within the time that O_2 uptake was linear. In this example, O_2 uptake was linear for the first 5 hours; indicating that, during this time, the chamber was not significantly perturbing the nutrient dynamics of the system. Therefore, solute fluxes (TCO_2 in this particular example) were determined using only data points from the first 5 hours of the incubation.

For core incubations, we measured solute concentrations at the beginning, and end of each incubation (at time t_0 and time t_1) and assumed the rate of uptake or release of solutes between these times was linear. If however, the bottom water became anoxic (< 10 % O_2-saturation) over the course of the incubation ($t_1 - t_0$), the system was considered too perturbed and the fluxes invalid.

We used the following equation to calculate the total flux (J) for each solute (x) in μmol m^{-2} day^{-1} for benthic chamber and core incubation data.

$$J(x) = \frac{(C_1 - C_0)Vol}{Øt}$$

Where:
C_1-C_0 is the linear change in solute concentration over time t
Vol is the volume of water above the sediment
$Ø$ is the surface area of sediment

We also calculated the coefficient of variance of dark chamber replicates at each site shown in Table 3-2 using:

$$Co.Var. = \sqrt{\frac{\sum (x-\mu)^2}{(n-1)}} \div \mu \times 100$$

Where:
x is each concentration value
μ is the sample mean
n is the number of replicate measurements at each site

This gives a measure of the degree of variance as a percentage of the mean.

A5b. Denitrification Efficiency

Denitrification efficiency is the percentage of total N released from the sediment as N_2 gas. We calculated N_2 fluxes using two methods: (1) by directly measuring the change in N_2 concentrations inside each chamber, and (2) by using a Redfield ratio organic matter source (106C:16N:1P), calculating the total N flux expected based on TCO_2 fluxes, and subtracting the NH_4^+ flux component. For method (2), we assumed NO_x fluxes were negligible, as in previous Geoscience Australia studies, in similar environments, the majority of NO_x fluxes were close to zero. N-fixation and TCO_2 flux from calcium carbonate dissolution were also assumed negligible.

The equations for calculating denitrification efficiencies for each of the two methods were:

(1) $$Denitr.eff.[\%] = \frac{6.6J(N_2)}{J(TCO_2\_org)} \times 100$$

(2) $$Denitr.eff.[\%] = \frac{\left(\frac{J(TCO_2\_org)}{6.6} - J(NH_4^+)\right)6.6}{J(TCO_2\_org)} \times 100$$

Where:
$J(N_2)$ is the N_2 flux measured in each chamber
$J(TCO_2\_org)$ is the TCO_2 flux related to organic matter decomposition in the sediment
$J(NH_4^+)$ is the NH_4^+ flux measured in each chamber

A5c. Diffusive Fluxes at the Sediment-Water Interface

Vertical pore water profiles show concentration gradients, which drive molecular diffusion. Therefore, we used pore water concentration profiles to calculate diffusive fluxes according to the methods of Schulz (2000), where the solute concentration gradient between the bottom water and the uppermost pore water sample (top 0.5 cm) gave an estimate of molecular diffusion at the sediment-water interface.

Firstly, the molecular diffusion coefficient in seawater (D_{SW}), at a given temperature, was corrected for the *tortuosity* in sediments, using porosity measurements (ϕ) and the following equation:

$$D_{sed} = \frac{D_{SW}}{1 - \ln(\phi^2)}$$

The diffusive flux was then calculated as:

$$J_{diff} = -\phi D_{sed} \frac{\partial C}{\partial z}$$

Where:
$\partial C / \partial z$ is the change in concentration over the depth interval ∂z.

A5d. The Diffusion and Irrigation Models

The modelling of tracer (caesium) loss from the benthic chamber to the sediments was undertaken in two parts. Firstly, we modelled the loss of tracer attributed to molecular diffusion. This diffusion model simulated the tracer loss using a finite difference model described by Townsend (1998) and Berelson *et al*. (1999) and given below:

$$C_{ch} = C'_{ch} + [\Delta t D_m/(\Delta z h)][2\phi_1^3(C_i - C_{i-1})]$$

Where:
C_{ch} is the concentration of tracer in the chamber
C'_{ch} in the tracer concentration in the previous time-step
Δt is the model time-step
Δz is the thickness of model sediment interval
h is the chamber height
D_m is the molecular diffusivity of the tracer
ϕ is the porosity of the sediment
C_i or C_{i-1} refers to the concentration of tracer in one cell and adjacent to it

The simulated tracer loss by diffusion was then compared to the measured tracer loss. The difference between the measured tracer loss and the simulated tracer loss by diffusion was attributed to other non-diffusive transport processes (primarily bioirrigation). Loss of tracer via adsorption was assumed negligible (Berelson *et. al*. 1996).

An irrigation term was then added to the model to take into account loss of a tracer by bio-irrigation. This model therefore simulated the loss of tracer from the chamber into the sediments via the transport processes of molecular diffusion and bioirrigation, and is given below:

$$C_{ch} = C'_{ch} + [\Delta t D_m/(\Delta z h)][2\phi_1^3(C_i - C_{i-1})] + [\Delta t \Delta z/h]\Sigma[I_i\phi_i(C_i - C_{i-1})]$$

Where:
I [m y^{-1}] is the non-local irrigation exchange rate constant

From the irrigation model, an irrigation velocity was derived. This was the rate, beyond molecular diffusion, at which the tracer was irrigated from the chamber into the sediments

APPENDIX 6 – SOLUTE VS TIME PLOTS

All solute concentrations are in μM except alkalinity, which is in μeq/L. Linear regressions are only drawn through data points used to calculate benthic fluxes, i.e. the data points corresponding to the time over which the O_2 uptake rate was linear. The same scale is used for each particular solute, except N_2. It was not possible to have a scale large enough to incorporate the range of absolute N_2 concentrations across all the sites and still be able to see the changes in

SGB - Central Basin (1A_1)

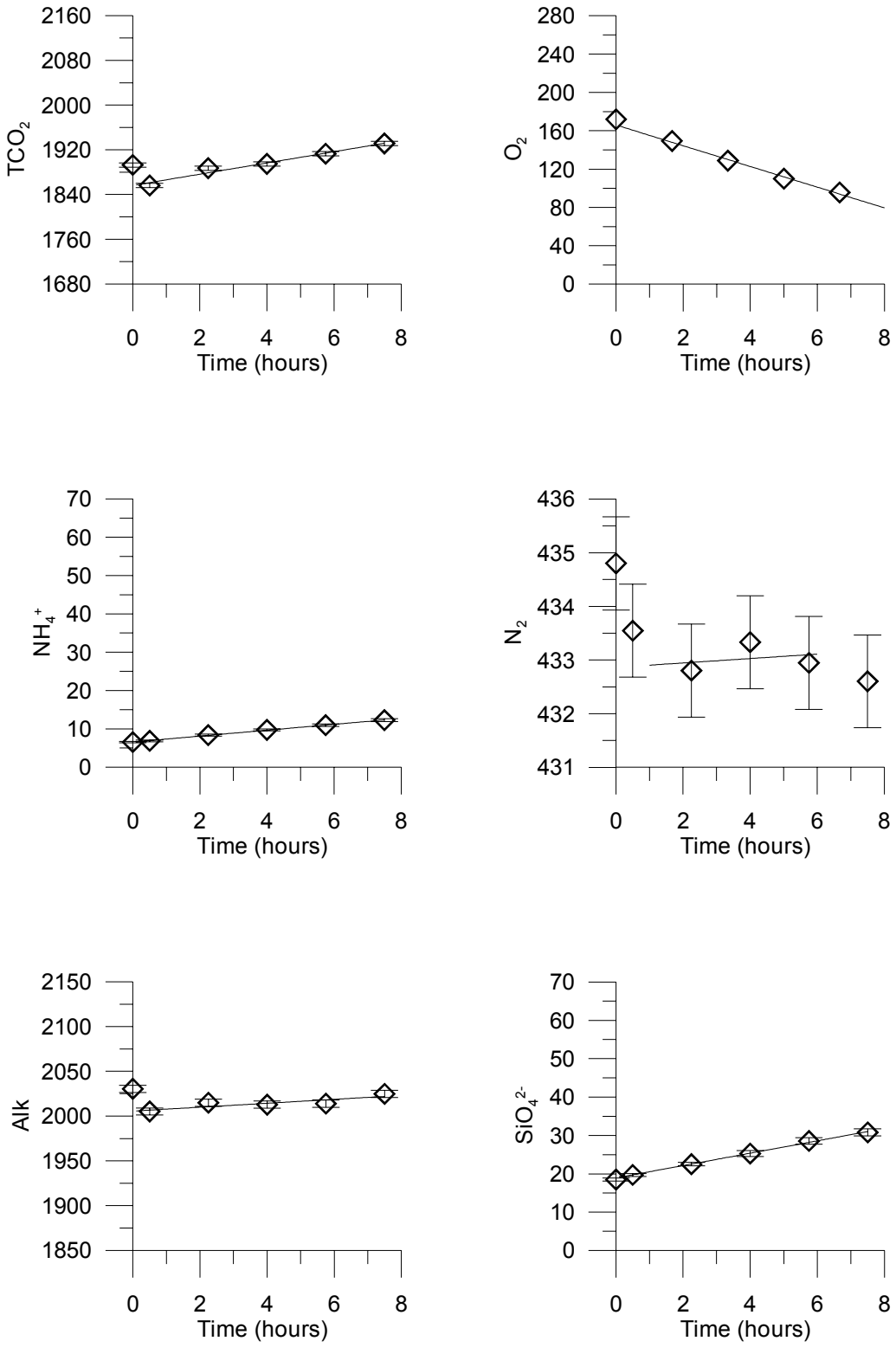

N_2 concentration over time in each plot.

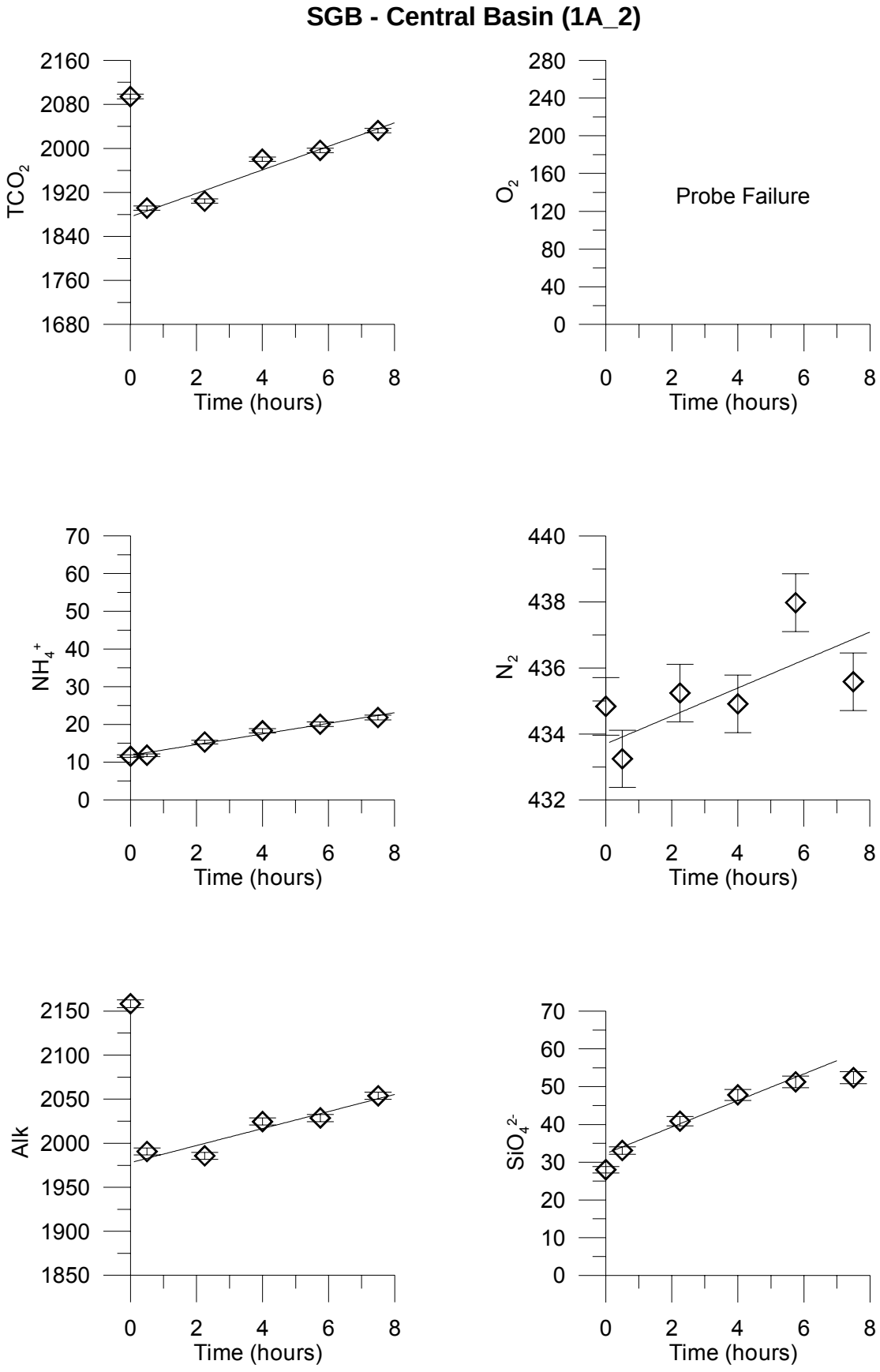

SGB - Erowal Bay (2A_3)

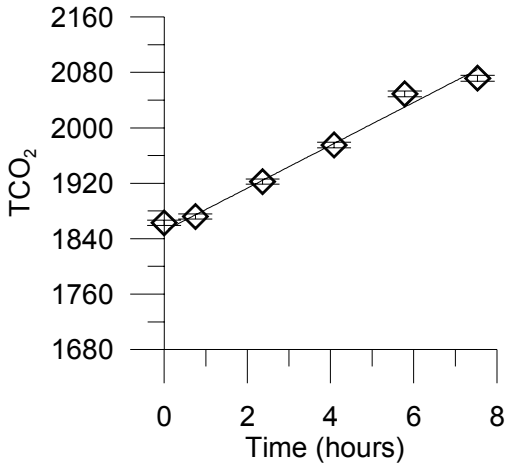

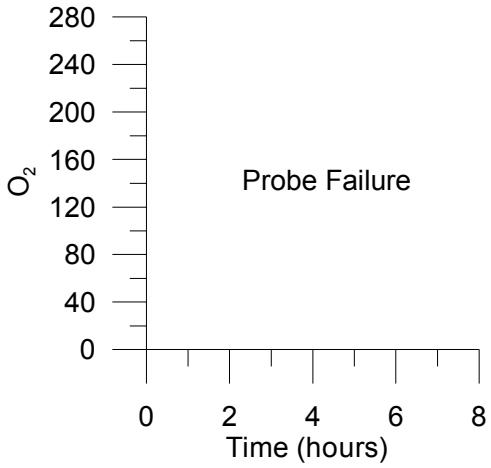

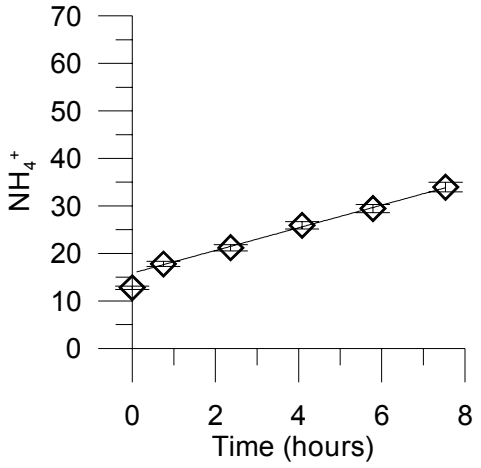

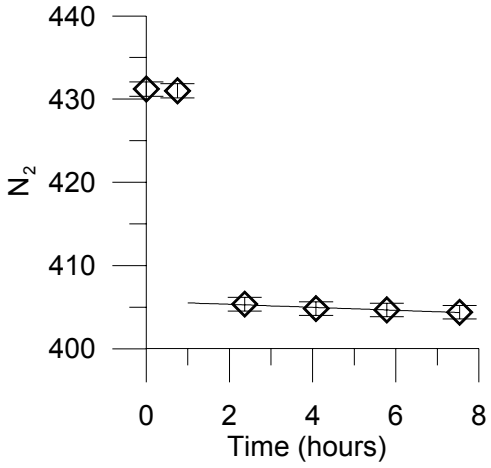

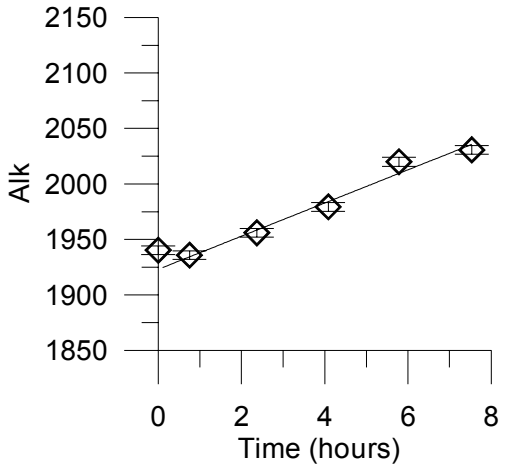

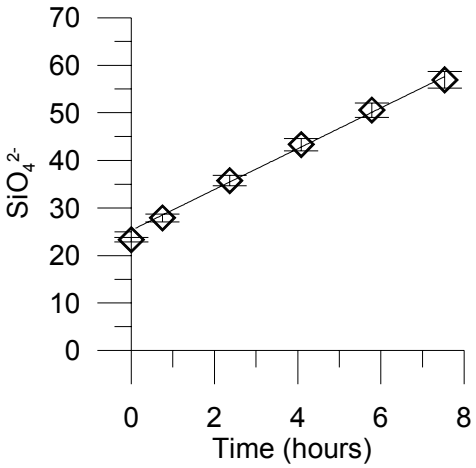

SGB - Erowal Bay (2A_4)

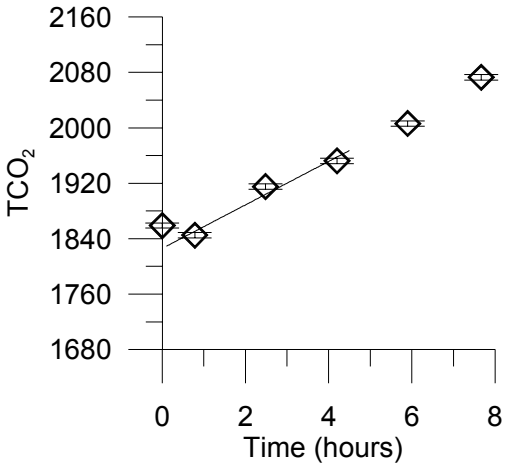

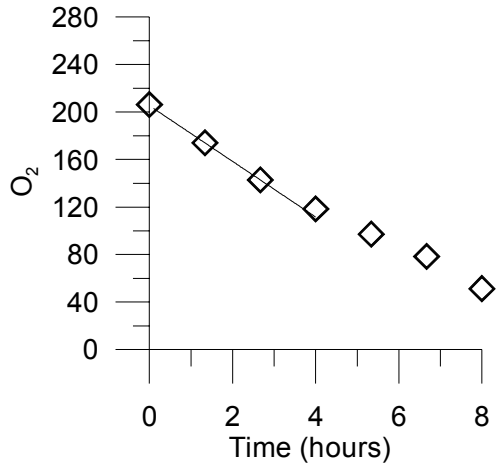

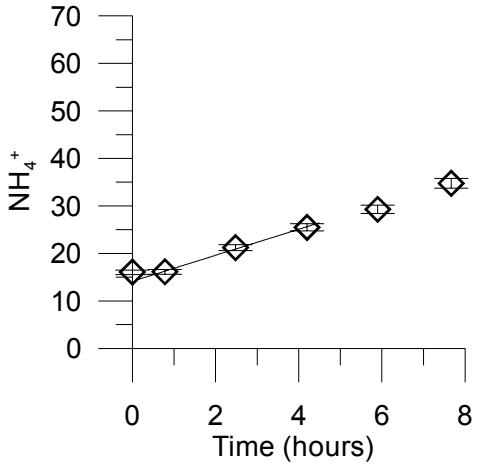

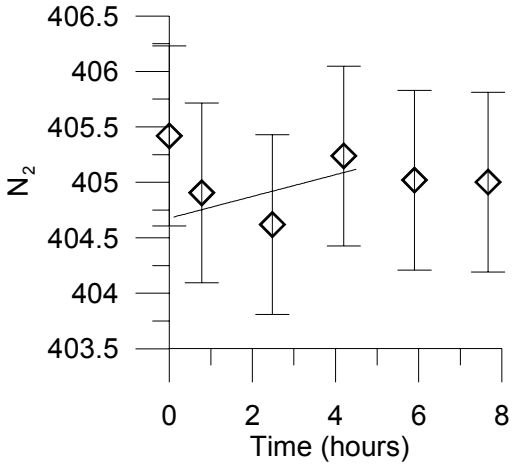

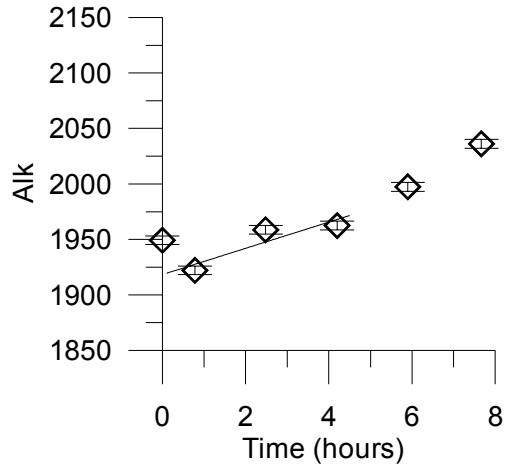

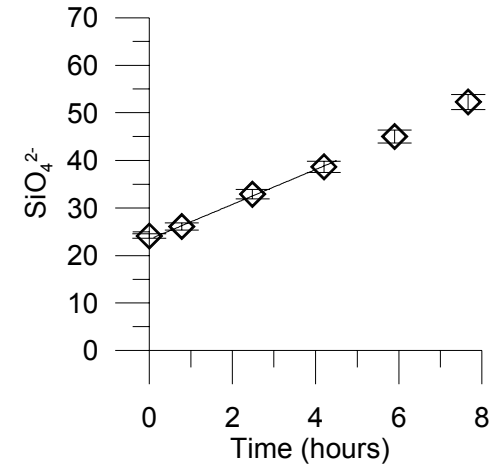

SGB - Erowal Bay (2A_7)

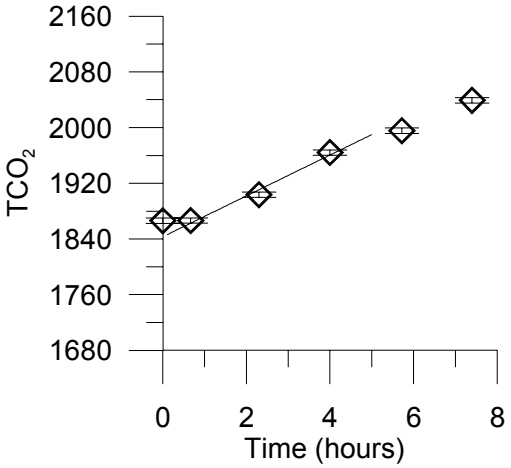

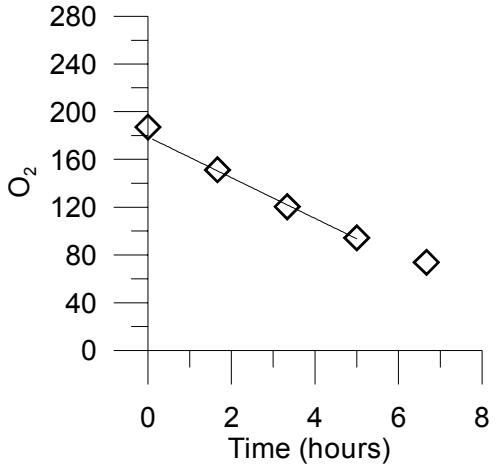

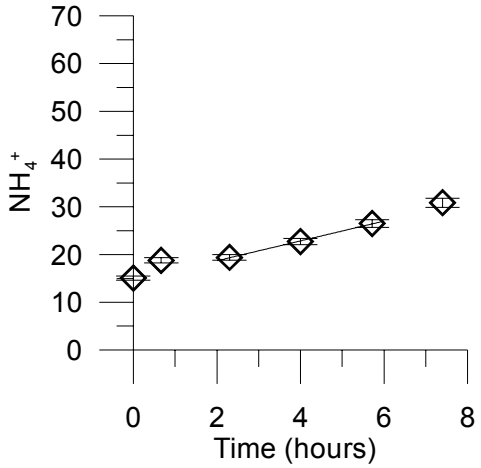

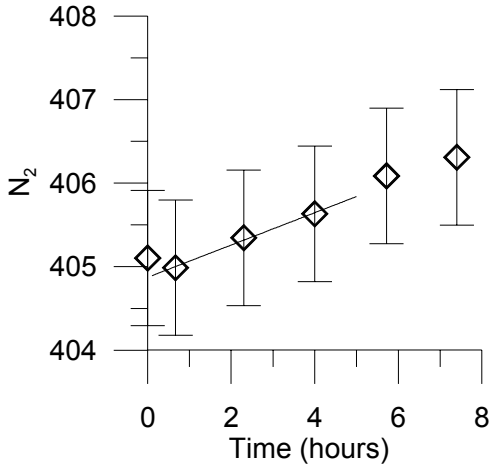

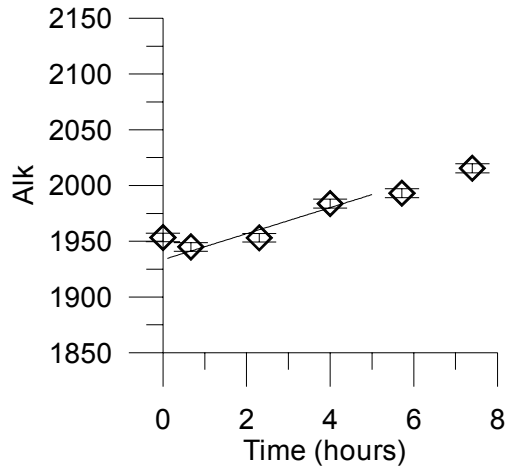

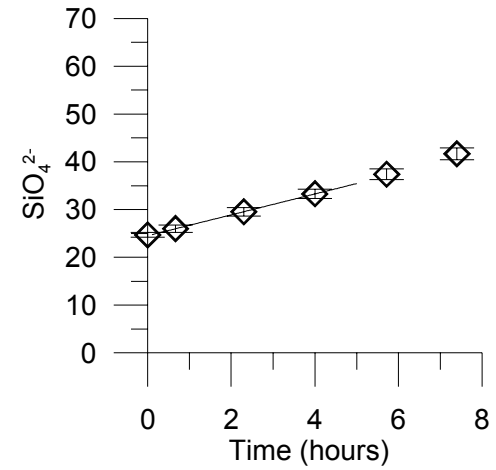

SGB - Erowal Bay (2A_8)

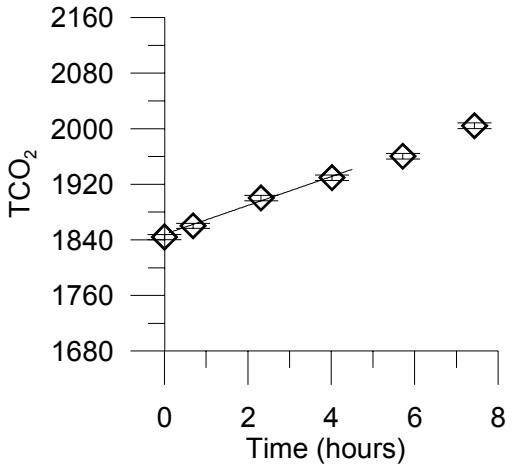

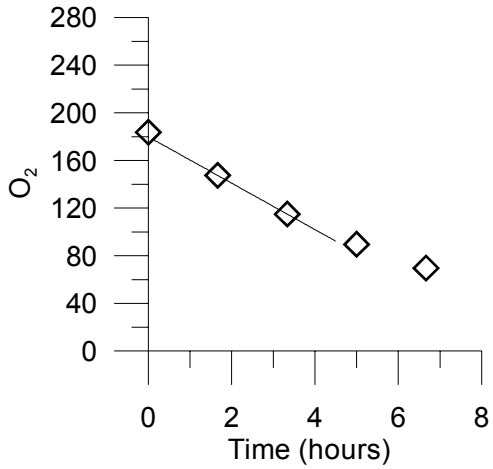

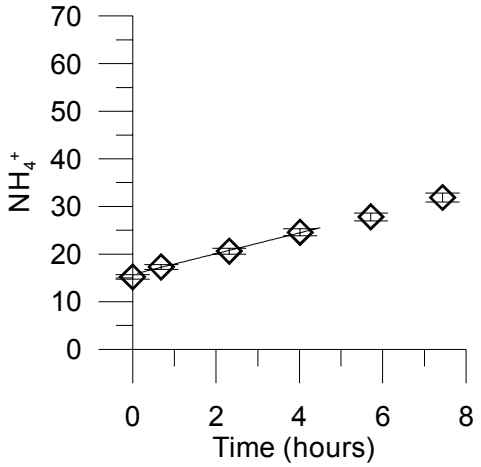

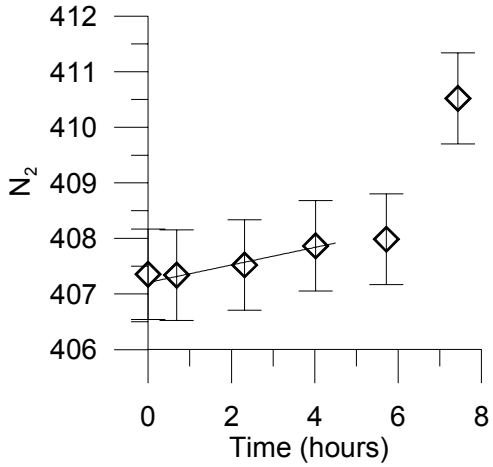

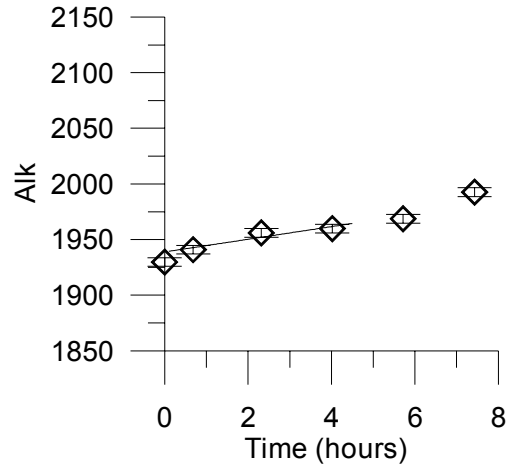

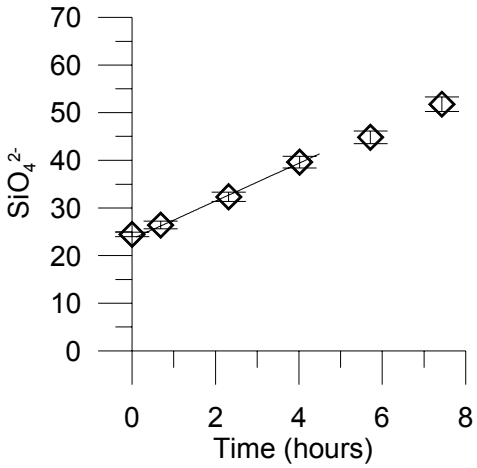

SGB - Erowal Bay (2A_9)

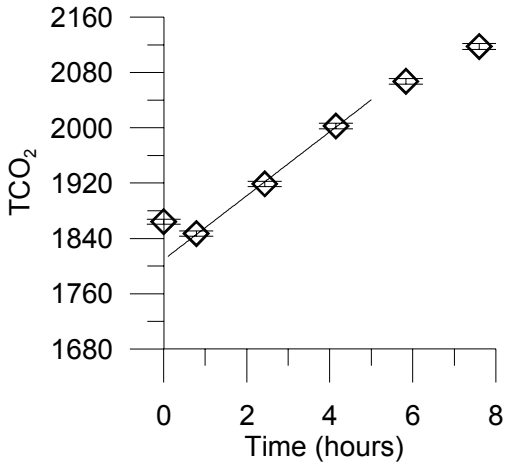

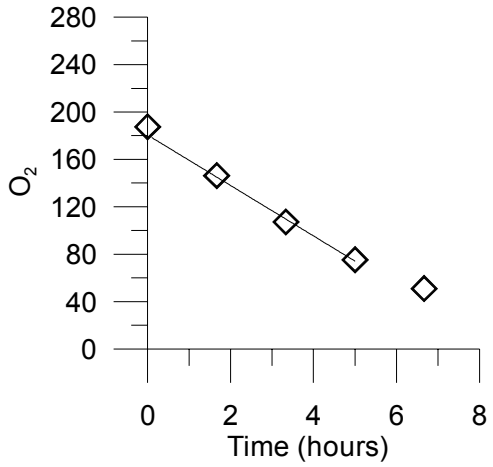

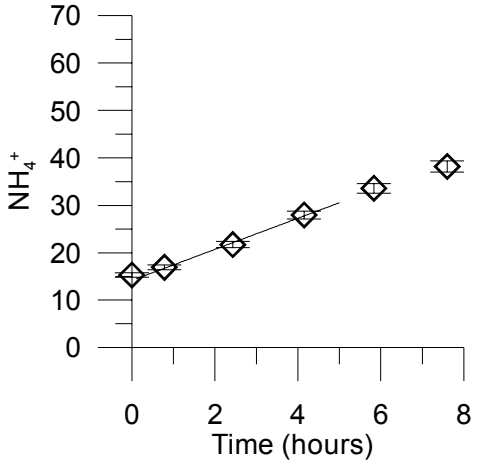

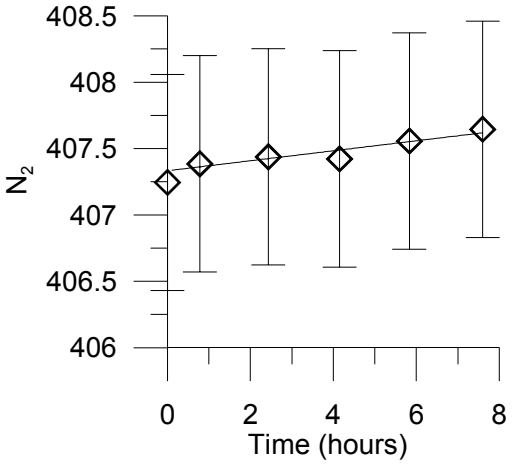

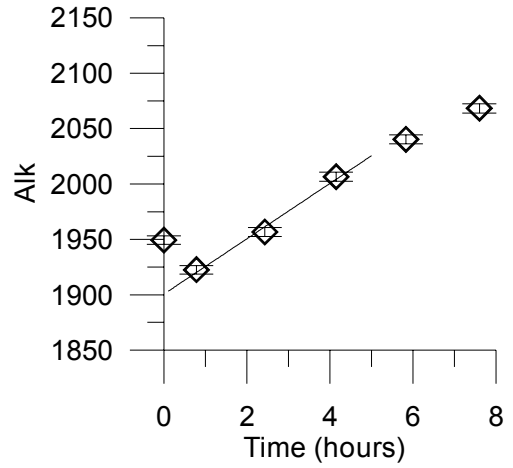

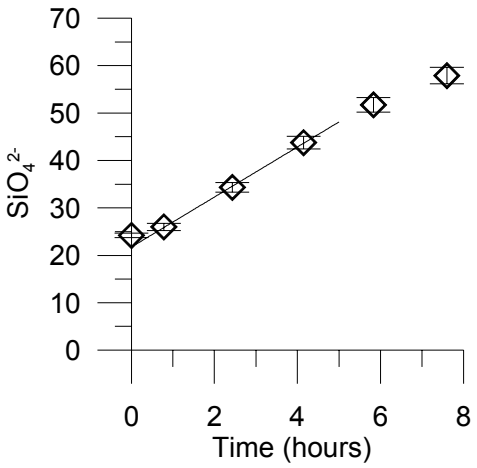

SGB - Wandandian Creek (3A_3)

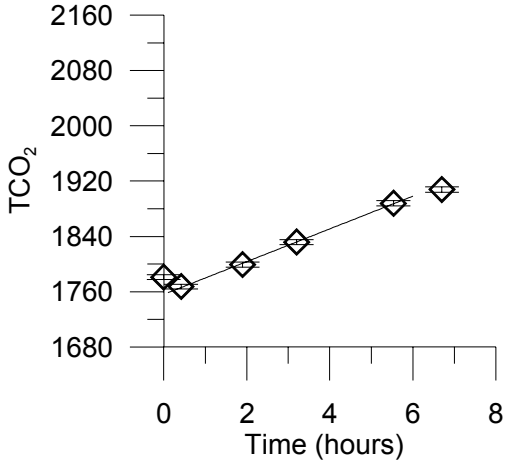

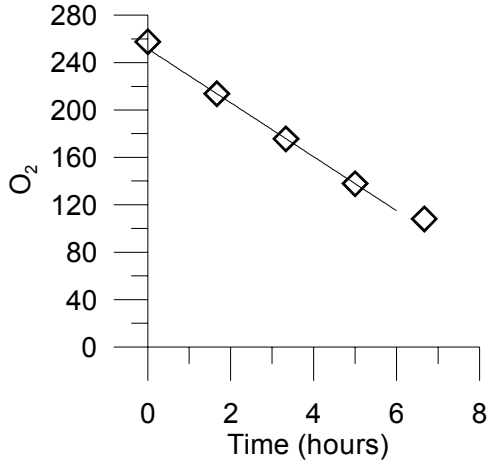

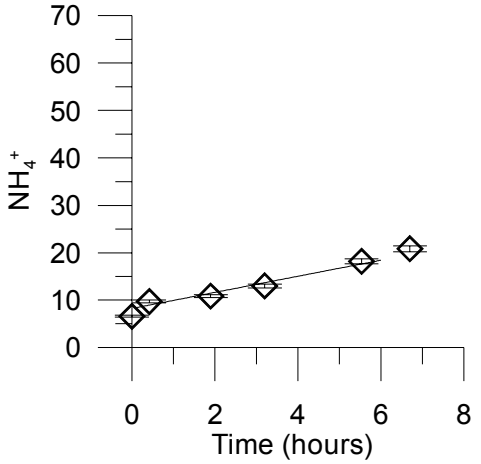

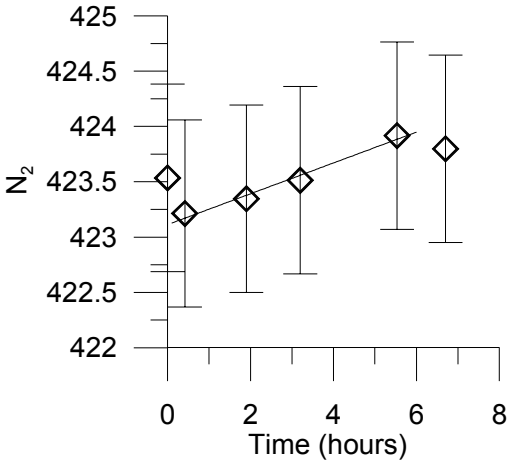

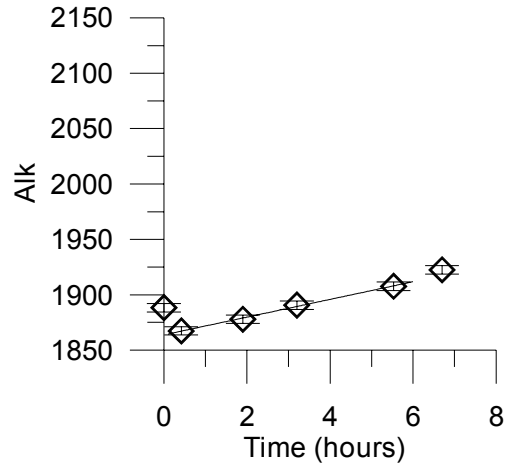

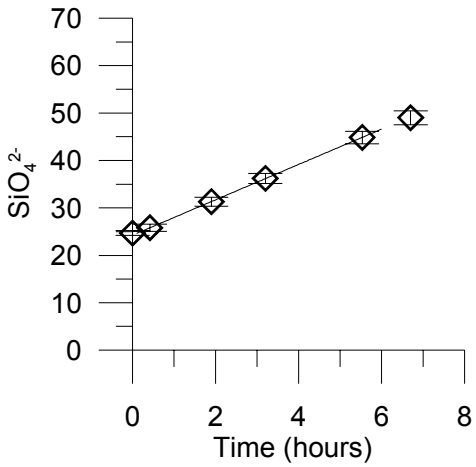

SGB - Wandandian Creek (3A_4)

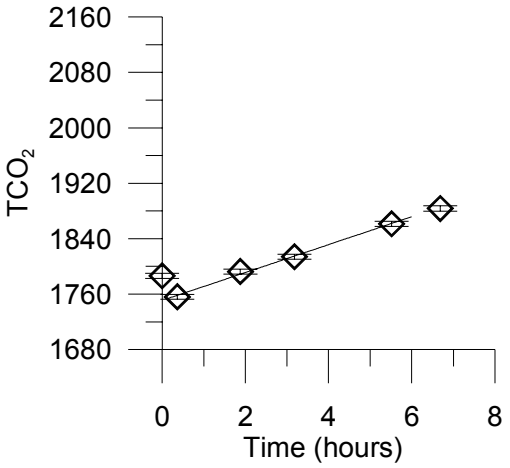

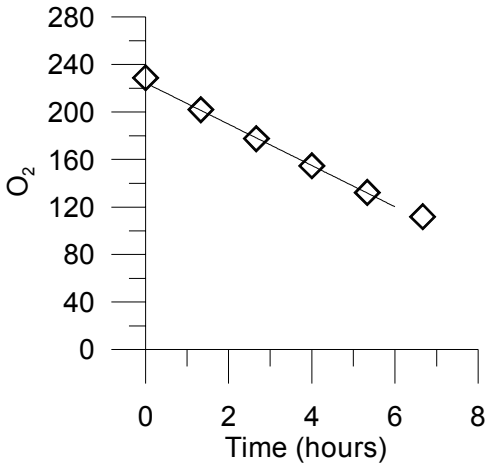

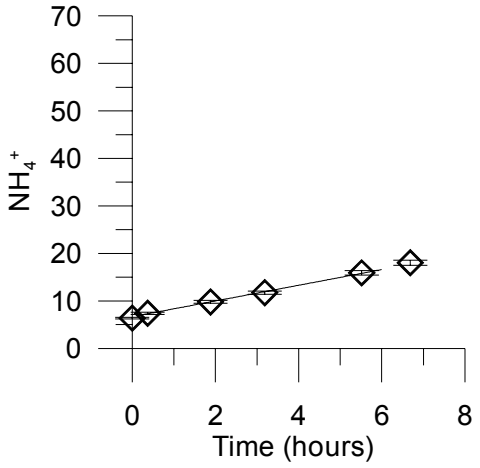

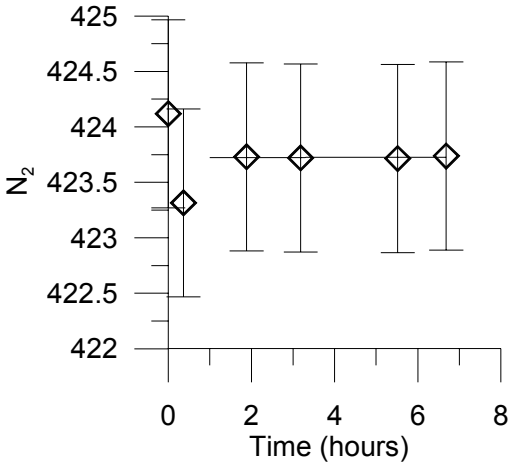

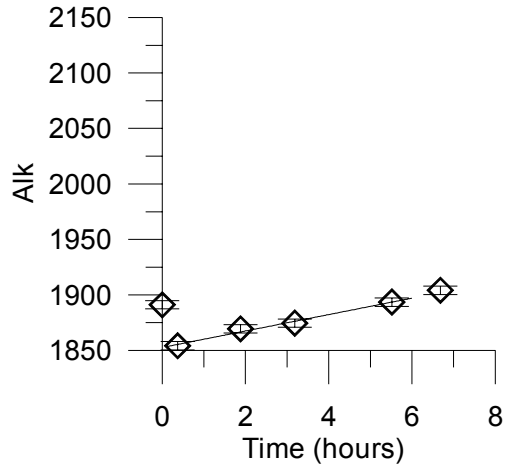

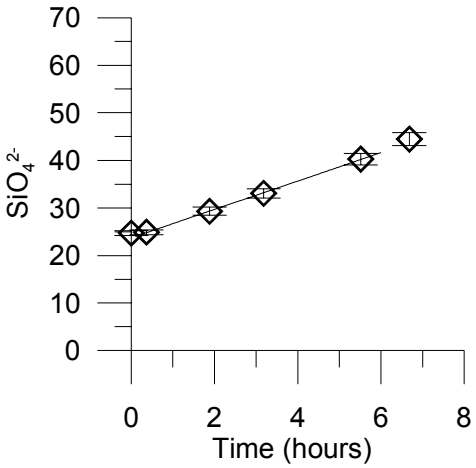

SGB - Wandandian Creek (3A_7)

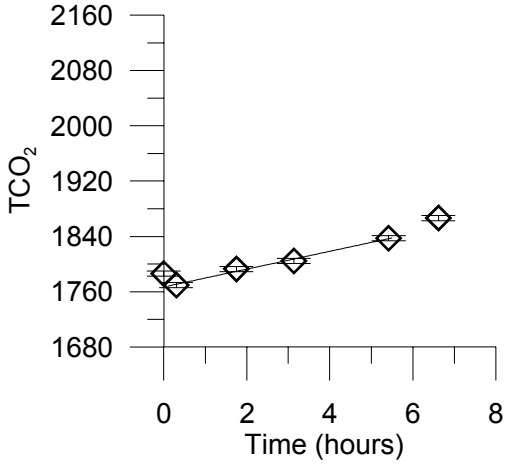

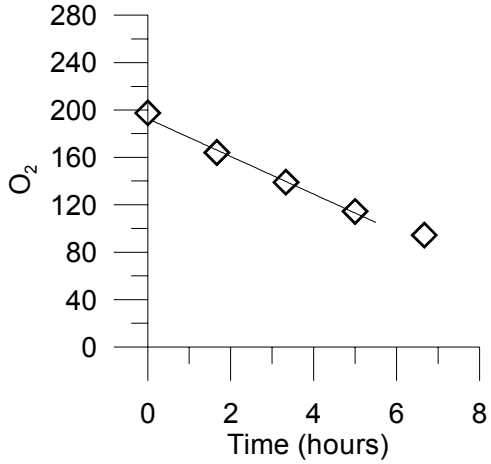

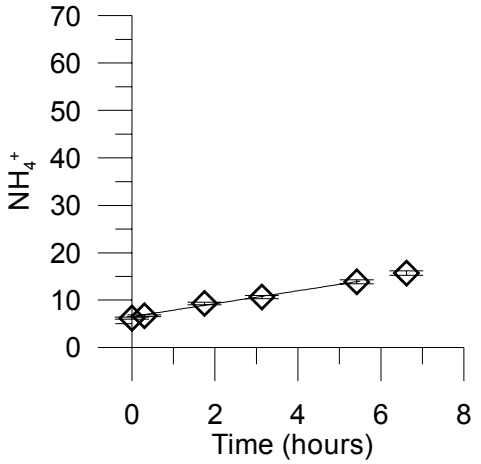

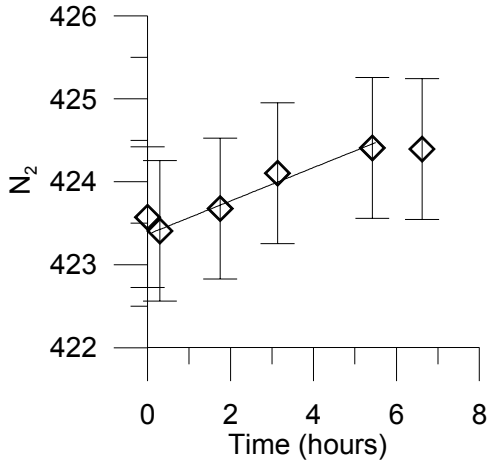

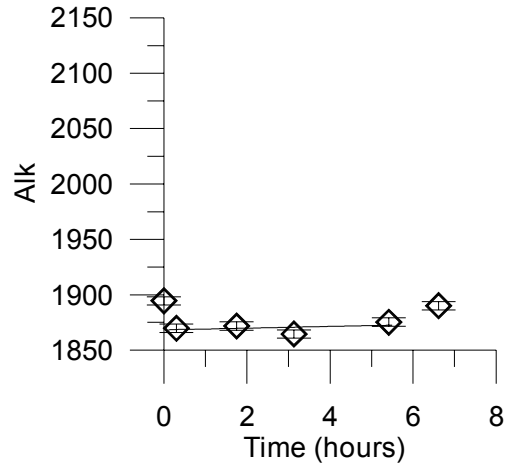

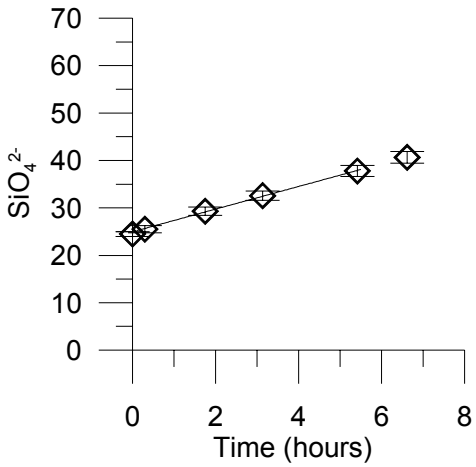

SGB - Wandandian Creek (3A_8)

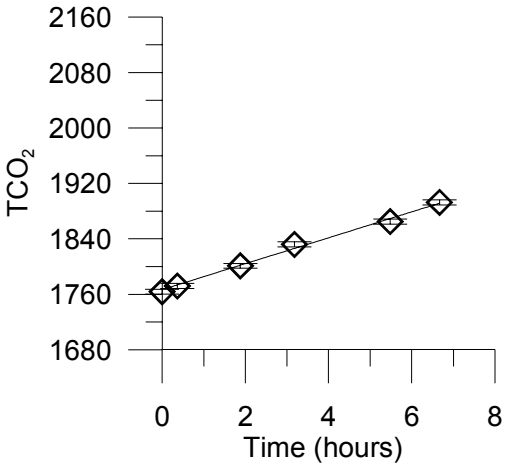

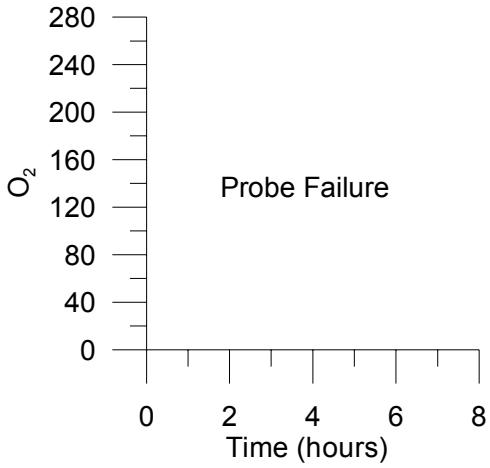

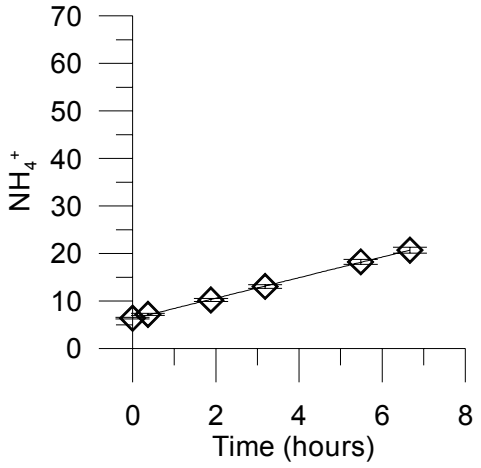

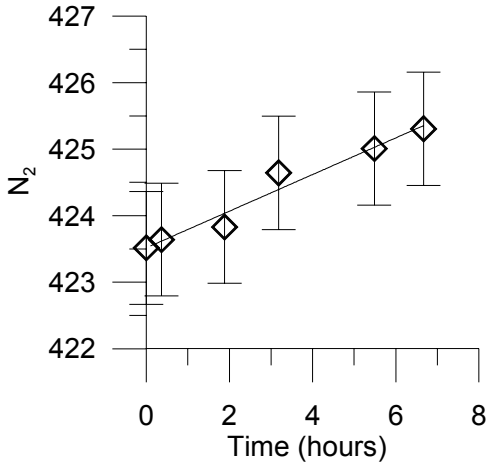

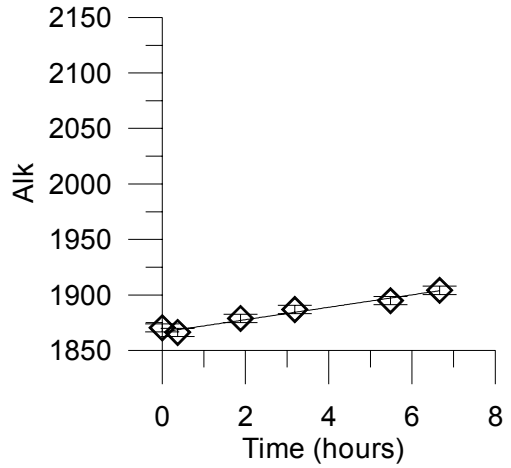

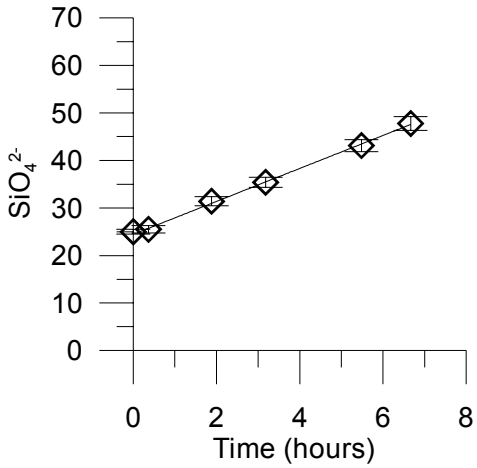

SGB - Wandandian Creek (3A_9)

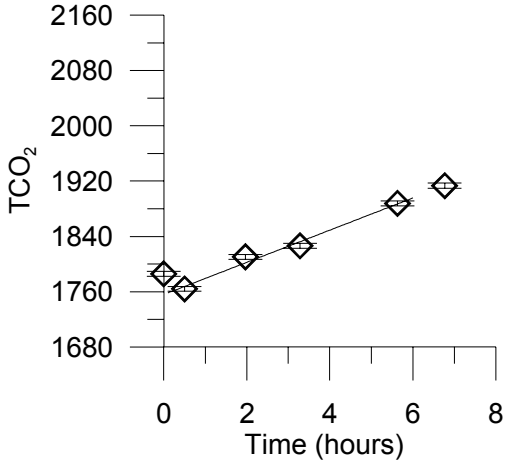

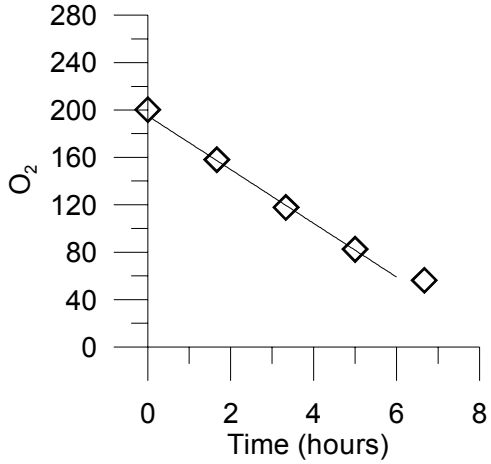

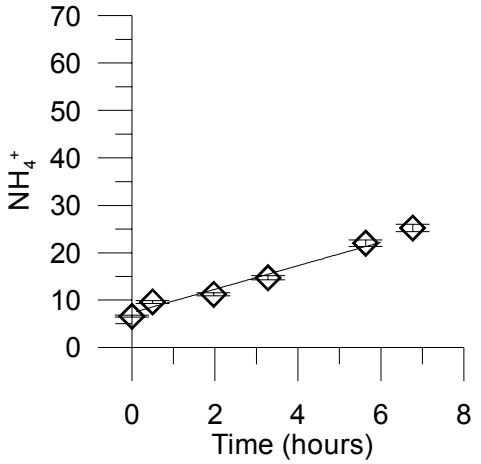

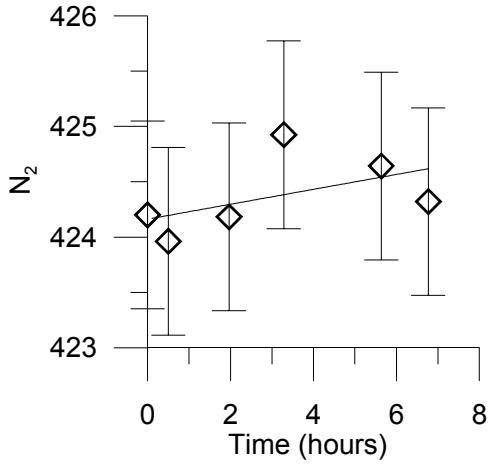

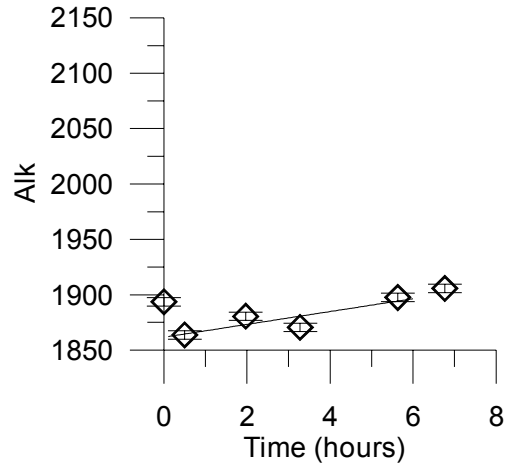

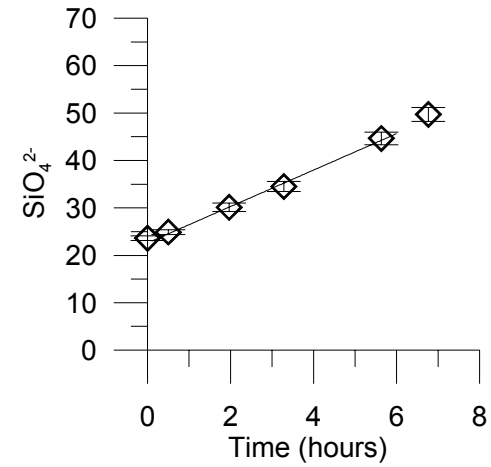

SGB - One Tree Bay (4A_3)

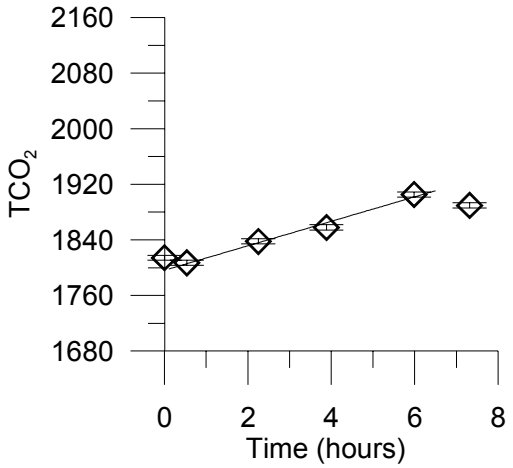

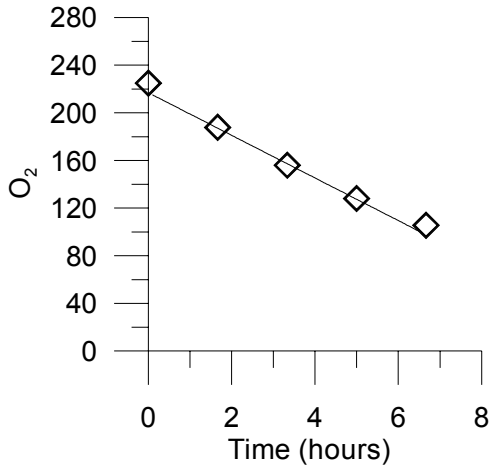

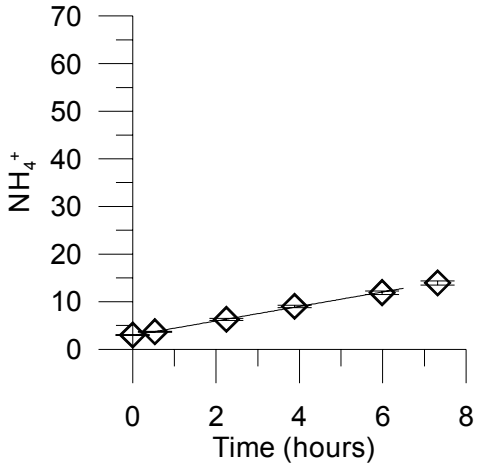

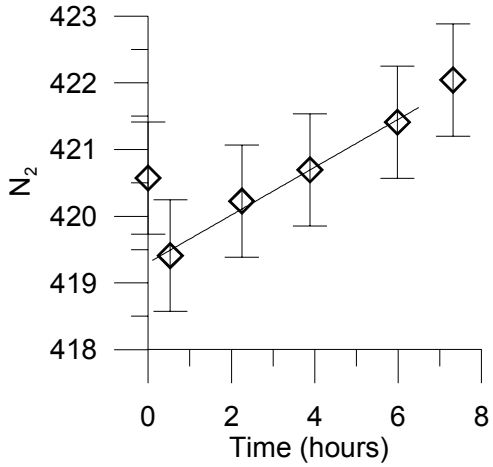

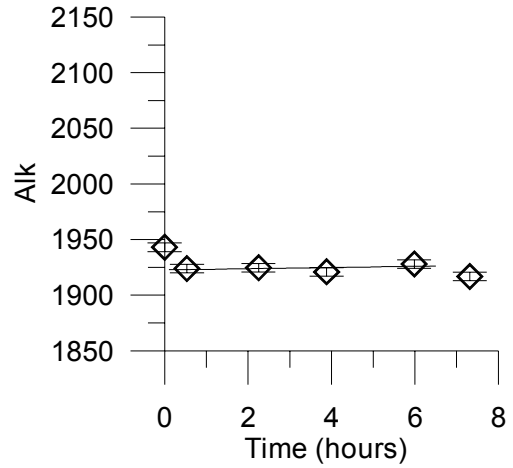

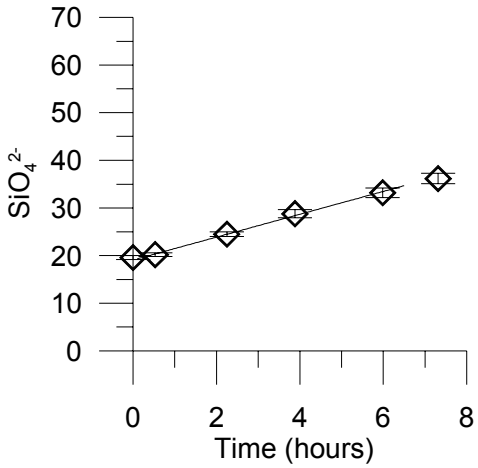

SGB - One Tree Bay (4A_4)

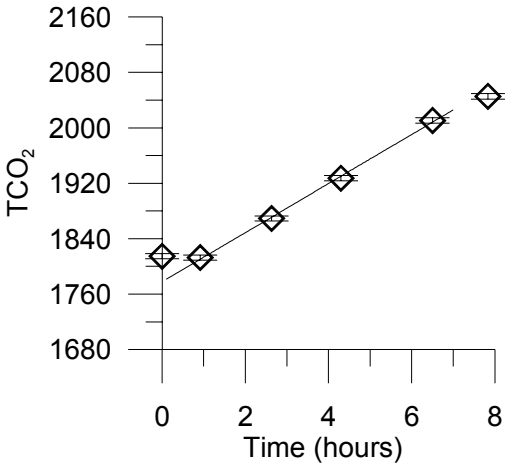

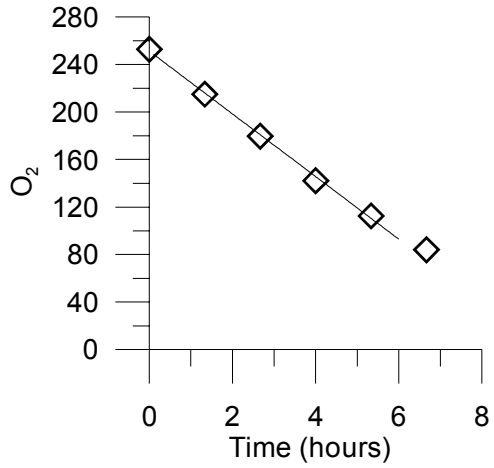

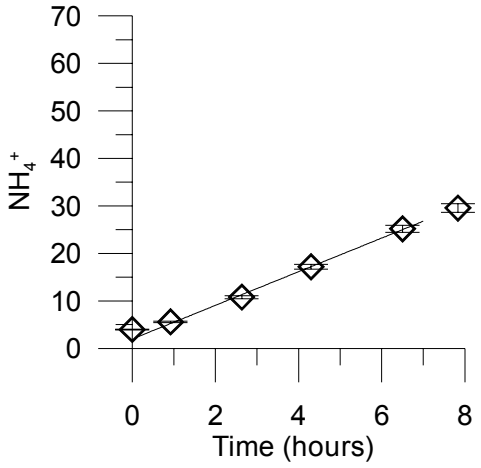

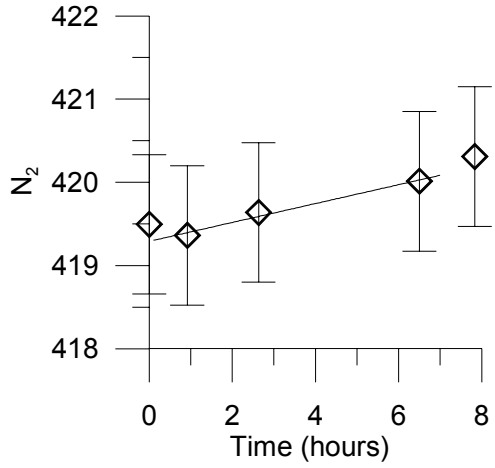

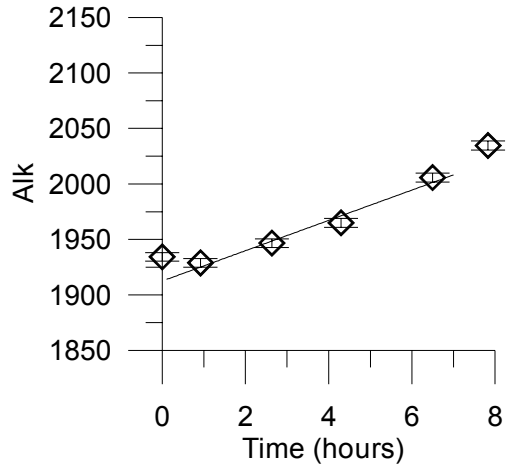

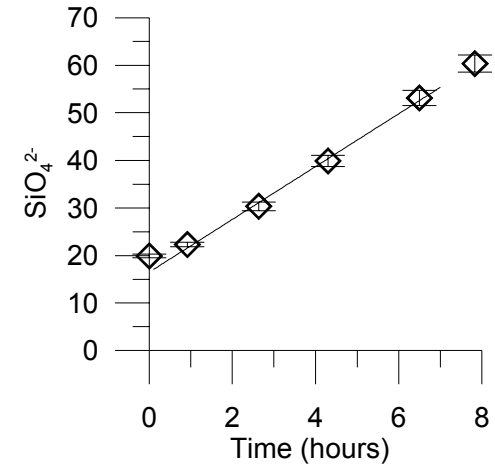

SGB - One Tree Bay (4A_7)

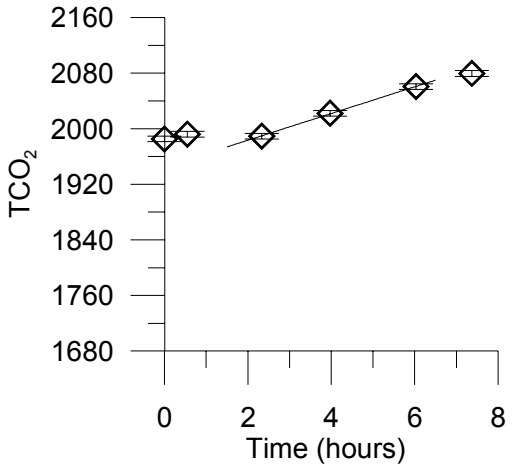

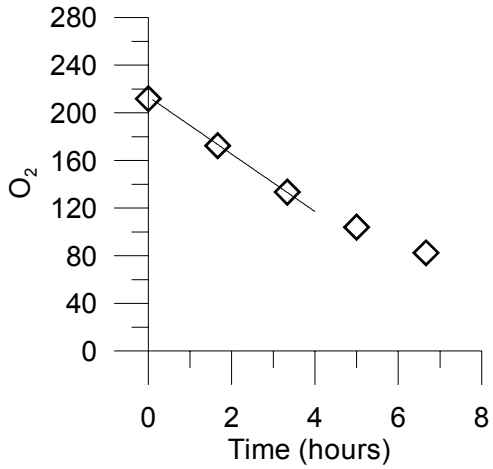

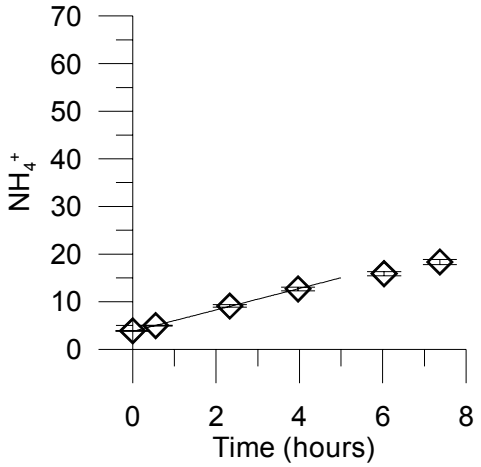

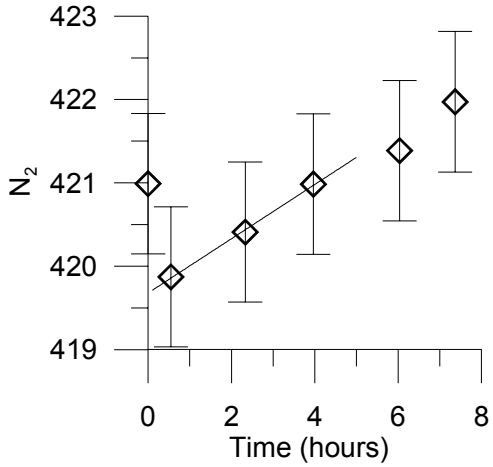

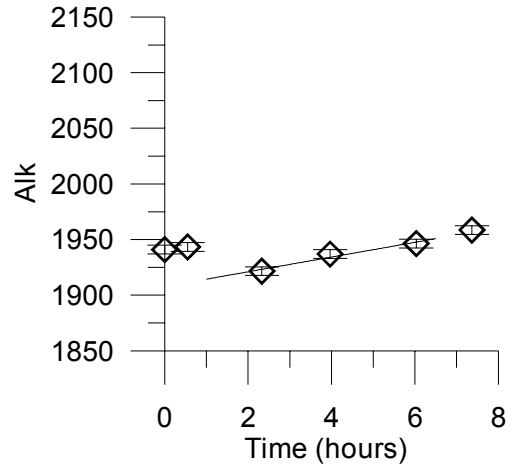

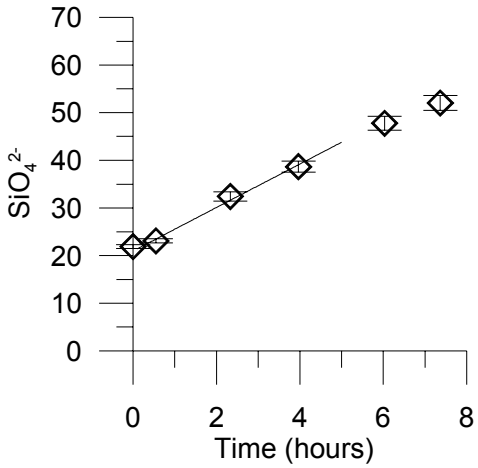

SGB - One Tree Bay (4A_8)

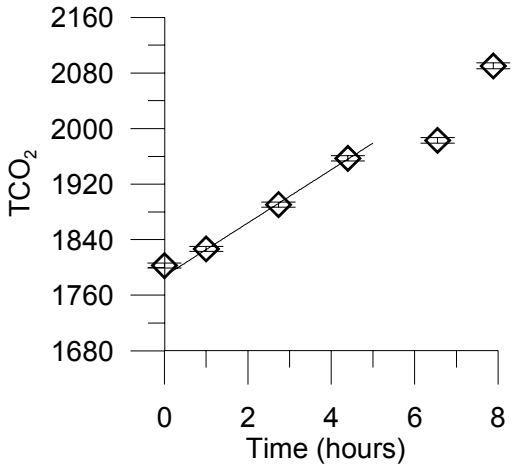

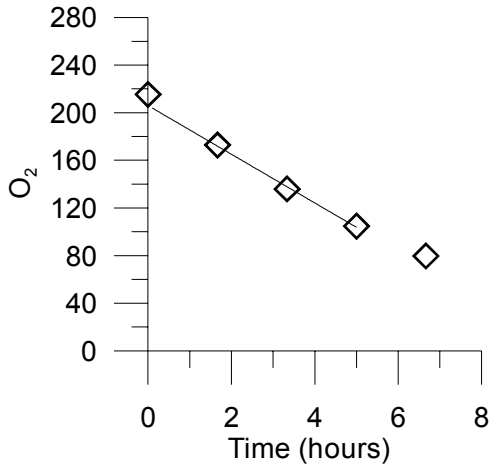

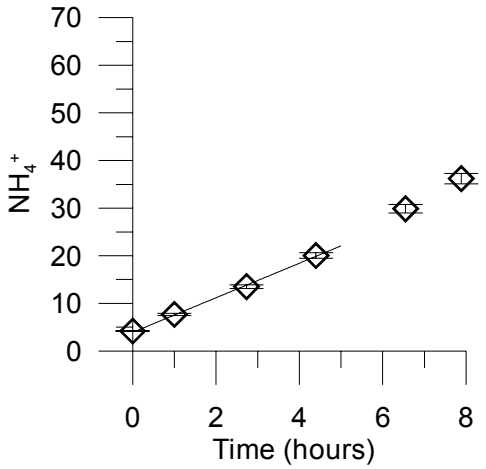

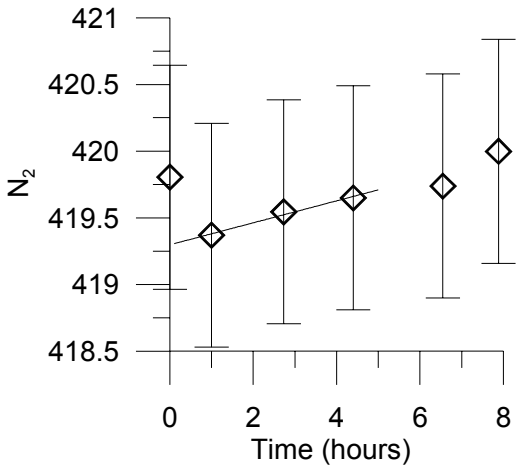

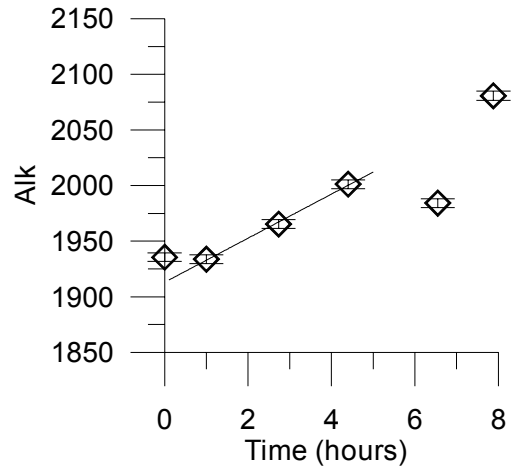

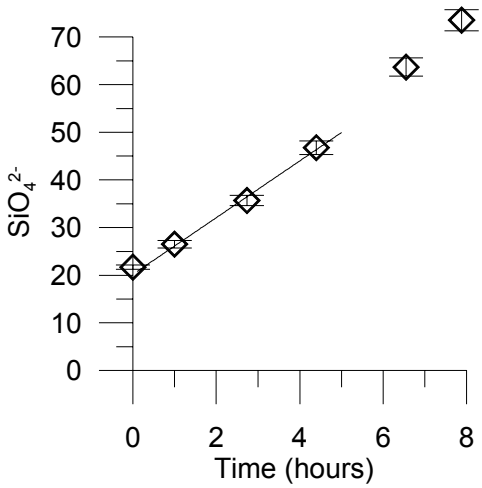

SGB - One Tree Bay (4A_9)

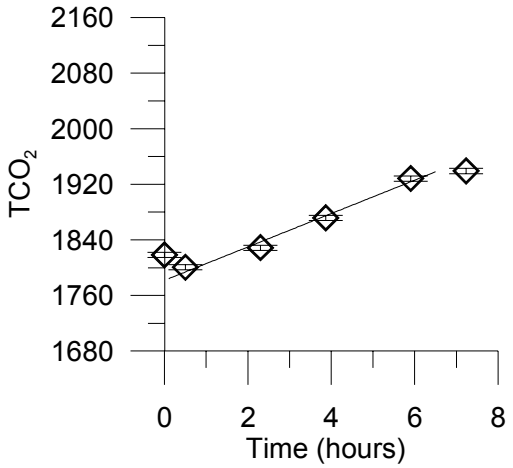

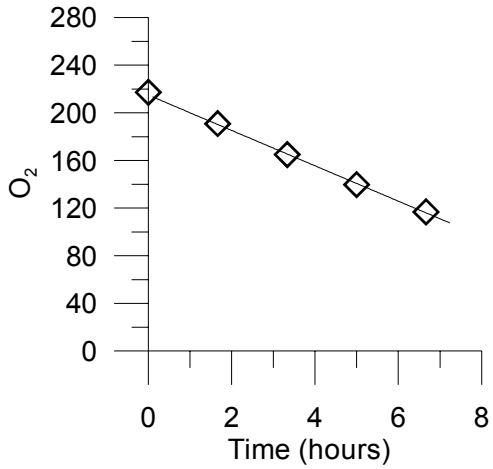

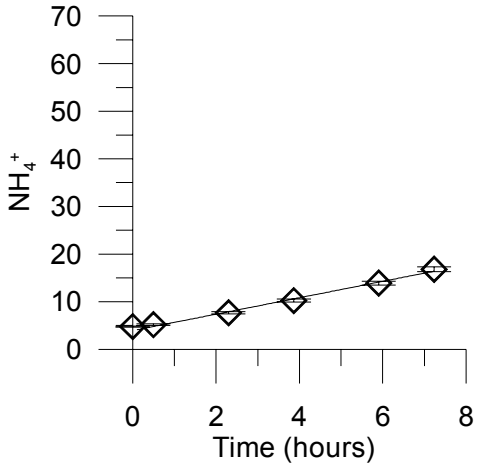

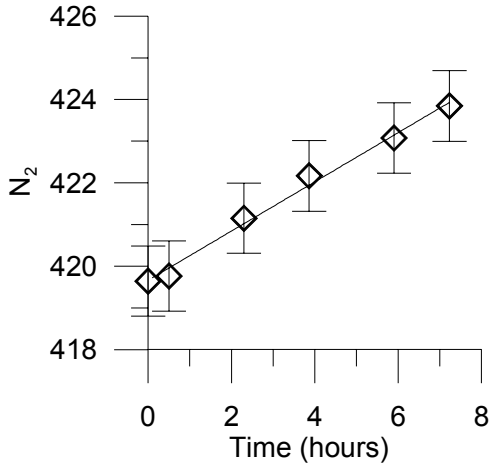

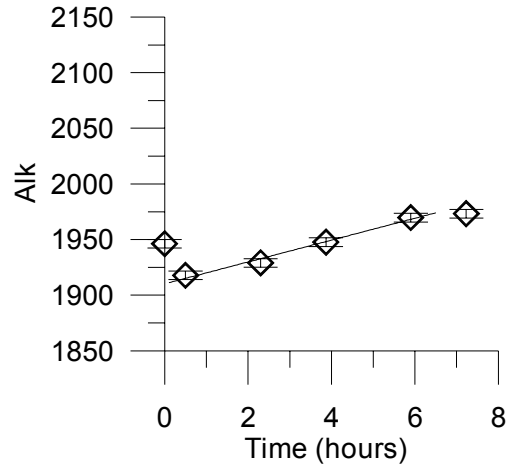

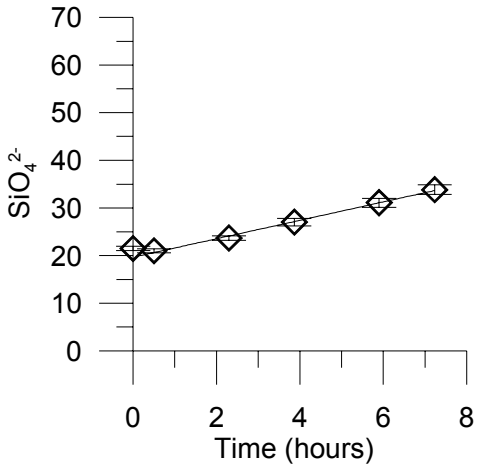

SGB - Pats Bay (5A_3)

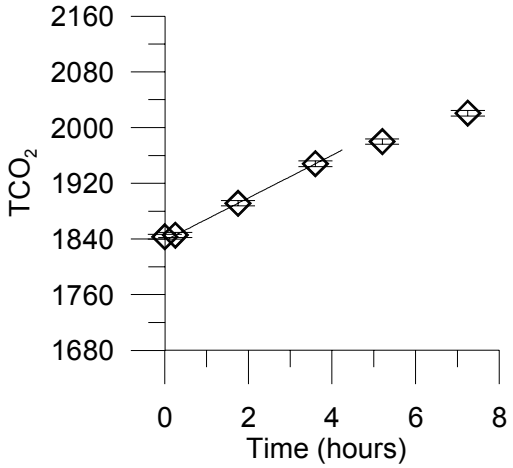

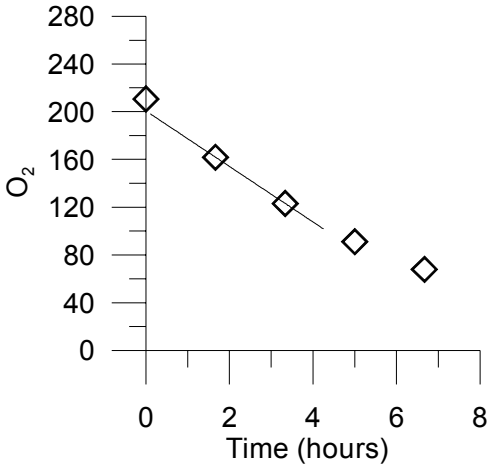

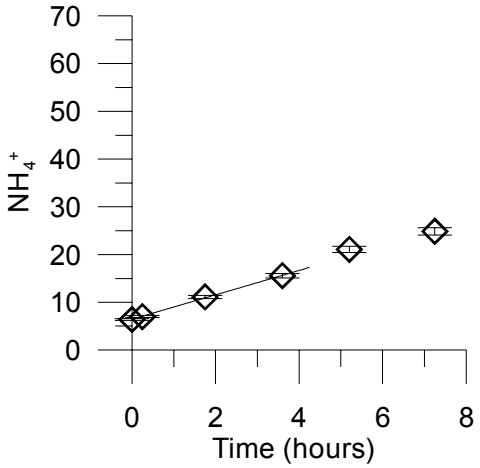

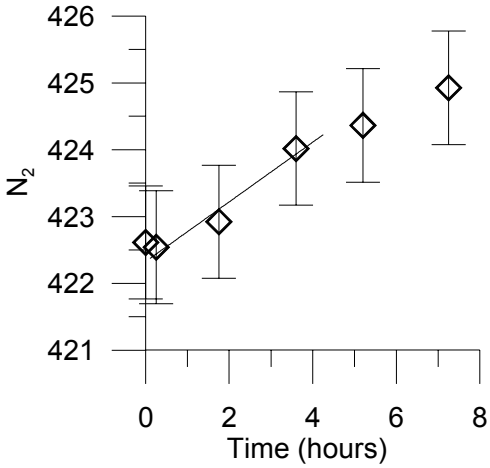

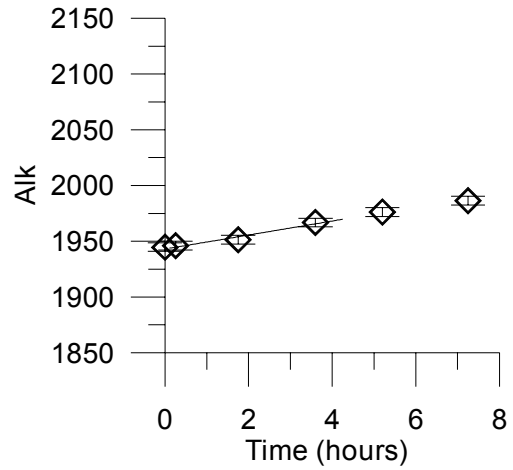

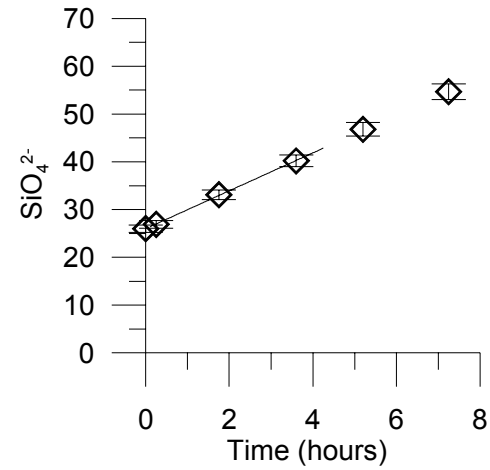

SGB - Pats Bay (5A_4)

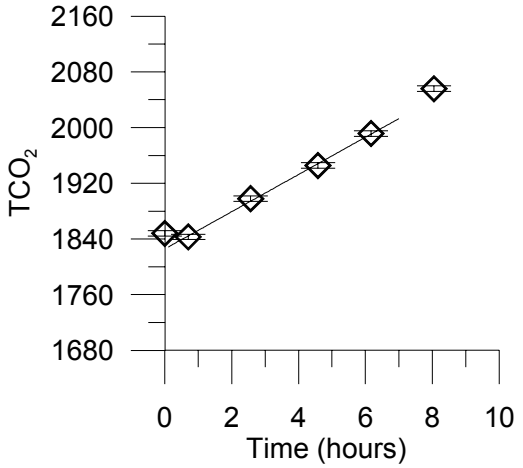

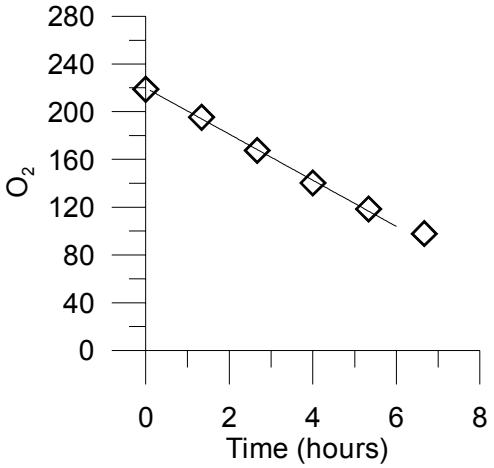

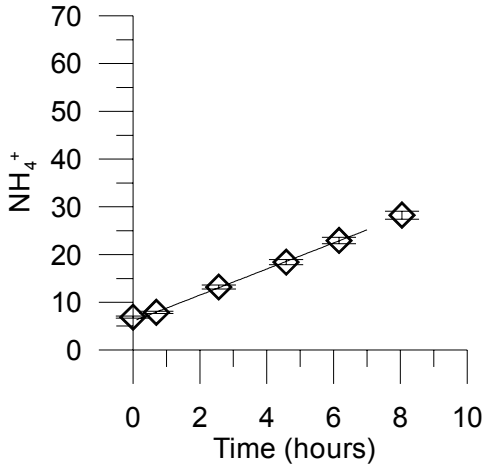

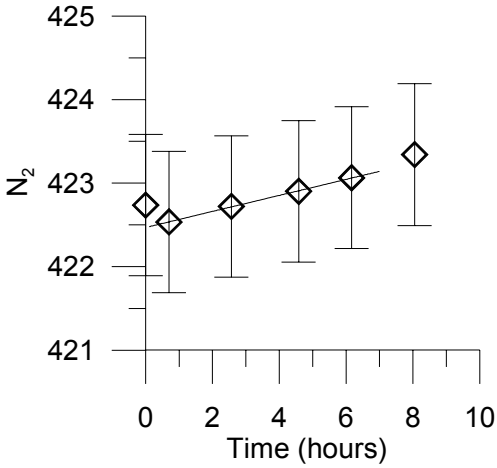

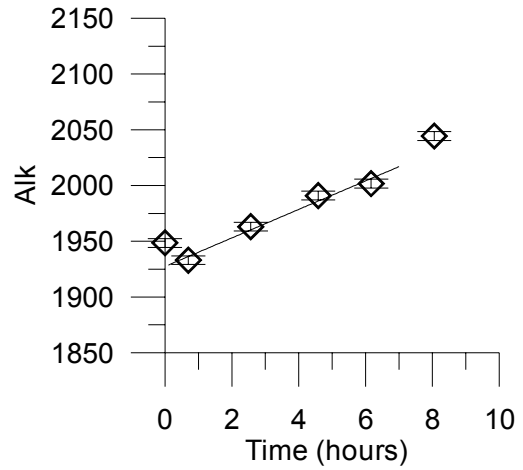

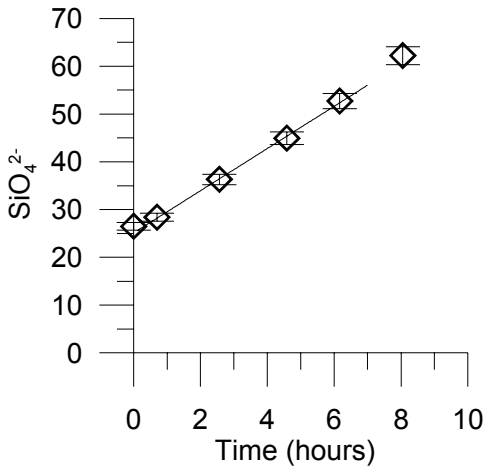

SGB - Pats Bay (5A_7)

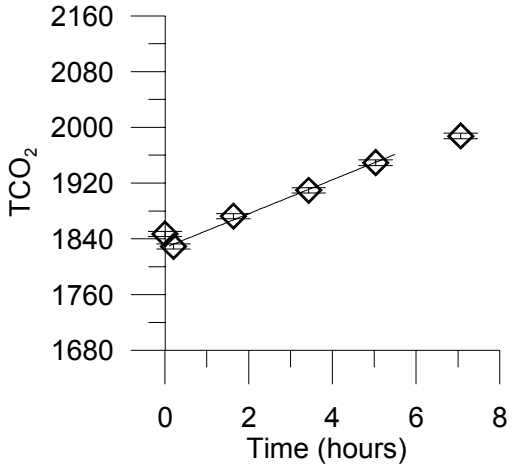

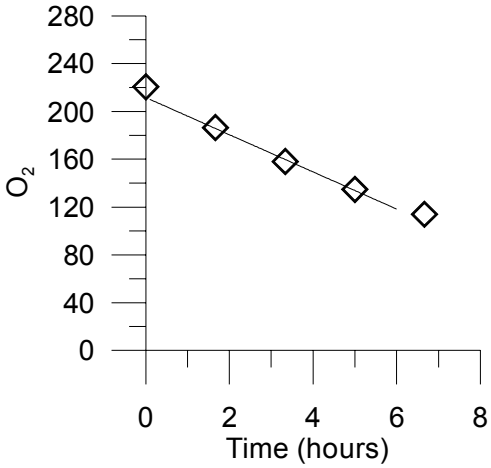

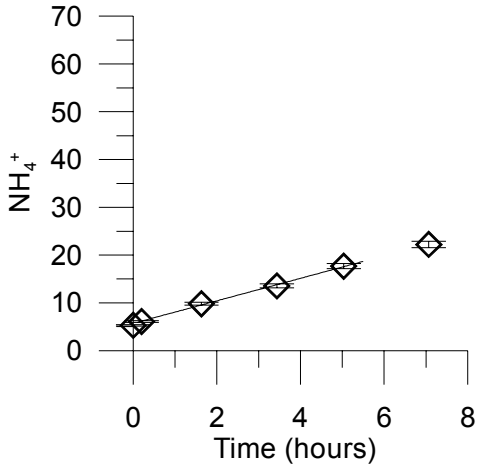

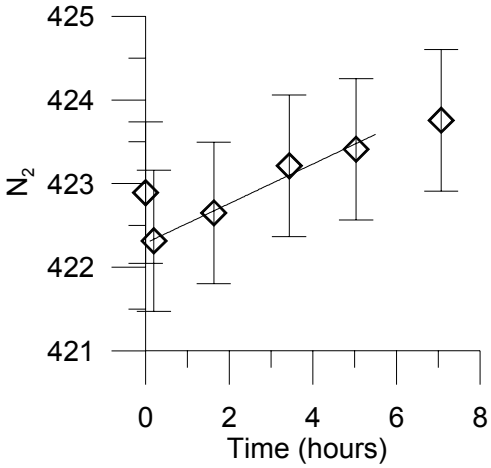

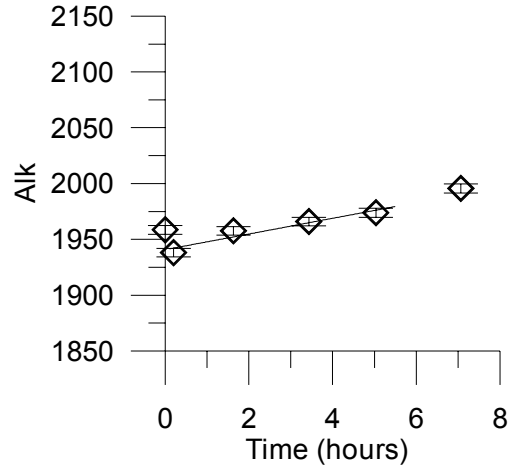

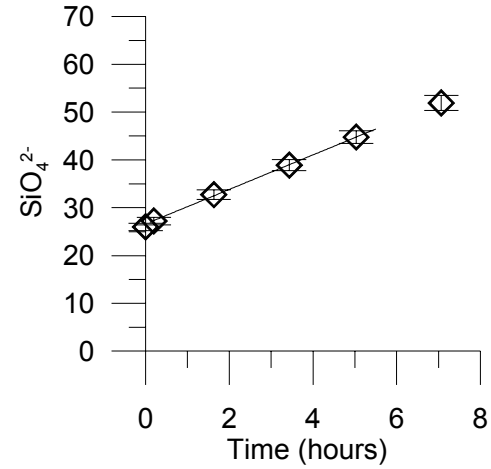

SGB - Pats Bay (5A_8)

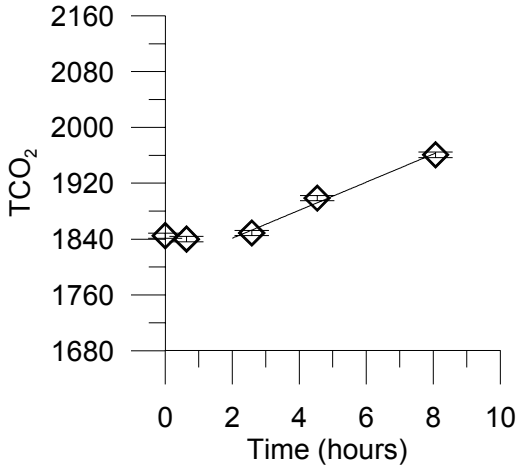

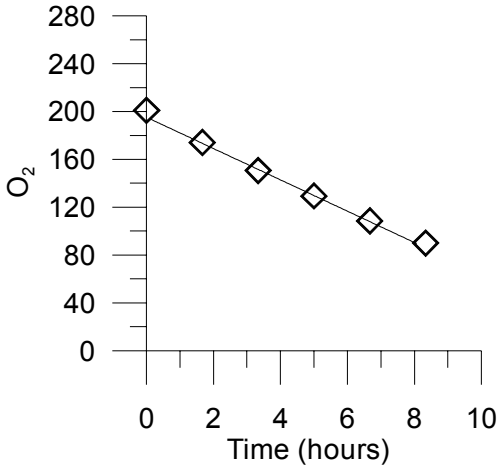

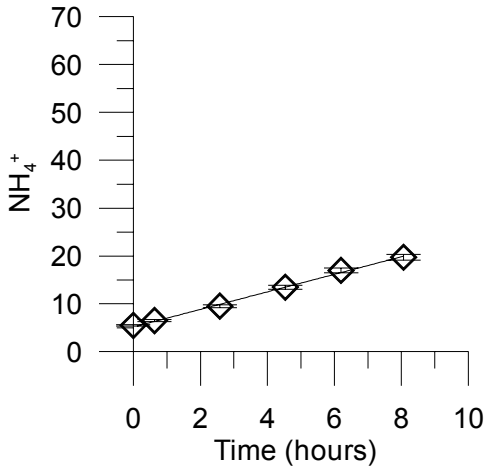

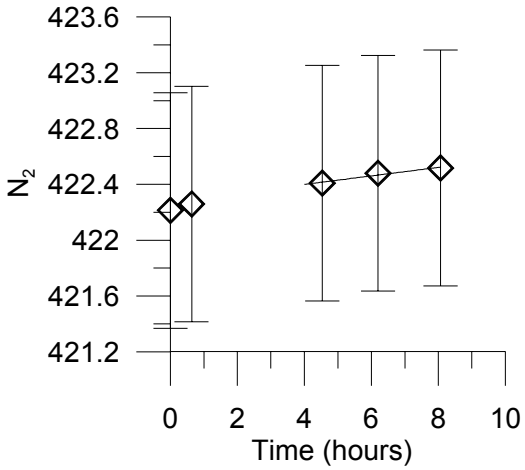

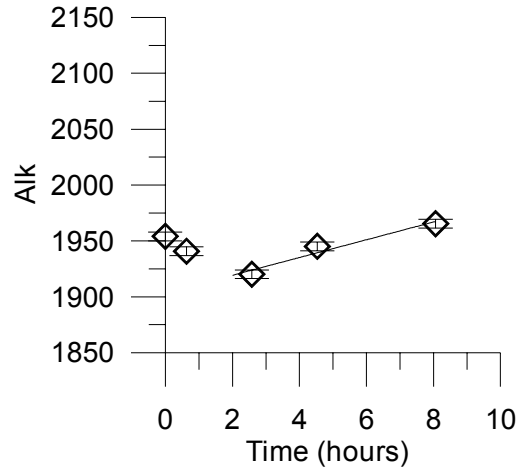

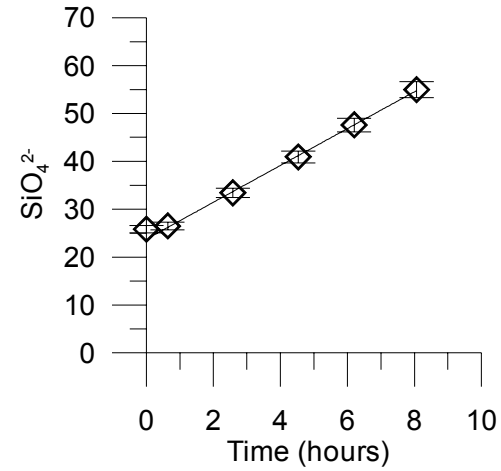

SGB - Pats Bay (5A_9)

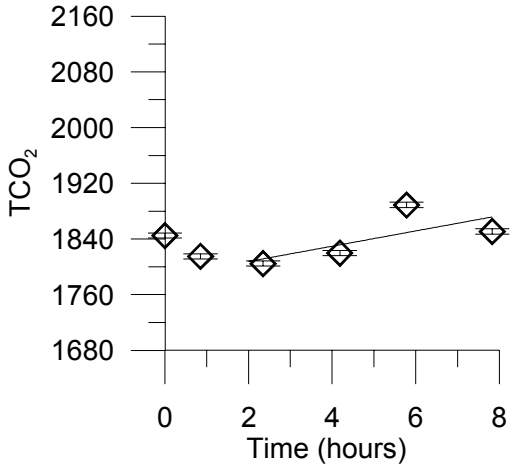

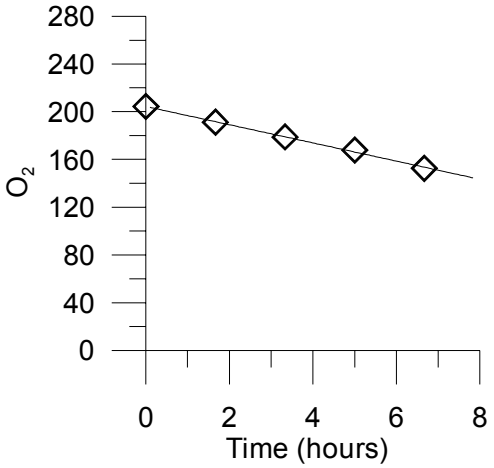

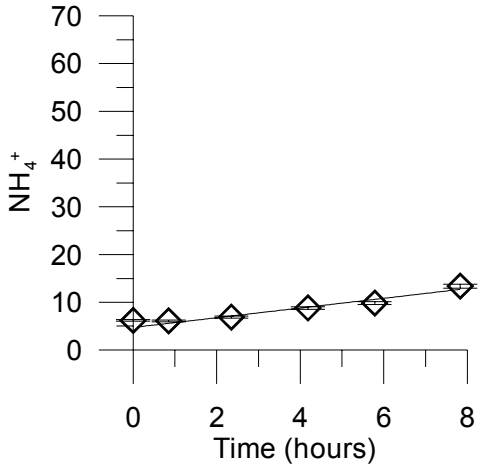

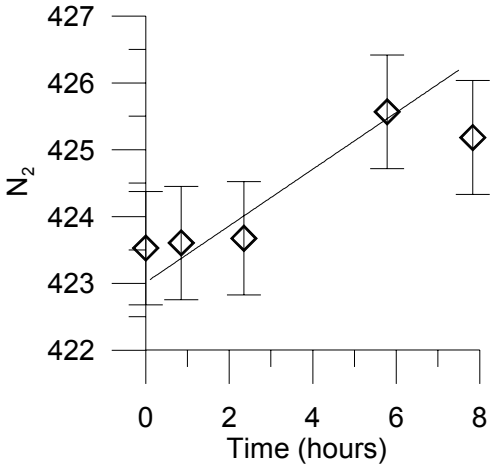

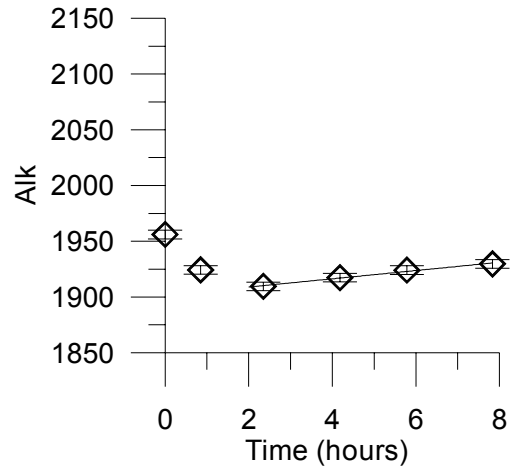

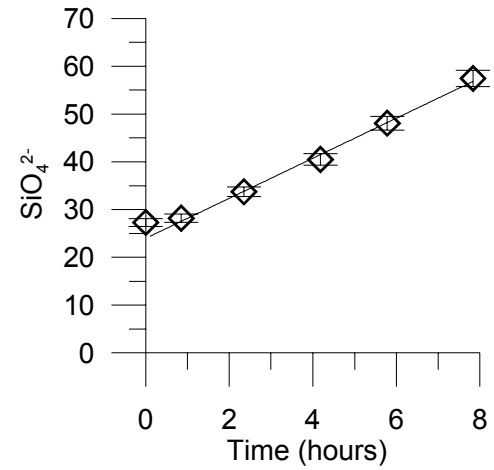

APPENDIX 7 – DOWN CORE SOLID PHASE AND POREWATER PLOTS

The area shaded in grey in each of the chlorophyll-a plots, represents background values. Crosses (+) represent core 1 for each site and closed circles (•) represent core 2. Open circles (o) represent δ^{13}C-TOC and δ^{15}N-TN data. The same scale is used for each particular parameter across sites.

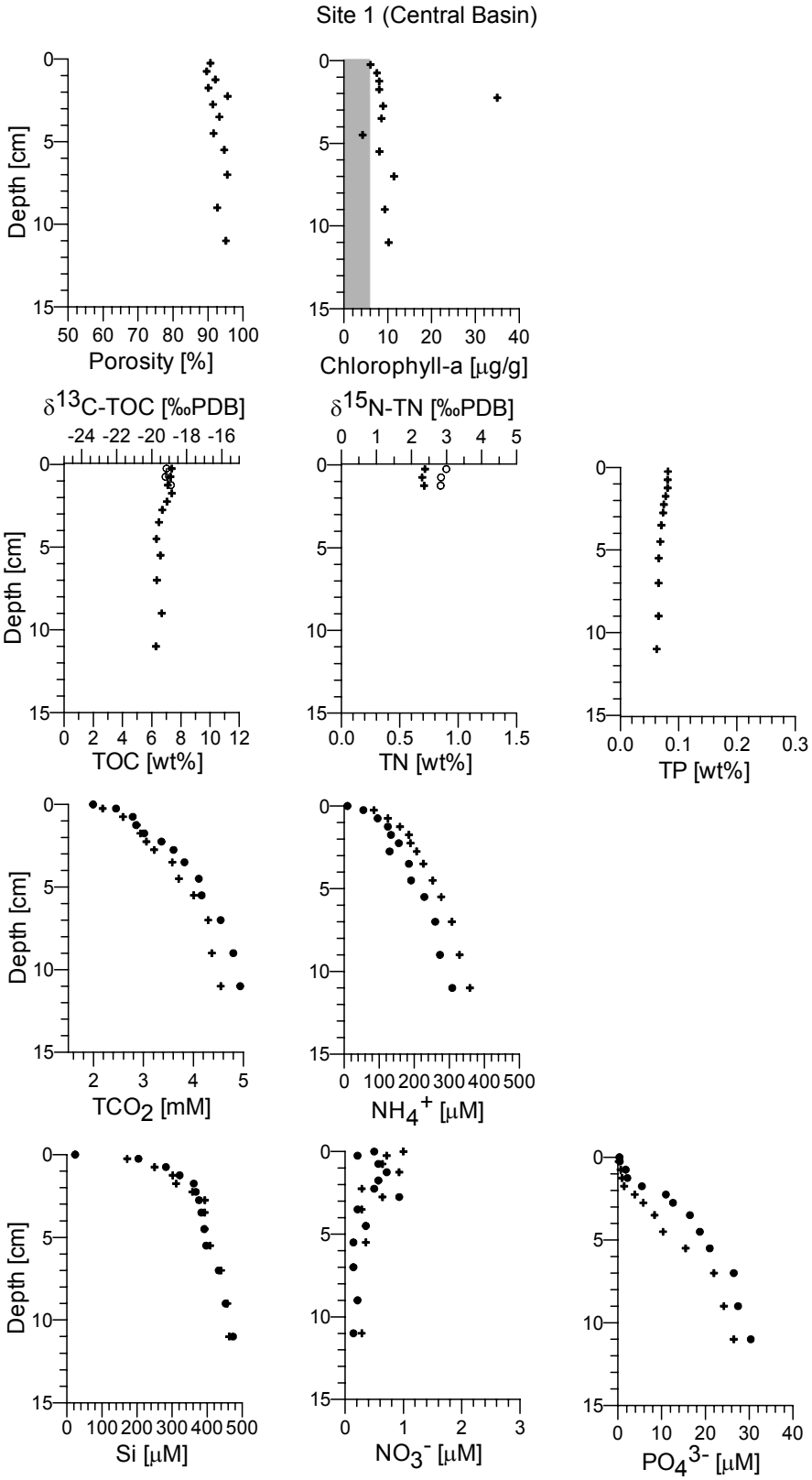

Site 2 (Erowal Bay)

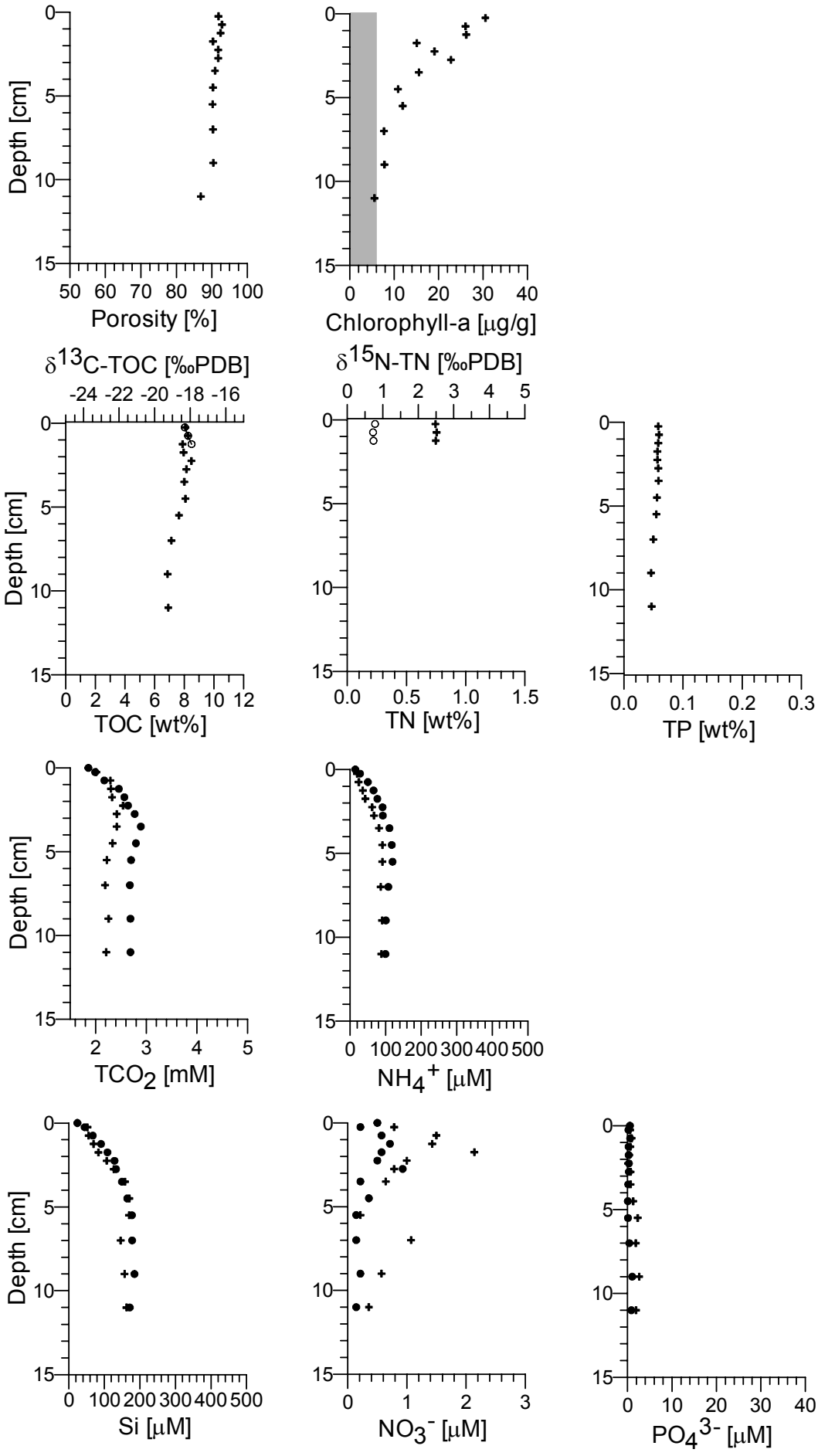

Site 3 (Wandandian Creek)

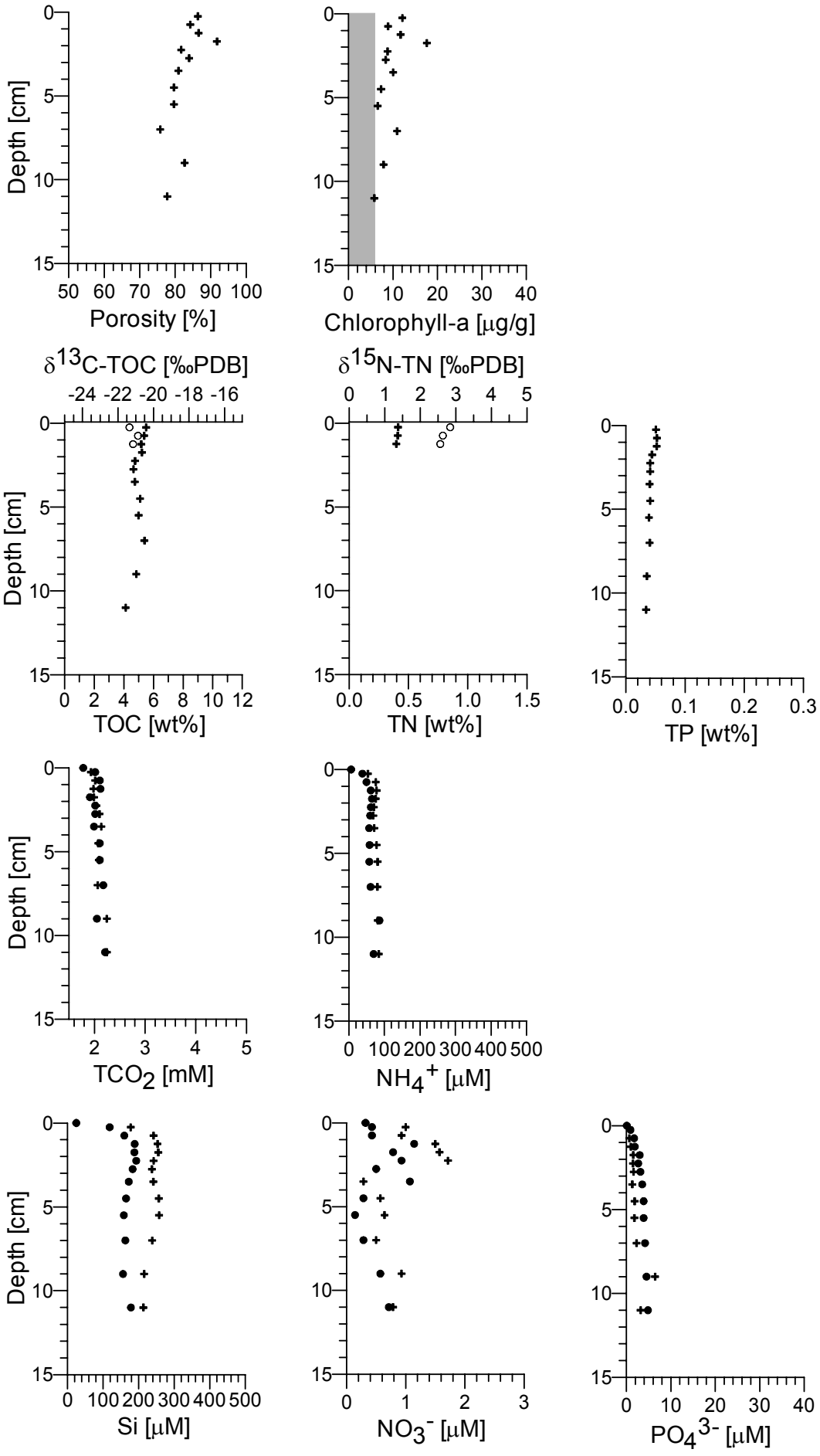

Site 4 (One Tree Bay)

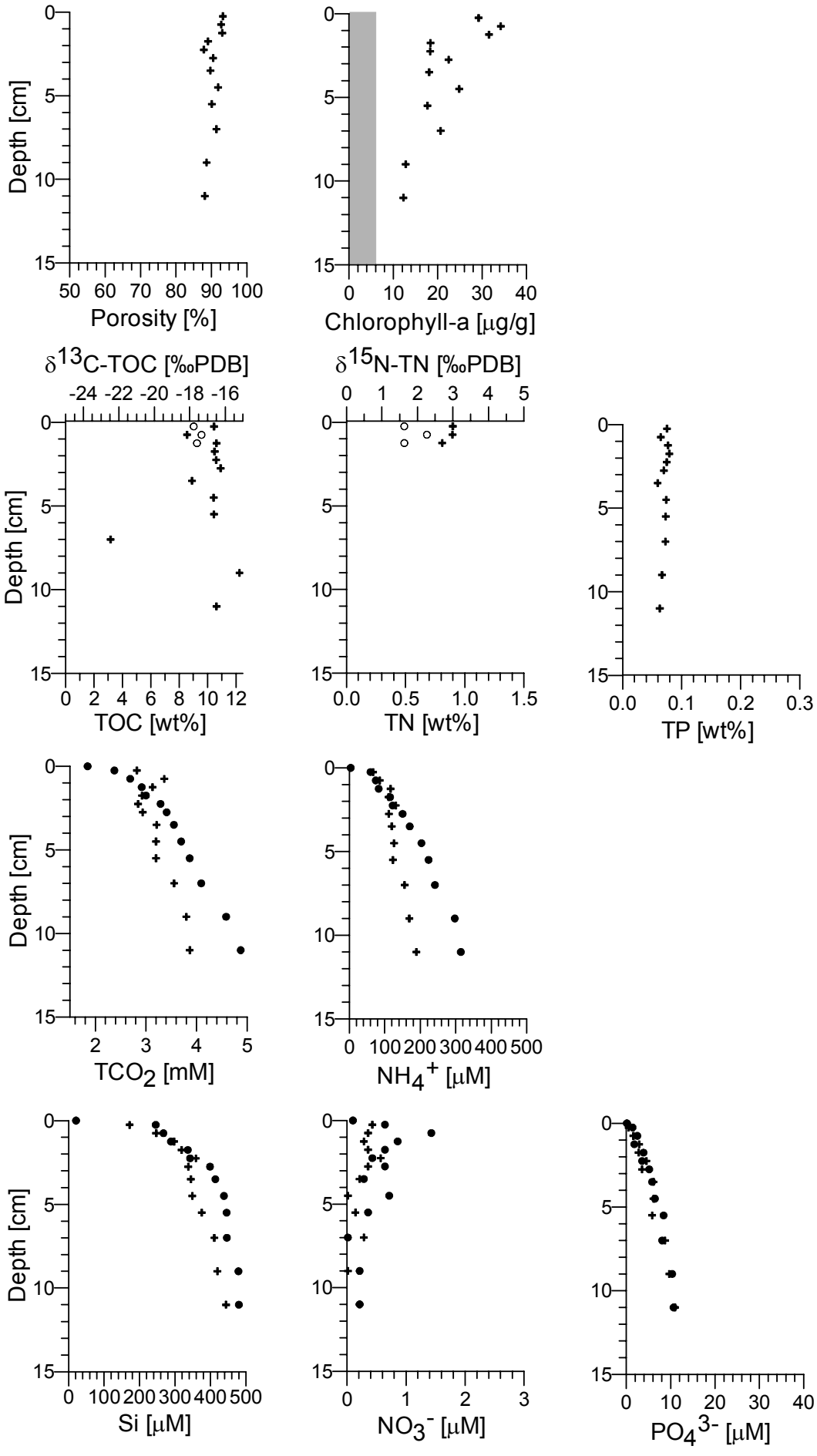

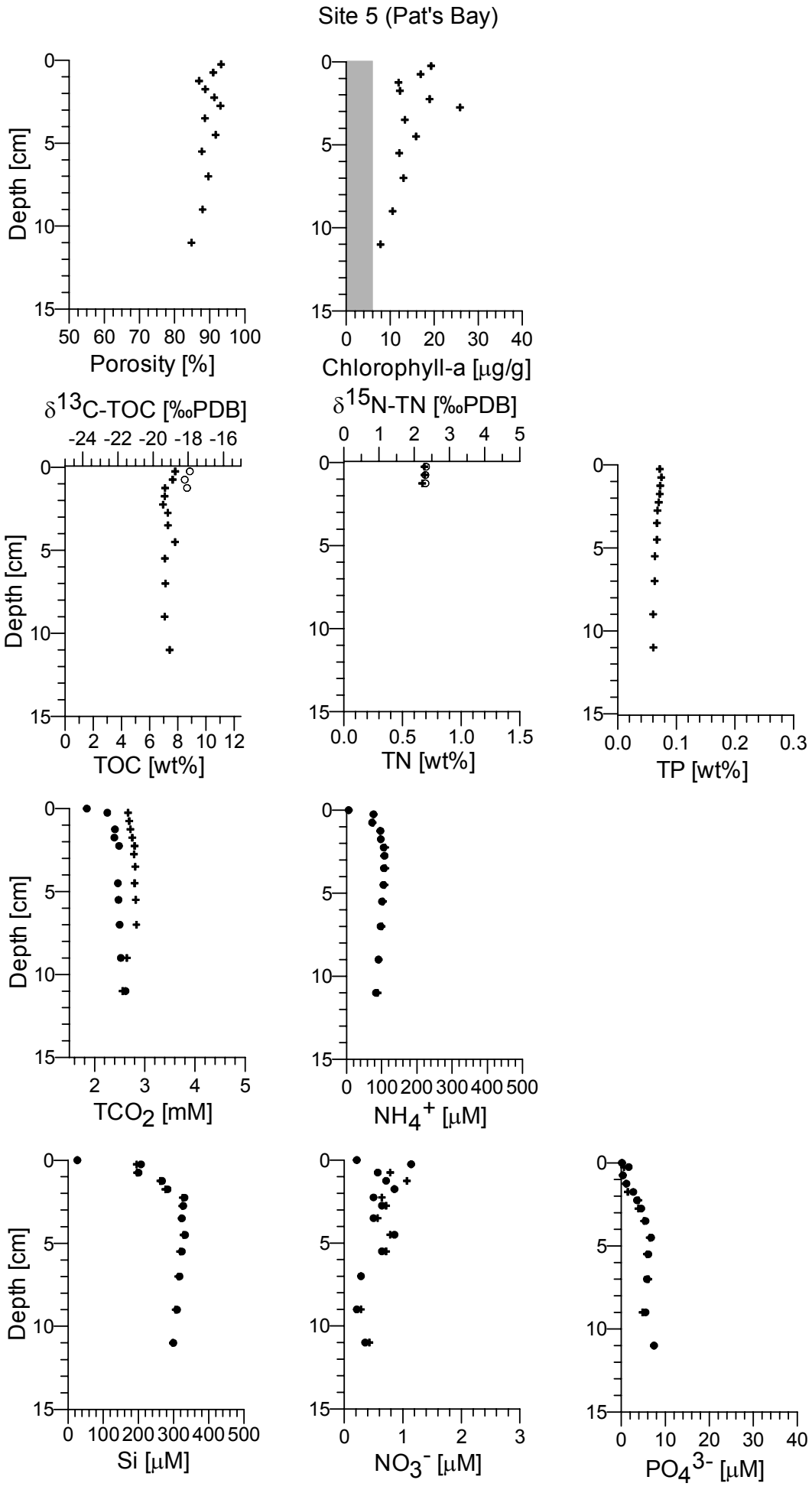
Site 5 (Pat's Bay)
Depth [cm]
Porosity [%]
Chlorophyll-a [μg/g]
δ13C-TOC [‰PDB]
TOC [wt%]
δ15N-TN [‰PDB]
TN [wt%]
TP [wt%]
TCO2 [mM]
NH4+ [μM]
Si [μM]
NO3- [μM]
PO43- [μM]